UNIVERSITY OF CAPE COAST

WAVE CLIMATE PREDICTION IN WEST AFRICA: COMPARING THE ACCURACY OF ERA5 AND CMENS REANALYSIS USING BUOY AND SATELLITE MEASUREMENTS

YUSIF OWUSU

2024

UNIVERSITY OF CAPE COAST

WAVE CLIMATE PREDICTION IN WEST AFRICA: COMPARING THE ACCURACY OF ERA5 AND CMENS REANALYSIS USING BUOY AND SATELLITE MEASUREMENTS

BY

YUSIF OWUSU

Dissertation submitted to the Department of Physics of the College of Agriculture and Natural Sciences, University of Cape Coast, in partial fulfillment of the requirements for the award of Master of Philosophy in Physics.

FEBRUARY 2024

DECLARATION

Candidate's Declaration

I hereby declare that this dissertation is the result of my own original research and that no part of it has been presented for another degree in this university or elsewhere.

Candidate's Signature:  Date: 26th August, 2024

Name: Yusif Owusu

Supervisors' Declaration

We hereby declare that the preparation and presentation of the dissertation were supervised under the guidelines on supervision of dissertation laid down by the University of Cape Coast

Supervisor's Signature:  Date: 26th August, 2024

Name: Prof. Anthony Twum

Co-supervisor's Signature: 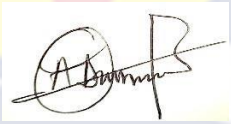 Date: 26th August, 2024

Name: Dr. Donatus B. Angnuureng

ABSTRACT

This research underscores the pivotal role of wave climate in the coastal activities and marine operations of West Africa, highlighting the necessity for accurate estimation to facilitate effective planning and management. The primary objective involves a comparative analysis of wave conditions and extreme wave events using the ERA5 and CMENS reanalysis datasets, focusing on the coastal regions of West Africa. The findings reveal that CMENS reanalysis datasets offer the most accurate description of wave conditions in West Africa. Utilizing CMENS reanalysis datasets, the study comprehensively estimates the wave climate, considering both global parameters and partitions (swell and wind sea). The predominant wave influence in the region is identified as swell, constituting approximately 95% of the sea state energy with wind sea contributing 5%. The origin of these swells is traced to the south and south-west region of the Atlantic Ocean. Through seasonal analysis, it is observed that high waves are most prevalent in the West Africa region during the month of August. Additionally, the research highlights 2017 as a year with the highest recorded anomaly for the region, contrasting with the least anomaly recorded in 2010. From 1993 to 2021, it seems that the wave power increases at an average rate of approximately 0.048kW/m per year.

KEY WORDS

CMENS hindcast

ERA5 hindcast

Satellite

Sea state

Significant wave height

Wave buoy

ACKNOWLEDGEMENTS

I would like to express my sincere gratitude to my esteemed supervisors, Prof. Anthony Twum and Dr. Donatus Angnuureng, whose unwavering guidance, insightful feedback, and motivational support have been instrumental in the successful completion of this dissertation. Their expertise and encouragement have truly enriched my academic journey.

I extend my heartfelt appreciation to Dr. Komlan Agbeko Kpogo-Nuwoklo, my dedicated coach, for sharing his profound knowledge, providing invaluable assistance, and enhancing my computational skills. His mentorship has been a source of inspiration throughout this research endeavor.

Furthermore, I am deeply thankful for the financial support received from the Harmony Coast Project and GMES Thesis Completion grant. Their generous funding has played a pivotal role in facilitating the execution of this research, enabling me to delve into meaningful exploration and analysis.

This dissertation would not have been possible without the collective contributions of Prof. Anthony Twum, Dr. Donatus Angnuureng, Dr. Komlan Agbeko Kpogo-Nuwoklo, Harmony Coast Project and GMES-UG. I am truly grateful for their support and mentorship which have significantly enriched my academic and research experience.

DEDICATION

To my beloved family.

TABLE OF CONTENTS

LIST OF TABLES

LIST OF FIGURES

LIST OF ABBREVIATIONS

CMENS: Copernicus Marine Environment Monitoring Service

ECMWF: European Centre for Medium-Range Weather Forecasts

ERA5: ECMWF Reanalysis 5

GPD: Generalized Pareto Distribution

Hs: Significant wave height

HY-2B: Hai Yang 2B

HY-2C: Hai Yang 2C

ML: Maximum Likelihood

POT: Peak Over Threshold

CHAPTER ONE

INTRODUCTION

Wave climate plays a crucial role in coastal activities like shipping, offshore operations, erosion management, and infrastructure projects. Accurate wave condition estimates are essential for safe and efficient coastal planning and management. In West Africa, where marine resources and coastal infrastructure are vital, understanding wave climate is necessary for sustainable development and protecting coastal communities. This study aims to estimate the wave climate in West Africa, focusing on extreme wave events, using historical data. The geographic scope includes coastal regions of Ivory Coast, Ghana, Togo, Benin, and Nigeria, within the 5°N to 20°N latitude and 20°W to 10°E longitude.

Background to the study

The Democratic Republic of the Congo, Equatorial Guinea, Ghana, Benin, Nigeria, Cameroon, Equatorial Guinea, Sao Tome & Principe, Gabon, Senegal, The Gambia, Guinea, Sierra Leone, Liberia, Cote d'Ivoire, and Togo occupy almost 11,000 km of the West African coastline. Low-lying coastal plains, estuaries, and mangrove swamps characterize the area, which is home to more than 350 million people (Abdul et al., 2020). The coastal area supports a variety of economic activities like tourism, oil and gas exploration, and fishing because it is also rich in natural resources.

Coastal erosion, flooding, and sea level rise are all wave-induced calamities that the West African coastline is particularly susceptible to. The vulnerability of the area is a result of a number of issues, such as climate change,

sea level rise, inefficient land use, and insufficient coastal protection measures (Hounkpe et al., 2019). The loss of property, the eviction of people, and the interruption of economic activity are just a few of the substantial socioeconomic effects of these risks.

The frequency and severity of wave-induced disasters in West Africa have increased during the past few years. The Greater Accra Region and the Volta Delta, for example, were both severely impacted by catastrophic coastal flooding in Ghana in 2015. (Amponsah et al., 2021). Almost 5,000 people were forced to leave their homes as a result of the flooding, which seriously damaged the infrastructure, possessions, and way of life. Similarly, wave-induced coastal erosion poses a serious problem in Nigeria, where estimates indicate that the nation loses more than 1.5 m of beachfront every year (Folorunsho et al., 2023).

To identify wave-induced dangers and create efficient mitigation strategies, wave climate data is essential. Designing coastal structures, predicting storm surges and coastal floods, and scheduling marine operations are all made easier with the use of accurate wave climate data. There is a need for more complete and precise information because the amount of wave climatic data for West Africa is small.

When there are few observational data points available, reanalysis datasets like ERA5 and CMENS offer a way to estimate wave climate data. The databases combine existing observations with mathematical models to provide gridded datasets of many sea state parameters including significant wave height, wave period, wave direction, etc. When these datasets are compared, it will be possible to pinpoint each dataset's advantages and disadvantages as well as learn more about how wave conditions vary across West Africa and how they often

resemble one another. We can better understand the wave conditions in West Africa thanks to the findings of this study, which will also help us create mitigation strategies that will effectively reduce the risks associated with wave.

Previous studies have evaluated reanalysis datasets such as ERA5 and NNR-II to determine their suitability for modeling wave conditions, revealing both strengths and limitations. ERA5, while consistent with annual mean significant wave heights (SWH), tends to overestimate SWH in most locations and underestimates maximum SWH during extreme weather events, making it less reliable without site-specific validation. Other studies, such as those by Sun et al. (2024) and Steinkopf et al. (2022), have highlighted biases in ERA5 data, particularly in shallow waters and coastal areas, with some studies suggesting that CMENS may offer more accurate results for West African coastlines. However, direct comparisons between ERA5 and CMENS in this context are limited. Despite some improvements in the available data, further research is required to clarify which dataset provides the most accurate representation of wave conditions. Based on the above, the accuracy of reanalysis datasets for estimating wave conditions in West Africa remains unclear.

Statement of the Problem

Coastal engineering, coastal management, and marine navigation are just a few of the industries that are greatly impacted by the varied wave conditions found along West Africa's coastlines. Reliable wave climate data are essential for understanding and mitigating the impacts of waves in this region. However, the accuracy and suitability of reanalysis datasets, such as ERA5 and CMEMS, for estimating wave climate parameters in West Africa remain

unclear. This research aims to address this critical gap by conducting a comprehensive comparison and validation of ERA5 and CMEMS reanalysis data, ultimately contributing to a more accurate assessment of wave conditions and their long-term trends in this important coastal area.

Purpose of the Study

The main aim of this research is to estimate wave climate and analyze extreme wave events in West Africa. This research also aims to address this critical gap by conducting a comprehensive comparison and validation of ERA5 and CMEMS reanalysis data, ultimately contributing to a more accurate assessment of wave conditions and their long-term trends in the West Africa region.

Objectives of the Study

The primary objectives of this research are focused on understanding and assessing wave conditions in West Africa using reanalysis datasets.

First, it aims to evaluate and assess the ERA5 and CMENS reanalysis datasets in estimating wave conditions in the region. Additionally, the study seeks to compare ERA5 and CMENS reanalysis data with available wave buoy and satellite data to determine which dataset better represents wave conditions in West Africa.

Based on the identified best-performing dataset between ERA5 and CMENS, the study will estimate the wave climate, concentrating on both global wave parameters and partitions. Furthermore, the research will analyze the

seasonal and inter-annual variability of wave conditions off the coast of West Africa.

Lastly, it aims to examine extreme wave events that could lead to coastal flooding and erosion.

Significance of the Study

This study aims to enhance the accuracy of wave climate estimations in the West African region by comparing two prominent global reanalysis datasets against observational reference data. By identifying the most reliable dataset, the research supports the planning, design, and maintenance of coastal and marine infrastructure, thereby aiding engineers and planners in making informed decisions to build resilient structures. The findings will also assist policymakers and environmental managers in developing sustainable coastal zone management strategies, mitigating risks like coastal erosion, flooding, and marine submersion to protect ecosystems and coastal communities. Furthermore, the study contributes to climate change adaptation efforts by providing long-term wave climate data, which is crucial for anticipating the impacts of sea-level rise and extreme weather events. Improved wave climate models will enhance marine safety and navigation, benefiting operations such as fishing, shipping, and offshore energy extraction by reducing risks associated with inaccurate wave predictions. Academically, the research enriches the scientific understanding of wave dynamics in tropical regions, particularly in West Africa, and offers valuable insights for future studies aiming to validate and improve reanalysis datasets on a global scale.

Limitations

The limitations of this study include the resolution of reanalysis data, which may not capture small-scale variations, especially near coastlines. The quality of reanalysis data depends on the accuracy of observational inputs, which may be sparse along the West African coast. Limited availability of buoy and satellite data for validation can introduce biases, and discrepancies may arise due to mismatches in the temporal coverage of reference data. Model uncertainties, particularly under extreme weather conditions, and challenges in capturing long-term climate variability like ENSO also affect the results. Finally, the findings are specific to the West African coast and may not apply to other regions.

Delimitations

The study is focused on the West African coast, comparing ERA5 and CMEMS reanalysis data for one year and estimating wave climate over 30 years. It excludes other global reanalysis datasets and validation sources beyond buoy and satellite data. Key metrics like significant wave height, wave period, and wave direction are prioritized, while more complex metrics are excluded. The analysis is quantitative, excluding qualitative assessments or extreme wave events like storm surges, to focus on average wave climate patterns relevant to the region.

Organization of the Study

This thesis is classified into five (5) chapters. The scope of each chapter is explained as follows:

Chapter two is about the literature review, in which terminologies and theories related to this project are discussed. The literature review provides a background of this project and also gives the direction for this research. In chapter three, the best of CMENS and ERA5 reanalysis is determined on the basis of comparisons with observations. In chapter Four, wave climate is estimated based on global parameters and partitions, seasonal and inter-annual variability are also analyzed in this chapter. Chapter four also unveils the extreme wave conditions for the region of study. Finally, chapter five is made up of the conclusion and recommendations of the work.

CHAPTER TWO

LITERATURE REVIEW

Introduction

This chapter provides a comprehensive review of the existing literature related to wave conditions and reanalysis datasets, with a focus on the West African region. It begins by exploring the importance of wave climate studies and their relevance to coastal management, marine operations, and infrastructure development. The chapter also examines the role of reanalysis datasets, particularly ERA5 and CMEMS, in estimating wave climates and their application in previous studies. Furthermore, it delves into the strengths and limitations of reanalysis data for wave prediction, including their use in regions with sparse observational data, such as West Africa. Comparative studies between different reanalysis datasets, and their relevance to understanding wave dynamics in tropical coastal environments, will also be discussed. Finally, the chapter highlights the gaps in the literature, particularly the limited focus on the West African coastline, and sets the stage for the research aims of this study.

Notations about Sea State and Wave Climate

The significance of wave climate resonates across various domains. In maritime navigation, an in-depth grasp of wave climate facilitates route optimization, ensuring safe and efficient passage for vessels. Coastal engineers rely on wave climate data to design structures capable of withstanding the forces exerted by waves, storm surges, and coastal erosion. Coastal erosion which has been a crisis for the West African coast is most specifically caused by swell waves (Hounguè et. al. 2018). Offshore industries, including oil and gas and

renewable energy, depend on precise wave climate information for the design, maintenance, and safety of offshore installations. Moreover, environmental scientists employ wave climate data to assess coastal vulnerability, study beach erosion, and safeguard ecosystems (Rusu et al., 2018).

Wave climate data and insights find applications across diverse sectors. Meteorology leverages this information for improved weather forecasting, particularly for coastal and maritime regions, where waves can have a substantial impact on weather patterns. Coastal management authorities utilize wave climate data to develop effective strategies for shoreline protection, beach nourishment, and flood risk assessment. Moreover, the shipping and maritime industries employ wave climate data for route planning, voyage optimization, and safety management, ensuring the well-being of vessels and crew (Appeaning Addo et al., 2011).

In light of these considerations, the accurate estimation of wave conditions becomes a fundamental necessity. This accuracy is indispensable for the effective planning, design, and overall management of coastal regions. In essence, comprehending historical wave patterns and predicting future wave behavior is vital for making informed decisions regarding coastal development and safeguarding (Dodet et. al, 2019). West Africa, a region characterized by its heavy reliance on marine resources and extensive coastal infrastructure, stands out as a primary focus for this research. Understanding the wave climate within this area becomes imperative for the sustainable management of coastal zones and the livelihoods of its coastal communities.

From previous studies, the evaluation of ERA5 and NNR-II reanalysis datasets in the marine domain of West Africa was examined to identify the

reanalysis data that best represents the wind regimes of the sub-region for use in climate studies and ocean wave modeling (Foli et. al, 2021).

Recent studies have assessed the quality of wave height and wave period data in the ERA5 reanalysis by comparing them to buoy measurements, revealing several limitations and areas for improvement. For instance, Shi et al. (2021) found that ERA5 significant wave height (SWH) data showed positive biases, indicating an overall overestimation for most locations, and a significant underestimation of maximum SWH during tropical cyclone periods, suggesting that ERA5 data may not be reliable for design applications without site-specific validation. Furthermore, while ERA5 was consistent with the annual mean SWH, its performance for the average wave period was less accurate, particularly in shallow water areas.

Similarly, Sun et al. (2024) highlighted the limitations of ERA5 by comparing it with Sentinel-1 SAR ocean wave spectra and NDBC buoy data, noting discrepancies in the spectral values and presenting RMSE and bias values that indicated the need for improvement in ERA5's wave height estimations. Steinkopf et al. (2022) emphasized the improvements in ERA5 over ERA-Interim for climate investigations in Africa, particularly in reducing wet biases and better representing the annual precipitation cycle, although their study did not specifically address coastal regions.

In the context of West Africa, Almar et al. (2023) and Angnuureng et al. (2022) investigated coastal changes and erosion management using various satellite and reanalysis data, but their findings suggested that employing CMENS could yield better results. My findings further support this by demonstrating that CMENS performs better than ERA5 in the coastal regions

of West Africa. Despite the valuable insights provided by these studies, there is a lack of direct comparison between ERA5 and CMENS in this specific context. Future research should focus on region-specific evaluations that directly compare these datasets to validate the superiority of CMENS and guide the selection of appropriate datasets for coastal studies in West Africa.

Previous studies tackling wave climate estimation in West Africa have either used data from a single buoy (Olagnon et. al, 2014) or ERA5 or ERA-interim reanalyses (Almar et. al, 2015, Hounguè et. al, 2018). Recently, other reanalysis data, notably CMENS, have become available with better spatial resolution. To our knowledge, these CMENS data have never been used for similar studies in West Africa. It is therefore worth investigating the added value of CMENS data compared with ERA-5 data, which has been used to date for studies requiring wave data in West Africa.

Sea State

The description of the ocean's surface or its condition in relation to wave motion is known as the "sea state." The term "sea state" also refers to the condition of the sea's surface, which is primarily determined by the size, frequency, and steepness of the waves, as well as the presence of other phenomena like wind and surge. These factors work together to influence the behavior of the water and add to its complicated dynamics, creating special difficulties for a variety of applications (Wimbush et al., 2021). Figure 1 shows an illustration of the definition of a sea state for a particular region. The sea state of a particular region comprises the wind sea and swell.

Wind Sea

The wind sea is the local pattern formed by the current wind conditions in the area. Larger waves eventually arise from ripples caused by wind blowing across the ocean's surface. Waves in the wind sea are often shorter than swell waves in wavelength and more frequent (shorter in period). The height of a sea is dependent on the strength of the wind, the duration of time the wind has blown, and the distance over which the wind has blown (fetch).

Swell

Waves that originate from distant storms or weather systems are known as swell. Compared to wind sea, swell waves have longer wavelengths and lower frequencies (longer periods). Generally speaking, their shape and orientation are more uniform.

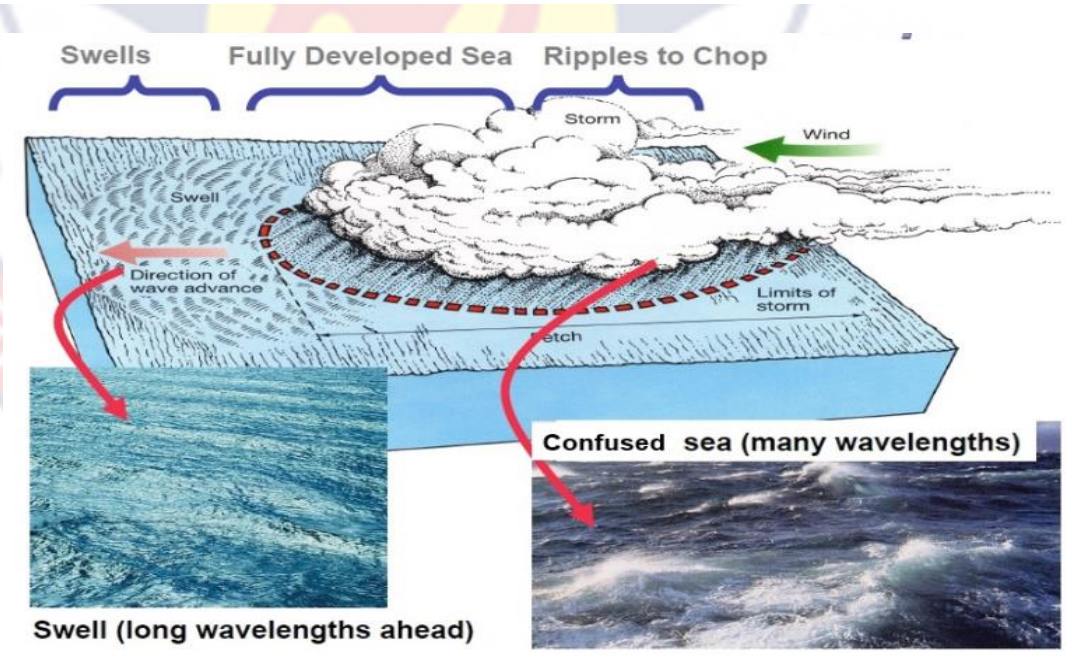

Figure 1: An illustration of sea state definition with the difference between swell and wind sea (Source: Retrieved from https://www.eoas.ubc.ca/courses)

Sea State Observations

Sea state observation encompasses the systematic collection of data and information related to the sea's surface. This includes critical parameters such as wave height, wave period, wave direction, and the presence of factors like wind and swell (Ardhuin et al., 2019).

Wave Buoy

A wave buoy, also known as a wave rider buoy or oceanographic buoy, is a specialized marine instrument designed to observe and measure various parameters related to ocean waves and sea states. These buoys are typically anchored or moored at sea and equipped with sensors and instruments to collect data on wave characteristics, water conditions, and meteorological variables. Wave buoys play a crucial role in oceanography, meteorology, maritime safety, and various coastal and offshore engineering applications.

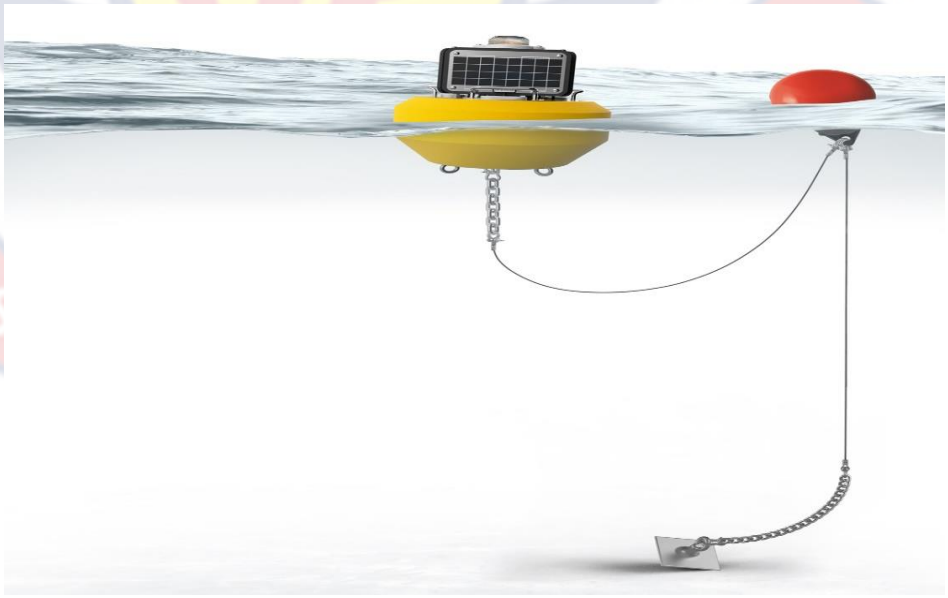

Figure 2: CB-25-SVS wave buoy. (Source: Retrieved from nexsens.com/systems/wave-buoy)

Wave buoys are engineered to withstand harsh marine environments and provide reliable, real-time data. The operation of a wave buoy involves the following steps:

Deployment: The wave buoy is deployed at a predetermined location in the ocean, typically by a research vessel or through automated systems. The mooring system is carefully set up to ensure the buoy remains in place.

Data Collection: The sensors on the wave buoy continuously collect data on wave height, wave period, wind speed and direction, water temperature, salinity, and other relevant parameters. This data is logged in real-time.

Data Transmission: Many wave buoys are equipped with communication systems that transmit the collected data to onshore facilities or research institutions. This allows scientists and researchers to access and analyze the data remotely.

Maintenance: Wave buoys require periodic maintenance to ensure their sensors remain calibrated and operational. This may involve routine inspections, sensor cleaning, and occasional repairs.

Data Analysis: Researchers and scientists use the data collected by wave buoys to analyze ocean conditions, study wave patterns, and improve our understanding of sea states. This information is valuable for various applications, including weather forecasting, maritime safety, and coastal engineering.

Wave buoys are invaluable tools for advancing our knowledge of the oceans and improving safety in maritime and coastal environments. Their continuous data

collection and transmission capabilities contribute significantly to scientific research and practical applications.

Satellite Observation

Satellite observation refers to the collection of data and information about Earth's oceans and their behavior using remote sensing instruments onboard orbiting satellites. Satellite observation has revolutionized our ability to monitor and analyze oceans on a global scale, enabling insights that were previously unattainable (Tatem et al., 2008; Front. Mar. Sci., 2019).

Numerous satellites monitor oceanographic features, providing vital information for scientific research, weather forecasting, environmental monitoring, and maritime operations. The following are a few of the satellites with an oceanic observational focus:

HY-2 Series (HY-2A, HY-2B, HY-2C): These Chinese satellites are a part of the Haiyang (HY) series and are outfitted with instrumentation to measure ocean parameters like wave height, wind speed, and sea surface temperature.

The Jason Series (Jason-3, Jason-2, and Jason-1): These satellites are equipped with altimeters that measure sea surface height. This information is used to track ocean circulation patterns, sea-level rise, and climatic events like El Niño and La Niña.

CryoSat-2: This satellite from the European Space Agency is equipped with a radar altimeter that measures changes in the thickness of sea ice and polar ice sheets, providing information about ocean conditions in polar regions.

Sentinel-3 Series (Sentinel-3A and Sentinel-3B): These satellites, which are a part of the Copernicus program of the European Space Agency, are equipped with a variety of equipment for ocean and land monitoring, including altimeters, radiometers, and sea and land surface temperature radiometers.

SARAL (Satellite with ARGOS and ALTIKA): A combined Indian-French satellite mission outfitted with radiometers and altimeters to gauge wind speed and other oceanographic variables.

GCOM-W1 (Global Change Observation Mission - Water): This is a Japanese satellite outfitted with the Advanced Microwave Scanning Radiometer 2 (AMSR2) to track ocean-related information such as sea surface temperature and sea ice concentration.

These and numerous additional satellites aid in the study of Earth's oceans and are essential for climate research, weather forecasting, oceanography, and environmental preservation.

Satellite missions that have been carried out to measure wave parameters in the past, present, and future are displayed in Figure 3.

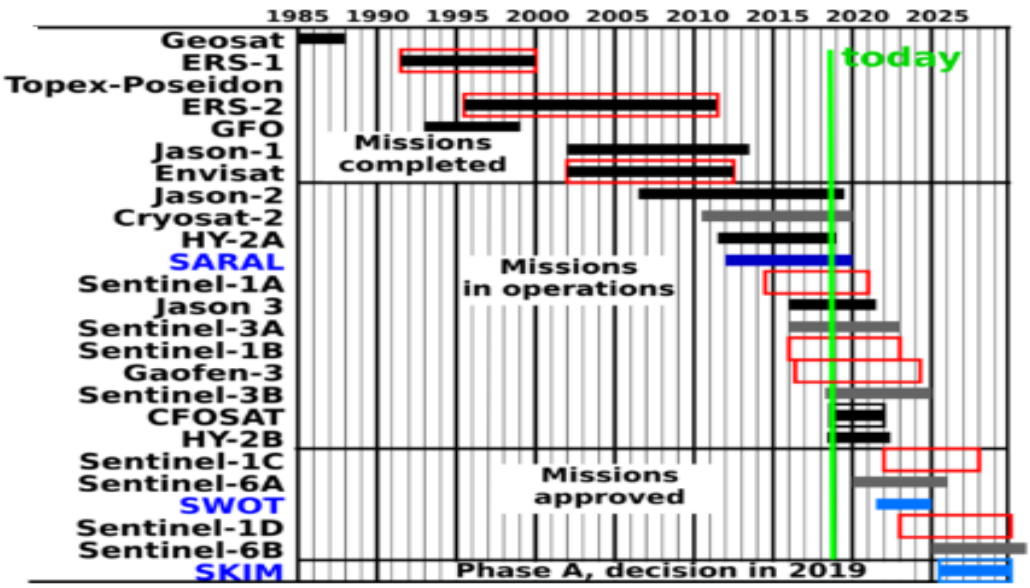

Figure 3: Time history of past, existing and planned satellite missions that

measure waves (Source: Retrieved from www.umr-lops.fr/Donnees)

Numerical Modeling of Sea State

Numerical modeling refers to the use of mathematical and computational models to simulate and predict the behavior of ocean waves and sea states. Numerical modeling allows to recreate complex oceanic conditions, including wave height, wave period, and wave direction, under various scenarios. It serves as a powerful tool for understanding and forecasting sea states, aiding in numerous maritime and coastal applications.

At the heart of our investigation lie the methodologies and tools employed in numerical modeling. This process involves the utilization of computer-based models that simulate the physical processes governing wave generation and propagation. These models leverage mathematical equations and input data to generate realistic representations of sea states, which allows us to explore the behavior of waves in different oceanic conditions.

Wave space-time evolution of the distribution of wave energy with wave frequency and direction is given as Equation 1 based on De Carlo et al, (2020):

$$\frac{\partial F}{\partial t} + \nabla\left(C_g . F\right) = S_{net} = S_{in} + S_{nl} + S_{ds} + S_{btm} \quad (1)$$

where $F\ (f,\ \theta,\ x,\ t)$ is the two-dimensional spectrum dependent on the frequency f and the wave direction θ.

$C_g\ (f,\ \theta,\ x)$ is the group velocity

S_{net} is the net source function

S_{in} is the energy input from wind

S_{nl} is the nonlinear energy transfer by resonant interaction

S_{ds} is the energy dissipation due to wave breaking

S_{btm} is the energy loss by bottom friction

Here are some examples of numerical wave models:

Copernicus Marine Environment Monitoring System (CMENS): CMENS is a numerical model produced by the Copernicus Marine Service. The wave products are the integrated parameters computed from the total wave spectrum (significant wave height, period, direction, Stokes drift... etc.), as well as the partitions into wind sea and swell (marine.copernicus.eu).

Fifth generation of the European Center for Medium-range Weather Forecasts (ECMWF) Reanalysis (ERA5): Is a numerical model of a climate reanalysis dataset produced by the ECMWF providing global atmospheric and land surface reanalysis data spanning several decades (https://www.ecmwf.int/en/forecasts/dataset).

WAVEWATCH III (WW3): WAVEWATCH III is one of the most widely used numerical wave models in the world. Developed by NOAA (National Oceanic and Atmospheric Administration), it simulates the generation, propagation, and transformation of wind-generated ocean waves. WW3 is used for weather forecasting, coastal engineering, offshore operations, and climate research.

Simulating Waves Nearshore (SWAN): SWAN is another wave model with a focus on nearshore wave processes. It is designed to simulate wave transformation and propagation in shallow coastal areas, where wave behavior can be highly complex due to interactions with the seabed. SWAN is used for coastal management, beach erosion studies, and nearshore infrastructure design.

Sea State Characterization

The characterization of sea states is of paramount importance in various marine applications and scientific endeavors. To initiate our exploration, it is essential to unveil the spectrum approach for sea state characterization. This approach is a mathematical framework used to analyze ocean wave data, offering a comprehensive view of wave energy distribution across different frequencies and directions. It helps to unravel the complexities of sea states and provides insights into their behavior, making it a cornerstone of oceanographic and coastal studies.

Directional Wave Spectrum

The wave spectrum is a mathematical representation of the distribution of wave energy across different frequencies and wave numbers. It provides a comprehensive and detailed description of the various wave components within a sea state. Understanding the wave spectrum is pivotal as it forms the basis for the estimation of key parameters that characterize sea states.

By taking into account both wave frequency and wave direction, a two-dimensional sea wave spectrum offers a more thorough description of the wave energy distribution. It provides a more accurate depiction of ocean wave patterns by taking into consideration the directional spread of wave energy. Wave energy is represented on a two-dimensional graph in a 2D wave spectrum, where wave direction and frequency are displayed on opposite axes. This makes it possible to comprehend how wave energy is dispersed across many frequencies and orientations better. It is especially crucial in situations when waves can originate from several directions, like in the open sea. When creating

constructions or vessels that can withstand waves coming from numerous directions, the 2D spectrum can be used to get insight into wave patterns.

An example of wave spectrum is shown in Figure 4. In this example, the sea state is made up of 3 wave systems:

1. A primary swell (Hs1 = 2m, Tp1 = 11s and θ1 = 55°)
2. A secondary swell (Hs2 = 1.7m, Tp1 = 17.8s and θ1 = 310°)
3. A wind sea (Hs0 = 1.6m, Tp1 = 7.5s and θ1 = 90°)

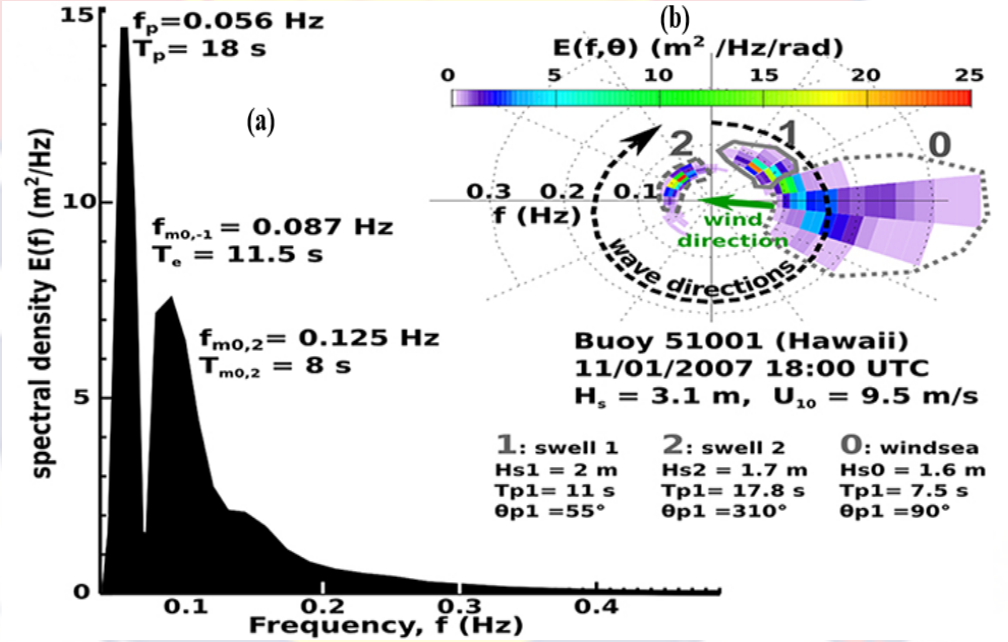

Figure 4: Example of sea state spectrum: (a) 1D spectrum and (b) directional wave spectrum (Hafez et. al., 2012).

Within the spectrum approach, we encounter the estimation of crucial wave parameters that shed light on sea state characteristics. These parameters include:

Significant Wave Height (Hs): Hs represents the average height of the highest one-third of waves in a sea state and serves as a fundamental measure of wave size.

$$H_s = 4\sqrt{m_o} \quad (2)$$

where m_o, is the zeroth-moment of the variance spectrum and is given by

$$m_o = \sqrt{\frac{\sum_{i=1}^{N}(H_i - \bar{H})^2}{n}} \quad (3)$$

where n is the measure of wave measurements, H_i is the individual wave height and $\bar{H}$ is the mean wave height.

Peak frequency (f_p): f_p is the spectrum's highest frequency. Typically, the greatest value in the spectrum corresponds to the peak period. If there are multiple peaks, they could also indicate the highest value within a certain category of sea state.

Wave Period (Tp): Tp signifies the average time interval between successive wave crests, providing insights into wave regularity.

$$T_p = \frac{1}{f_p} \quad (4)$$

where f_p is the peak frequency

Wave Direction (θ): Wave direction indicates the predominant direction from which waves approach, a vital aspect for navigation and coastal engineering.

Wave Power: The wave power represents the energy carried by waves and is critical for assessing their potential impact on maritime operations and coastal structures.

$$P_w = \frac{\rho g^2}{64\pi} T_e {H_s}^2 \quad (5)$$

where H_s is significant wave heights, T_e is wave energy periods. ρ is the density of the sea (1,025kg/m^3) and g is acceleration due to gravity.

Wave Climate

Wave climate refers to the long-term statistical characteristics of ocean waves in a specific region or location. It encapsulates vital parameters like wave height, wave period, wave direction, and wave energy distribution. Understanding wave climate serves as the foundation for predicting and mitigating the impacts of waves on coastal regions, maritime operations, and coastal structures (Jiang et al., 2023).

The significance of wave climate resonates across various domains. In maritime navigation, an in-depth grasp of wave climate facilitates route optimization, ensuring safe and efficient passage for vessels. Coastal engineers rely on wave climate data to design structures capable of withstanding the forces exerted by waves, storm surges, and coastal erosion. Offshore industries, including oil and gas and renewable energy, depend on precise wave climate information for the design, maintenance, and safety of offshore installations. Moreover, environmental scientists employ wave climate data to assess coastal vulnerability, study beach erosion, and safeguard ecosystems (Rusu et al., 2018).

Wave climate data and insights find applications across diverse sectors. Meteorology leverages this information for improved weather forecasting, particularly for coastal and maritime regions, where waves can have a substantial impact on weather patterns. Coastal management authorities utilize wave climate data to develop effective strategies for shoreline protection, beach nourishment, and flood risk assessment. Moreover, the shipping and maritime industries employ wave climate data for route planning, voyage optimization,

and safety management, ensuring the well-being of vessels and crew (Appeaning Addo et al., 2011).

In analysing the best of CMENS and ERA5 off the West African coast, using satellite observations and wave buoy, some scores of qualitative analyses were evaluated and compared. The scores calculated include:

Mean Bias: The mean bias represents the average difference or offset between the reference data (HY-2B/HY-2C and buoy) and the respective datasets (CMENS and ERA5). A lower relative error indicates a better agreement with the reference.

$$Bias = \frac{1}{N}\sum_{i=1}^{N}(X_i - Y_i) \quad (6)$$

Relative Error (RE): The relative error quantifies the percentage deviation between the reference data (HY-2B/HY-2C and buoy) and the respective datasets (CMENS and ERA5). A lower relative error indicates a better agreement with the reference.

$$RE = \frac{1}{N}\sum_{i=1}^{N}\frac{abs(X_i - Y_i)}{X_i} \quad (7)$$

Root Mean Square Error (RMSE): Is a measure of the overall difference or spread between the reference data (HY-2B/HY-2C and buoy) and the respective datasets (CMENS and ERA5). A smaller RMSE indicates a closer match to the reference.

$$RMSE = \sqrt{\frac{\sum_{i=1}^{N}(X_i - Y_i)^2}{N}} \quad (8)$$

Scatter Index (SI): The scatter index measures the dispersion of data points around the regression line. A lower scatter index suggests a tighter clustering of data points, indicating a better agreement with the reference.

$$SI = \frac{RMSE}{\bar{X}} \quad (9)$$

Correlation Coefficient (CR): The correlation coefficient is a measure of the linear relationship between two variables, ranging from -1 (perfect negative correlation) to +1 (perfect positive correlation), with 0 indicating no correlation.

$$CR = \frac{\sum(X-\bar{X})(Y-\bar{Y})}{\sqrt{\sum(X-\bar{X})^2 \sum(Y-\bar{Y})^2}} \quad (10)$$

Where X represents Hs of satellite or buoy and Y represents Hs of ERA5 or CMENS.

Extreme Wave Analysis

Extreme wave research is essential for coastal applications. These waves pose significant threats to coastal communities worldwide due to their exceptional height, force, and regularity. Their research is important because it provides the groundwork for creating practical plans to lessen their possibly disastrous effects on coastal areas. Researchers and coastal engineers can better predict, prepare for, and respond to these potent natural events by knowing their behavior and characteristics.

Studying severe waves is vital for sustainable coastal development, and its value goes far beyond intellectual curiosity. It is essential to incorporate study findings into risk assessment, catastrophe management, and coastal engineering procedures. Coastal towns can strengthen their resistance to these powerful natural forces by utilizing this information. Ensuring the safety and lifespan of coastal populations, infrastructure, and biological systems requires the effective use of research findings in policy-making and urban planning.

Description of Extreme Events

Extreme events in this view are the events that exceed a certain threshold which is above the expected wave events. The definition of an extreme event is shown in Figure 7. An extreme wave event is characterized by the maximum value of Hs reached (Hs_e), the peak period corresponding to the date of the Hs_e (Tp_e) and the duration of the event (Duration). To guarantee independence between events, two successive events must be at least 48 hours.

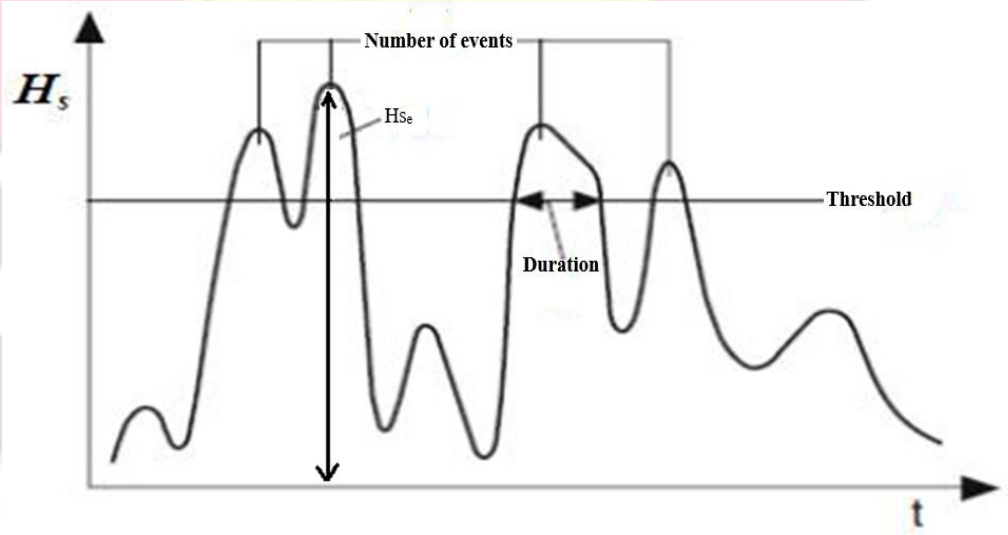

Figure 5: Graphical representation of extreme events

Peak Over Threshold (POT) and Annual Maxima are the two main methodologies used in the research of extreme wave analysis. POT technique was the method of choice for analyzing severe waves in this particular study. By evaluating wave events that surpass a predetermined cutoff, this approach allows for a more concentrated analysis of extreme occurrences as opposed to depending only on the largest wave recorded each year.

This analysis unfolds a comprehensive exploration of extreme event analysis methodologies within the context of the West African region. The analysis initiates with a detailed explanation of the POT method, intricately

employing the Generalized Pareto Distribution (GPD). It delves into the mechanics of this method, elucidating its application in identifying extreme values surpassing predefined thresholds. Following this, an in-depth analysis of the region's time series data unravels, unveiling underlying patterns, trends, and variations. The focus then transitions to a meticulous examination of extreme events, featuring histograms portraying the distribution of extreme significant wave heights (Hs) alongside their respective peak wave periods (Tp) and durations. The chapter further enriches its analysis through scatter plots, providing visual insights into the relationships between various extreme event parameters. Moreover, it conducts a thorough POT graph analysis, scrutinizing scale and shape parameters to comprehend the characteristics of extreme events. Conclusively, the chapter culminates with an intricate graph analysis, juxtaposing POT with GPD fitting graphs, and elucidating return levels and return periods to offer a holistic understanding of extreme event occurrences in the West African region.

Peak Over Threshold (POT) Approach with Generalized Pareto Distribution (GPD) Method

The POT approach, which is applied in this study, stands apart by focusing on wave events that exceed a predefined threshold. With this purposeful emphasis, severe wave events can be explored in greater detail and with greater nuance, giving rise to a thorough understanding of their properties, behaviors, and possible effects.

This study focused its attention on waves that exceeded a predetermined threshold by using the POT technique for extreme wave analysis, allowing for

a more thorough analysis of these severe occurrences. This methodological decision enables a more precise and in-depth examination of the unique traits and dynamics displayed by waves that exceed the threshold.

The POT approach was specifically used in this work to analyze severe waves. This methodology, which is distinguished by its emphasis on wave events that exceed a certain threshold, provides an exhaustive analysis of these extreme events, augmenting the study's accuracy and profundity in comprehending their characteristics and behavior.

The POT method is an approach that is based on high threshold exceedances. It involves fitting the GPD to the peaks of clustered excesses over a threshold, where the excesses are the observations in a cluster minus the threshold. Return values are calculated by accounting for the cluster occurrence rate. This process guarantees, under extremely generic conditions, that observations corresponding to various peak clusters are (roughly) independent and that the data can have only three possible, albeit asymptotic, distributions. In the POT method, the peak excesses over a high threshold u of a time series are assumed to occur in time according to a Poisson process with rate λ and to be independently distributed as a GPD, whose distribution function is given by (Sofia Caires, 2011):

$$F_u(y) = \begin{cases} 1 - \left(1 + \xi \frac{y}{\sigma_u}\right)^{-1/\xi}, for\ \xi \neq 0 \\ 1 - \exp\left(-\frac{y}{\sigma_u}\right),\ for\ \ \xi = 0 \end{cases} \quad (11)$$

Where $0 < y < \infty$, $\sigma_u > 0$ *and* $-\infty < \xi < \infty$. The two parameters of the GPD are called the scale (σ_u) and shape (ξ) parameters.

When $\xi = 0$, the GPD is equivalent to the exponential distribution with mean σ_u and is said to have a type I tail.

When $\xi > 0$, it has a type II tail and is the Pareto distribution

When $\xi < 0$, it has a type III tail and it is a special case of the beta distribution.

If $\xi < 0$, the support of the GPD is an upper-bond, $-\sigma/\xi$, which is called the upper end-point of GPD. The significance of this upper end-point is that (because when $\xi < 0$, equation 5.1 becomes $x < -\sigma_u/\xi$) the excesses over u modelled by the GPD cannot take values greater than $-\sigma_u/\xi$, which in turn means that the exceedances of the variable of interest cannot exceed the value

$$x^* = u - \sigma_u/\xi \tag{12}$$

x^* parameter is the upper-limit of the variable of interest.

The 1/m-year return value based on a POT/GPD analysis z_m, is given by

$$z_m = \begin{cases} u + \frac{\sigma}{\xi}\{(\lambda_u m)^{\xi} - 1\}, & for\ \xi \neq 0 \\ u + \sigma \log(\lambda_u m), & for\ \xi = 0 \end{cases} \tag{13}$$

The shape parameter and the scale parameter of the distribution are related by

$$\sigma_u = \sigma + (u - \mu) \tag{14}$$

In West Africa, extreme wave events occur during strong storms in the South Atlantic and push water surges towards coastlines, causing widespread flooding.

Chapter Summary

This chapter provided a detailed literature review on wave conditions and the use of reanalysis datasets, focusing on the West African coastline. It discussed the significance of wave climate studies in coastal management and marine operations, emphasizing the importance of accurate wave data for infrastructure development and safety. The chapter examined the use of ERA5 and CMEMS reanalysis datasets in wave climate estimation, comparing their strengths and limitations in regions with limited observational data. Comparative studies between different reanalysis models were reviewed, highlighting their relevance to understanding wave dynamics in West Africa. The chapter concluded by identifying gaps in the existing research, particularly the limited application of these datasets in the West African region, thus framing the importance of the current study.

CHAPTER THREE

METHODOLOGY

Introduction

This chapter outlines the methodology used to compare wave conditions in West Africa, utilizing ERA5 and CMEMS reanalysis datasets to estimate the wave climate. It describes the data collection process, including the selection of reanalysis data and the reference datasets, such as buoy and satellite observations, used for validation. The chapter details the statistical methods applied for comparing the datasets, as well as the criteria for assessing the accuracy and reliability of wave climate estimates. Additionally, it explains the temporal and spatial analysis techniques employed to evaluate the long-term wave patterns along the West African coast. This methodological framework provides the foundation for the analysis and comparison of wave conditions in the study area.

Comparison of ERA5 and CMENS Hindcast

Understanding and mitigating the effects of ocean waves in coastal zones requires precise wave climate estimation. Comparing ERA5 and CMEMS hindcast data in this work emphasizes the importance of wave climate estimation for modern marine research and coastal management.

Using datasets like ERA5 and CMENS proves to be a practical and effective method for precisely estimate wave conditions in West Africa. The region's long coastline presents several challenges that call for creative solutions. First, even though wave buoy deployment is a common technique for gathering data, it is logistically difficult and prohibitively expensive to apply widely across West

Africa. Second, the lack of wave data in the area is a critical problem that necessitates seeking alternate information sources. Finally, the scarcity of wave buoys in West Africa highlights the necessity for substitute techniques, considering that accurate and thorough wave measurements are essential for a range of coastal operations and environmental surveillance in the area. ERA5 and CMENS datasets offer a valuable solution, enabling researchers and stakeholders to gain insights into wave conditions in this vast and dynamic coastal region while overcoming the limitations of traditional data collection methods.

Establishing the main goals of comparing ERA5 with CMEMS hindcast wave data is crucial to before beginning this investigation. The main goals of this comparison are as follows:

Evaluation of Data Applicability: The comparison aims to evaluate the applicability of ERA5 and CMEMS hindcast data for precisely describing wave characteristics off West Africa.

Identification of Discrepancies: This goal involves identifying any differences or discrepancies between the two datasets in order to assess the consistency and reliability of each.

Improved Data Utilization: By contrasting these datasets, it promotes better data utilization across various industries, including coastal engineering, environmental monitoring, and maritime navigation.

Research Contribution: By improving the understanding of wave climate dynamics of wave climate, this comparison advances the fields of marine science and climate research as a whole.

Data

The data used in this study includes secondary datasets from ERA5, CMENS reanalysis, satellite observations, and buoy measurements. ERA5 and CMENS are reanalysis datasets that provide global climate and wave data, offering detailed insights into atmospheric and oceanic conditions. The HY-2B and HY-2C satellite data, which are independent from the wave models used in the reanalysis, offer valuable validation by measuring wave height and other sea state parameters. Additionally, buoy data, such as those from the Akpo buoy off the coast of Nigeria, provide localized, in-situ wave measurements. These secondary data sources collectively enhance the robustness of the wave condition analysis for West Africa.

ERA5 Hindcast

ERA5, short for ECMWF Reanalysis 5, is a high-resolution global atmospheric and oceanic reanalysis dataset produced by the European Centre for Medium-Range Weather Forecasts (ECMWF). ERA5 data is acquired by assimilating a wide range of observational data, including satellite information, into advanced numerical models. This process combines the strengths of both observational data and modelling to create a comprehensive dataset of atmospheric and oceanic conditions, making it a valuable resource for weather forecasting, climate research, and various other applications. This dataset provides comprehensive historical records of meteorological and oceanographic parameters dating back to 1950 (Munoz Sabater, 2019).

The ERA5 dataset consists of wave parameters such as significant wave height, wave period, and wave direction. The spatial resolution and temporal resolution were 0.5º (~50 km) for any grid point and 1 hour, respectively.

The temporal resolution was interpolated to 3 hours to match the temporal resolution of that of CMENS.

CMEMS Hindcast

CMEMS, the Copernicus Marine Environment Monitoring Service, provides hindcast model data specifically focused on oceanographic parameters. CMEMS data is acquired through a combination of satellite observations, in situ measurements, and numerical modelling. This multi-faceted approach ensures the availability of high-quality and comprehensive oceanographic data for various scientific, operational, and policy-related purposes. The global wave reanalysis from previous sea states since 1993 is described in the CMENS dataset. In the GLO-HR MFC, this product is also referred to as WAVERYS in order to correspond with other global multi-year goods such as GLORYS, BIORYS, etc. The MFWAM model, a third-generation wave model that computes the wave spectrum, that is, the distribution of sea state energy in frequency and direction on an uneven grid of 1/5°, is the foundation of WAVERYS. The significant wave height (Hs) and average wave period, two average wave variables obtained from this wave spectrum, are presented on a standard 1/5° grid with a 3h time step. Oceanic currents from the GLORYS12 physical ocean reanalysis are incorporated into WAVERYS, which also incorporates considerable wave height observed from past altimetry

missions and directed wave spectra from Sentinel 1 SAR starting in 2017 (Law-Chune et. al, 2021).

The CMENS dataset consists of wave parameters like significant wave height (Hs), wave period, wave direction, etc. The spatial resolution for the dataset was 0.2° (~ 20 km) for the period of 1993 to 2020 and 0.083° (~ 8 km) for the period of 2021 to 2022 for any grid point selected and its temporal resolution was 3 hours.

Satellite: HY-2B and HY-2C

For this study, significant wave height, Hs from the satellite (HY-2B and HY-2C) was used. HY-2B and HY-2C is a near-real-time mono-mission satellite-based along-track significant wave height (Hs), thus is a timely collection and transmission of significant wave height data obtained from the HY-2B and HY-2C satellite mission as it travels along its orbital path. Calibrated on in-situ buoy measurements and an along-track filter is applied to reduce the measurement noise. The along-track resolution of altimeter data is at approximately 7km. Significant wave height from January 2021 to December 2022 was the data used for the comparison.

The two wave models (ECWAM for ERA5 and MFWAM for CMENS) already assimilate the significant wave height of a number of satellites as seen in Figure 3 except for the satellites Hai Yang 2B (HY-2B) and Hai Yang 2C (HY-2C).

For the validation of data from wave models, it is common and preferable to use only independent data, i.e. data that have not been used in the assimilation process. HY-2B and HY-2C satellites are specifically chosen

because they are the only satellites whose data are available and not used in the data assimilation process by the two Wave models.

During the first week of August 2021, Figure 6 shows a significant wave height track from Hai Yang 2B and Hai Yang 2C.

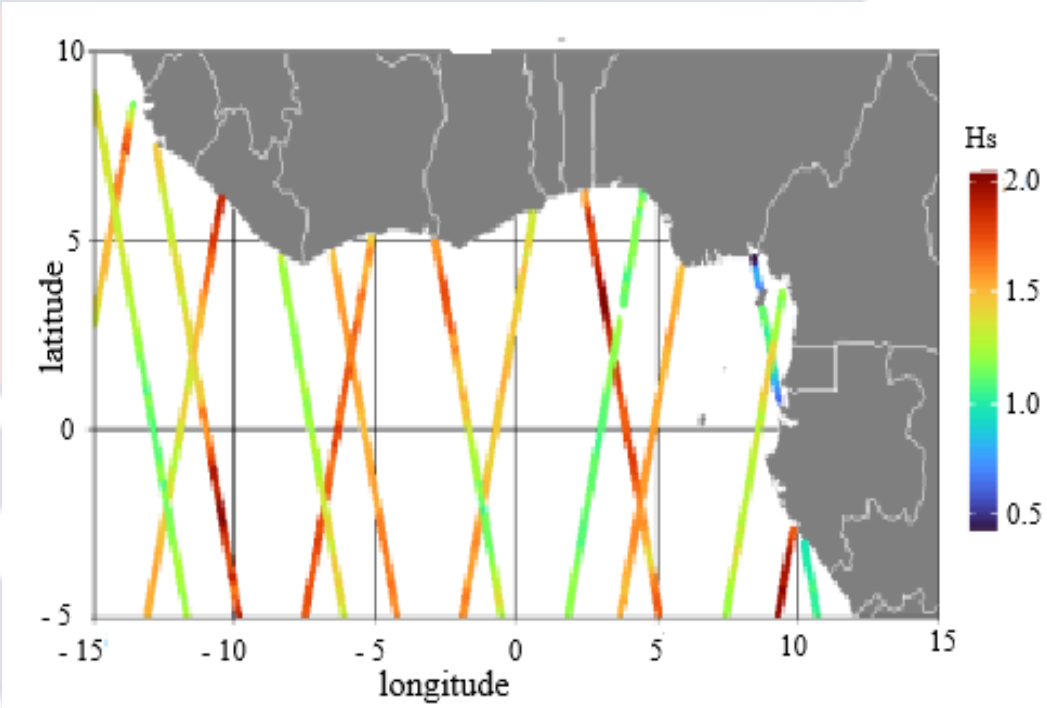

Figure 6: Significant wave height (in meter) track from Hai Yang 2B and Hai Yang 2C during the first week of August 2021

Buoy Data

The buoy data came from AKPO oil platform, anchored in the deep water of Nigeria. Its geographical position(coordinates) was longitude = 6.8224 and latitude = 3.1398.

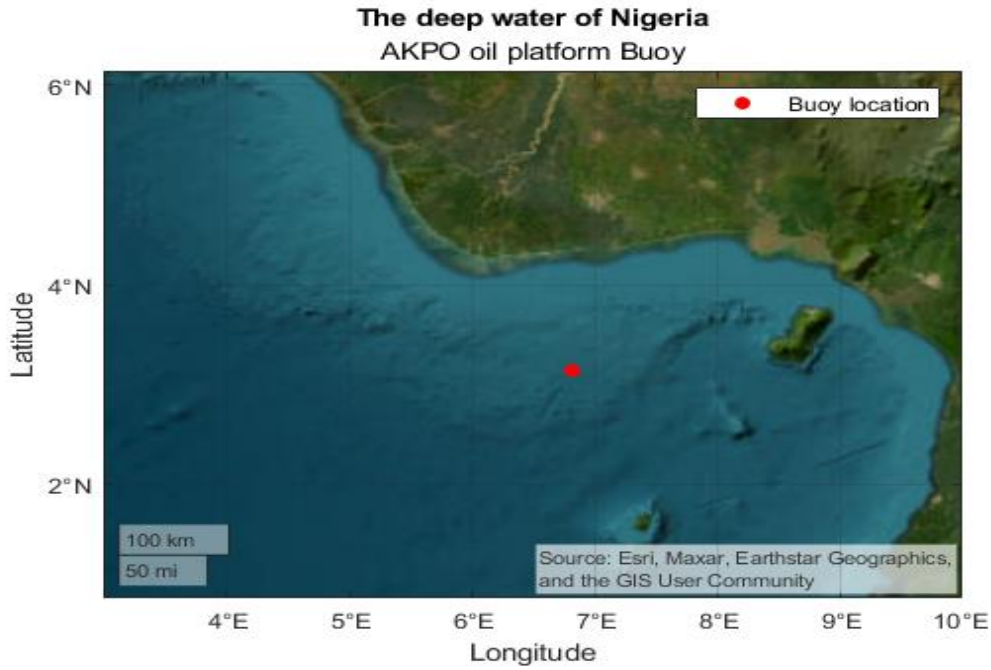

Figure 7: Position of the AKPO oil platform Buoy in the deep water of Nigeria.

Satellite image depicting where the buoy was mounted is presented in Figure 7. The AKPO oil platform installed this buoy in order to monitor the wave conditions in the area around their pipelines and determine what steps to take in the event that unfavourable wave conditions develop.

The parameters measured by this buoy include significant wave height, wave period, wave direction, etc. The temporal resolution of this buoy is 1 hour. Significant wave height from May 2003 to April 2004 was the data used for the comparison.

Data Pre-processing

The comparative analysis was focused on the significant wave height, Hs. The HY-2B and HY-2C satellites only provide Hs, and for the buoy, the other sea state parameters were not available. The acquired data for the

comparison was pre-processed to a temporal resolution of 3-hour intervals. The Hs from the HY-2Ba and HY-2C and Hs from ERA5/ CMENS are mapped by keeping the model grid containing the altimeter footprint. The buoy location, geographical coordinates of latitude 6.224 and longitude 3.1398 were selected and mapped and its significant wave height, Hs was acquired. The grid point of this coordinate for both ERA5 and CMENS significant wave height, Hs was also mapped.

A scatter plot of Hs from reference (satellite and buoy) against Hs from ERA5 and CMENS with regression lines are plotted. A quantile-quantile plot (QQplot) of Hs from reference (satellite and buoy) against Hs from ERA5 and CMENS are also plotted.

Mean Bias, Relative Error (RE), Root Mean Square Error (RMSE), Scatter Index (SI), Correlation Coefficient were evaluated.

Chapter Summary

This chapter presents the methodology used to compare wave conditions in West Africa based on ERA5 and CMEMS reanalysis datasets. It explains the data sources, including the reanalysis datasets and reference data from buoy and satellite observations, and the process of validating these datasets. The chapter outlines the statistical tools and techniques used for data comparison and analysis, focusing on temporal and spatial trends in wave climate. Additionally, it describes the methods for assessing wave metrics such as significant wave height, wave period, and direction. This methodology serves as the foundation for estimating the wave climate and identifying the best-performing dataset for

long-term wave analysis in the region. It also unfolds the methods employed in estimating the extreme wave events of this region.

CHAPTER FOUR

RESULTS AND DISCUSSION

Introduction

This chapter presents the results and discussions on the comparison of wave conditions in West Africa using ERA5 and CMEMS reanalysis datasets. It provides detailed findings on the performance of both datasets in capturing key wave climate metrics such as significant wave height, wave period, and direction. The chapter includes a comparison of these results with reference data from buoy and satellite observations, highlighting the accuracy and reliability of each reanalysis dataset. Additionally, the discussion explores the implications of the results for wave climate estimation in the region, identifying trends, patterns, and potential discrepancies between the datasets. This analysis is crucial for selecting the most suitable dataset for long-term wave climate estimation in West Africa.

Validation between CMENS and ERA5 Reanalysis Dataset

This section discusses the results on the analysis for comparing ERA5 and CMENS.

Comparison between ERA5 and CMENS Hs based on Satellite Hs Data

A scatter plot of **(a)** Hs of CMENS against Hs of HY-2B/HY-2C in meters (m) with linear regression line and **(b)** Hs of ERA5 against Hs of HY-2B/HY-2C in meters (m) with linear regression line is presented in Figure 8. The points are clustered around the linear regression line for both graphs. Even though both graph (**a**) and (**b**) show a strong relationship to the Hs of HY-

2B/HY-2C but the linear regression line for CMENS is closer to the reference line *(y = x)* than for ERA5, indicating that, the Hs of CMENS is closer to the altimeter observations.

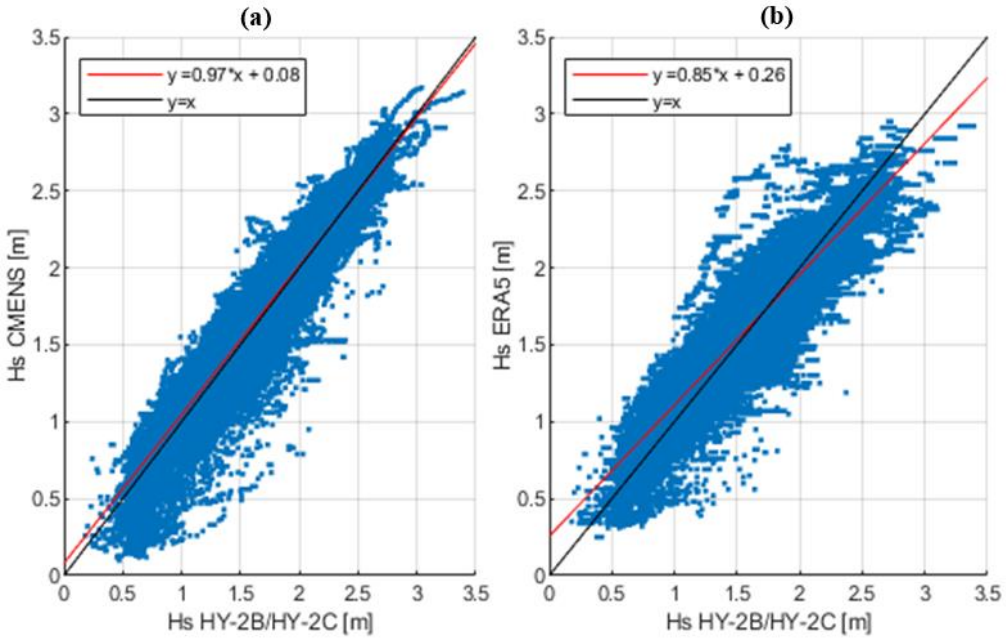

Figure 8: A scatter plot of Hs of (a) CMENS and (b) ERA5 against Hs of HY-2B/HY-2C with regression line.

A plot of Hs quantiles of CMEMS and ERA5 against the Hs quantiles of HY-2B/HY-2C is presented in Figure 9. Both the CMENS and the ERA5 followed the line of equality in spite of the little deviation at the tails of the graph (Hs < 0.5 m). It can also observe that, the quantile of ERA5 deviates at Hs > 2.5 m whiles that of CMENS deviates at Hs > 3.2 m. The Hs of CMENS is in line with HY-2B/HY-2C.

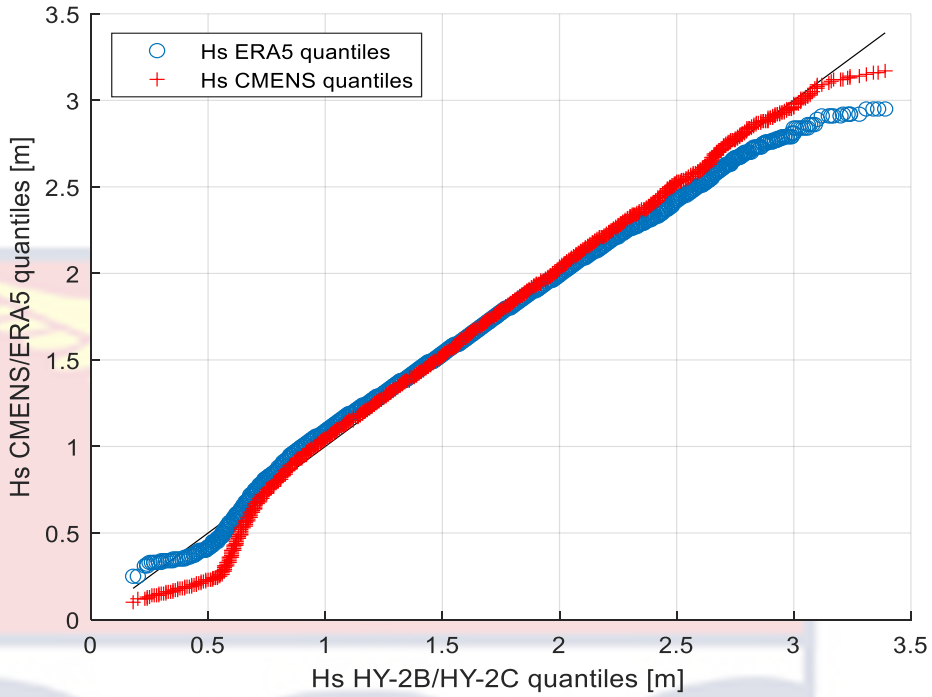

Figure 9: A quantile-quantile plot of Hs of ERA5/CMENS against Hs of HY-2B/HY-2C

The scores in Table 1 confirm the results of the graphical analysis. Both CMENS and ERA5 display low biases and the scatter indexes remain low. This shows that there is a good agreement between Hs from these two dataset and altimeter observations. Between the Hs from CMENS and that from ERA5, the former shows the best scores (smallest bias, SI, RE and greater correlation coefficient). We can conclude that the Hs from CMENS best matches the Hs from the HY-2B/HY-2C satellites as compared to ERA5.

Table 1: Scores for qualitative analysis between Hs of HY-2B/HY-2C against Hs of CMENS/ERA5

Scores	Hs of HY-2B/HY-2C against Hs of CMENS	Hs of HY-2B/HY-2C against Hs of ERA5
Mean Bias (m)	0.03	0.04
Relative Error, RE	6.04	8.37
Root Mean Square Error, RMSE (m)	0.11	0.14
Scatter Index, SI (%)	7.49	10.05
Correlation Coefficient, CR	0.96	0.92
Data size, N	256,430 observations	

(Source: Researcher, 2024)

Analysis for Comparing ERA5 and CMENS Hs based on Buoy's Data

Time series plot of Hs of buoy, Hs of CMENS and Hs of ERA5 is presented in Figure 10. It depicts the Hs recorded by the buoy, CMENS and ERA5 at an interval of one hour for a duration of one year.

It can be seen that, both Hs of CMENS and ERA5 are in line with that of the Hs of buoy.

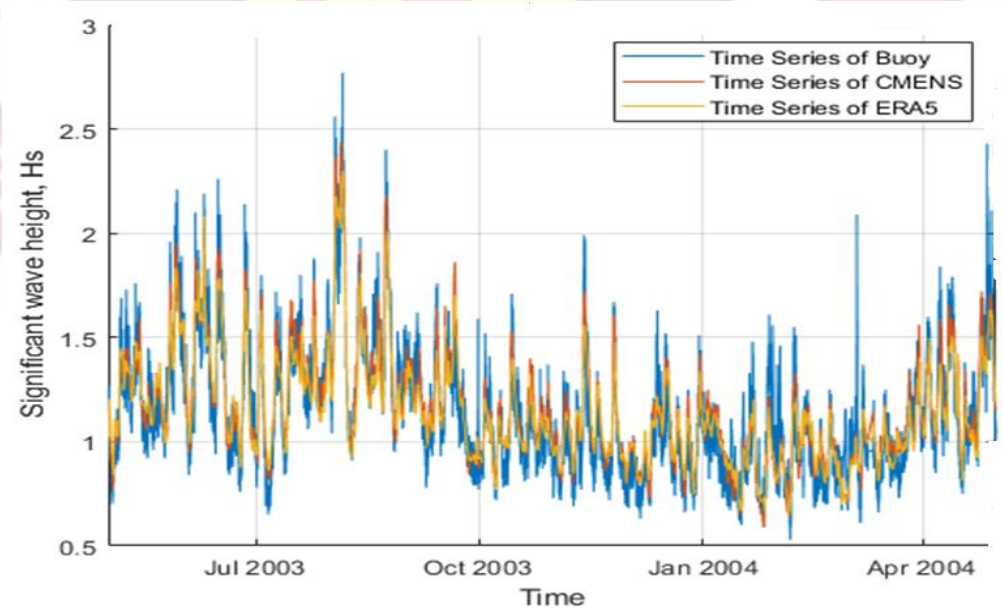

Figure 10: A time series plot of Hs of buoy, Hs of CMENS and Hs of ERA between May 2003 and April 2004

A scatter plot of **(a)** Hs of CMENS against Hs of buoy in meters (m) with linear regression line and **(b)** Hs of ERA5 against Hs of buoy in meters (m) with linear regression line is seen in Figure 11. The points are clustered around the linear regression line for both graphs. Both Hs of CMENS and Hs of ERA5 matches well with the Hs of buoy. Even though both graph **(a)** and **(b)** show a strong relationship to the Hs of buoy but the linear regression line for CMENS is closer to the equality line than for ERA5, indicating that the Hs of MENS is closer to the observations.

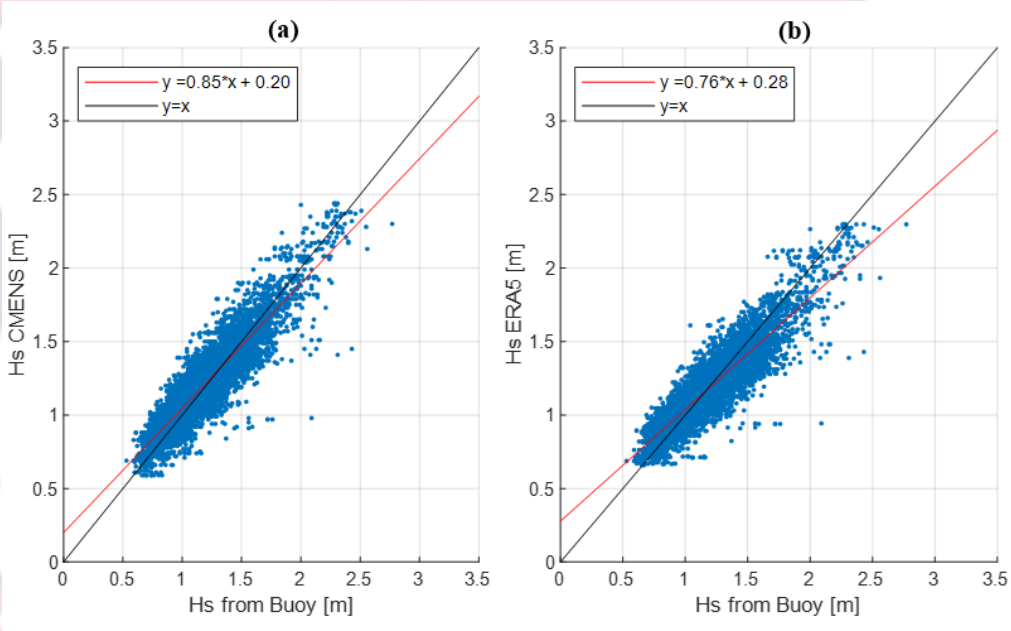

Figure 11: A scatter plot of Hs of (a) CMENS and (b) ERA5 against Hs of Buoy with regression line

From Figure 12, Hs quantiles of CMEMS and ERA5 were plotted against Hs quantiles of buoy. Both the CMENS and the ERA5 followed the line of equality in spite of the little deviation between the region of Hs > 0.7 m and Hs < 0.9 m. It can also be observed that, for high values of Hs > 1.7 m, ERA5 deviated from the buoy results whiles that of CMENS deviated at Hs > 2.4 m.

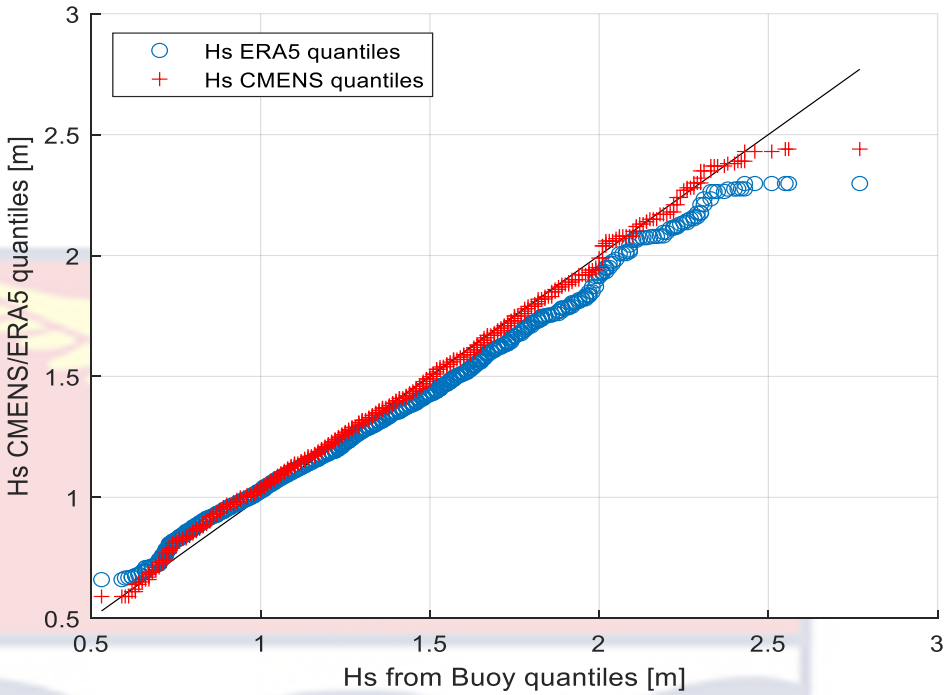

Figure 12: A quantile-quantile plot of Hs of buoy against Hs of ERA5/CMENS

Confirming the findings of the graphical analysis are the scores listed in Table 2. While the dispersion indices continue to be low, CMENS and ERA5 both exhibit modest biases. This demonstrates that there is good agreement between the Hs from these two datasets and the buoy measurements. The largest scores (smallest bias, SI, RE, and better correlation coefficient) are found between the Hs from CMENS and that from ERA5. Based on comparison with ERA5, we may conclude that the Hs from CMENS best matches the Hs from the buoy.

Table 2: Scores for qualitative analysis between Hs of Buoy against Hs of CMENS/ERA5

Scores	Hs of Buoy against Hs of CMENS	Hs of Buoy against Hs of ERA5
Mean Bias (m)	0.023	0.004
Relative Error	8.786	8.883
Root Mean Square Error, RMSE (m)	0.125	0.129
Scatter Index, SI (%)	10.936	11.276
Correlation Coefficient, CR	0.913	0.906
Data size, N	8,500 observations	

Source: Researcher, 2023

Validation Conclusion

In this study, a comparison of ERA5 and CMENS data against HY-2B/HY-2C and wave buoy was made. Focusing on the significant wave height, Hs, even if the two reanalysis are broadly representative of the sea states off West Africa, it seems that the HY-2B/HY-2C is better described by the Hs of CMENS. The higher correlation coefficient, lower mean bias, lower root mean square error, lower relative error, and lower scatter index indicate that, CMENS is more accurate and closer to the actual values compared to the Hs of ERA5. Comparison of the Hs of CMENS and ERA5 with the Hs of buoy led to the same results.

From the above propositions, it can be concluded that, West Africa wave conditions is best described by CMENS dataset. This can be explained by the fact that CMENS data has better spatial resolution and also assimilates data from more satellites than data than ERA5.

Wave Climate off West Africa based on CMENS Hindcast Data

This section explores the task of determining West Africa's wave climate, a region distinguished by its distinct marine environment. First, we examine the concept of a global sea condition and its two main divisions: swell and wind sea. Understanding the dynamics of waves in the coastal regions of West Africa requires knowledge of these elements. This section will address conditions including significant wave height (Hs), wave period (Tp), and wave direction. Next, we focus on the geographic locations of Ivory Coast (longitude = -3.6, latitude = 4.4), Ghana (longitude = 0.4, latitude = 5.2), Togo/Benin (longitude = 1.4, latitude = 5.2), and Nigeria (longitude = 5.2, latitude = 3.4).

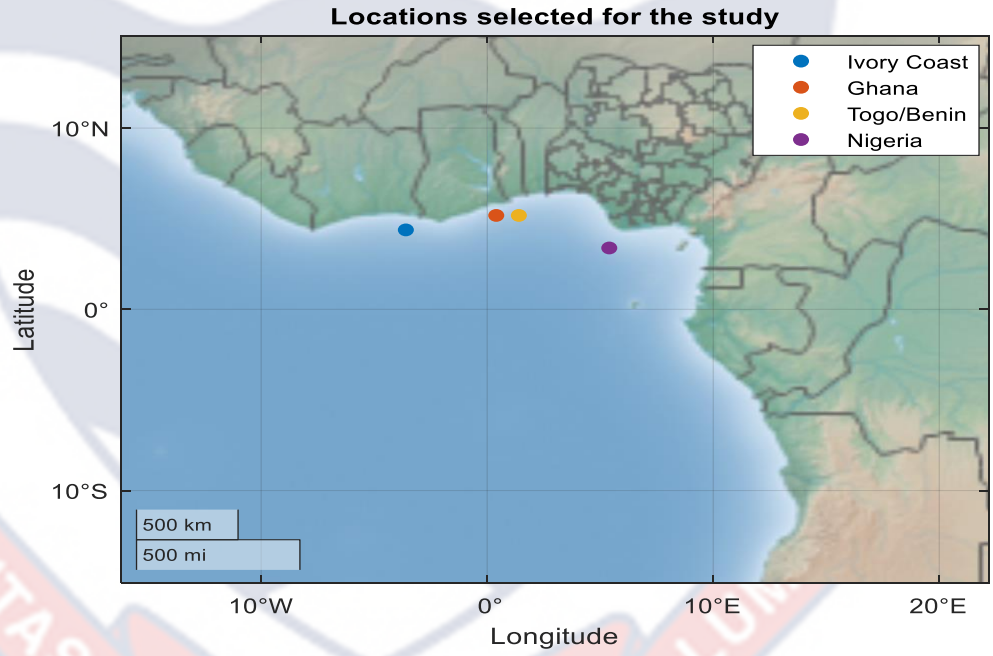

Figure 13: Map of the study domain and selected locations

A color terrain map indicating the regions where this study was focused is seen in Figure 13. These nations were deliberately selected to symbolize West Africa because of their advantageous locations around the Gulf of Guinea. Throughout the chapter, we examine why these particular nations are useful

proxies for understanding the wave climate of the region, highlighting the variety of their coastlines and climates that make them essential for research and decision-making concerning environmental management, coastal infrastructure, and maritime safety in this vital and dynamic coastal region. This chapter also analyzes the seasonal and inter-annual variability of sea state conditions off West Africa.

Global Sea State: Combination of Wind Sea and Swell

In this section, the wave climate is estimated based on the combination of wind sea and swell.

Distribution of Significant Wave Height

A histogram with a density curve depicting the global significant wave height, Hs for the selected regions is shown in Figure 14. The analysis for the regions of Ivory Coast, Ghana, Togo/Benin, and Nigeria is shown in Figure 14a, 14b, 14c, and 14d, respectively.

For Ivory Coast, the minimum significant wave height was estimated to be 0.57 m, and that of the maximum Hs value was determined to be 3.18 m, with a mode of 1.22 m. The density distribution plot shows that, 50% of Hs is less than 1.32 m and 10% of Hs is greater than 1.80 m.

For Ghana, the minimum and the maximum significant wave heights were 0.57 m and 3.04 m, respectively, with 1.18 m as the mode. The plot also shows that, 50% of Hs was less than 1.29 m while 10% of Hs was greater than 1.73 m.

In the case of Togo/Benin, the significant wave height for this region ranges from 0.54 m to 3.22 m, with 1.26 m being the mode. Additionally, the

histogram shows that the average Hs has risen over time. The density distribution figure shows that the 50% quantile of Hs was estimated to be 1.30 m, and the 90% quantile was estimated to be 1.76 m.

For Nigeria, the minimum and maximum significant wave heights were estimated to be 0.52 m and 3.04 m, respectively, with 1.15 m as the mode. The density distribution figure shows that 50% of Hs was estimated to be less than 1.26 m, and 10% of Hs was estimated to be greater than 1.77 m.

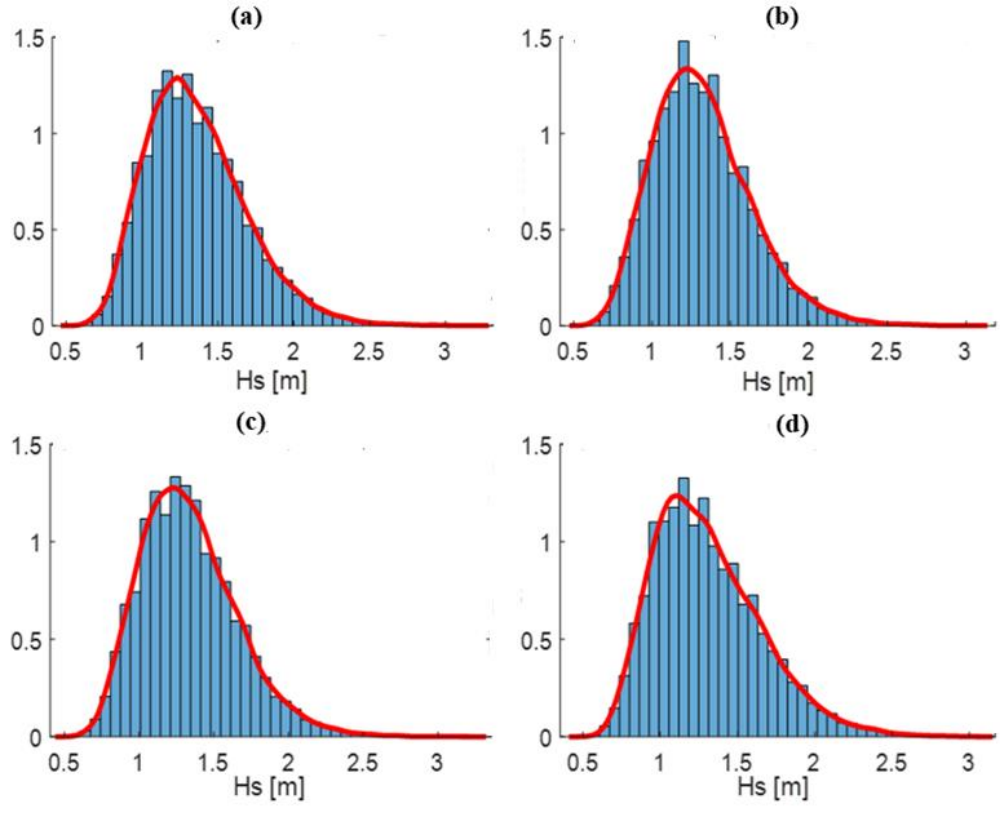

Figure 14: Histogram with density curve of Hs for (a) Ivory Coast, (b) Ghana, (c) Togo/Benin and (d) Nigeria

Distribution of Wave Peak Period, Tp

A histogram with a density curve was plotted to depict the wave peak period, Tp for the selected regions.The analysis for the regions of Ivory Coast, Ghana,

Togo/Benin, and Nigeria is shown in Figure 15a, 15b, 15c, and 15d, respectively.

For Ivory Coast, the wave period, Tp was between 4.09 s, and 24.03 s with the mode period, Tp as 13.08 s. From the density distribution plot, 50% of Tp was determined to be less than 12.49 s and 10% of Tp was determined to be greater than 15.75 s.

For Ghana, the minimum and maximum wave period, Tp were determined to be 3.83 s and 25.39 s, respectively with the mode period, Tp as 13.04 s. From the density distribution plot, 50% of Tp was determined to be less than 12.75 s, and 10% of Tp was determined to be greater than 15.84 s.

For Togo/Benin, the wave period, Tp was between 4.06 s and 25.61 s with 13.03 s as the mode. The density distribution plot shows that, the 50% quantile of the wave period, Tp was estimated to be 12.80 s and the 90% quantile of Tp was estimated to be 15.89 s.

In the case of Nigeria, the wave period, Tp was between 3.59 s and 25.06 s (minimum and maximum wave period, Tp respectively) with 13.23 s as the mode. The density distribution plot shows that 50% Tp was estimated to be less than 12.97 s and the 90% of Tp was estimated to be less than 15.98 s.

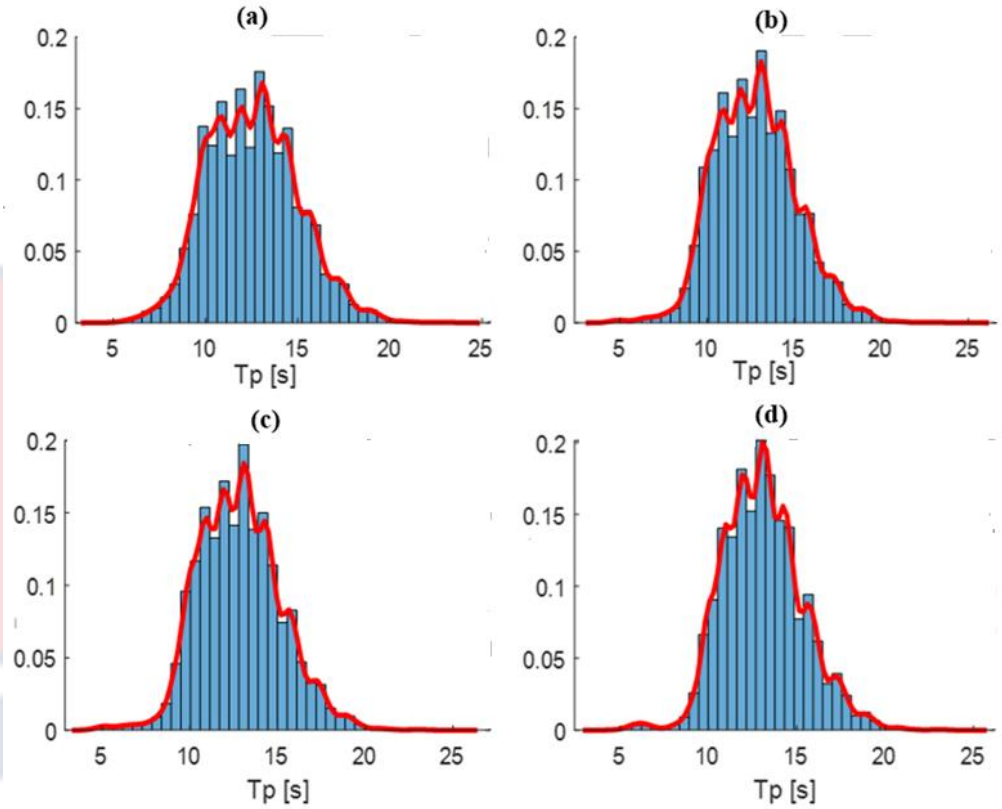

Figure 15: Histogram with density curve of Tp for (a) Ivory Coast, (b) Ghana, (c) Togo/Benin and (d) Nigeria

Mean Wave Direction

The direction of the waves is analyzed from directional roses.

Wave directions for the regions Ivory Coast, Ghana, Togo/Benin and Nigeria are presented in Figure 16a, 16b, 16c and 16d respectively.

For Ivory Coast, the most common wave direction is from the south (S) with 38%, south (S) and southwest (SW) with 42%, and 20% of the wave coming from the south (S) and the southeast (SE) region.

In the case of Ghana, the waves of this region is from the south (S) and southwest (SW) with 75% and 25% of the wave coming from the south (S) region.

For Togo/Benin, the majority of wave direction of this region is from the south (S) and the southwest (SW), with 80% and 20% of the wave coming from the south (S) region, respectively.

For Nigeria, at this region, all the waves are coming from the southwest (SW) region.

These figures also show that, the wave direction appears to be independent of Hs values.

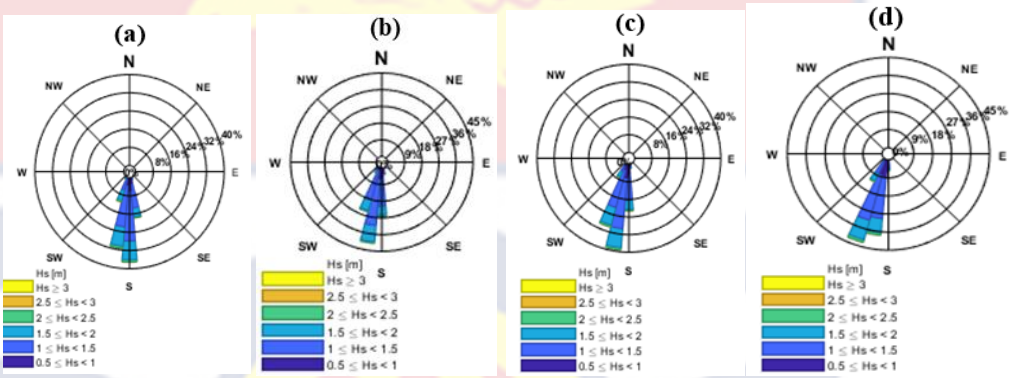

Figure 16: Directional rose of wave off: Ivory Coast (a), Ghana (b), Togo/Benin (c) and Nigeria (d)

Wave Climate based on Partitions: Wind Sea and Swell

Sea states are mostly composed of several superimposed wave systems, each with its own contribution to the total energy. For some coastal applications such as coastal defense design or erosion, one needs to estimate separately long-term statistics of wind sea (generated by local wind) and swell (generated by distant storms).

An example of a time series of Hs of swell (red), and wind sea (orange) and Hs of combined wind sea and swell between August 9, 2016 and October 9, 2016 of Ghana is shown in Figure 16. This period corresponds to the period during which the model simulated the maximum global Hs between 1993 – 2022 (3.04

m which occurred on September 4, 2016). This maximum of Hs is essentially the result of swells which Hs was 2.94 m, as the Hs of the wind sea is only 0.12 m. Overall, the significant wave heights of the swells are much higher than those of the wind sea.

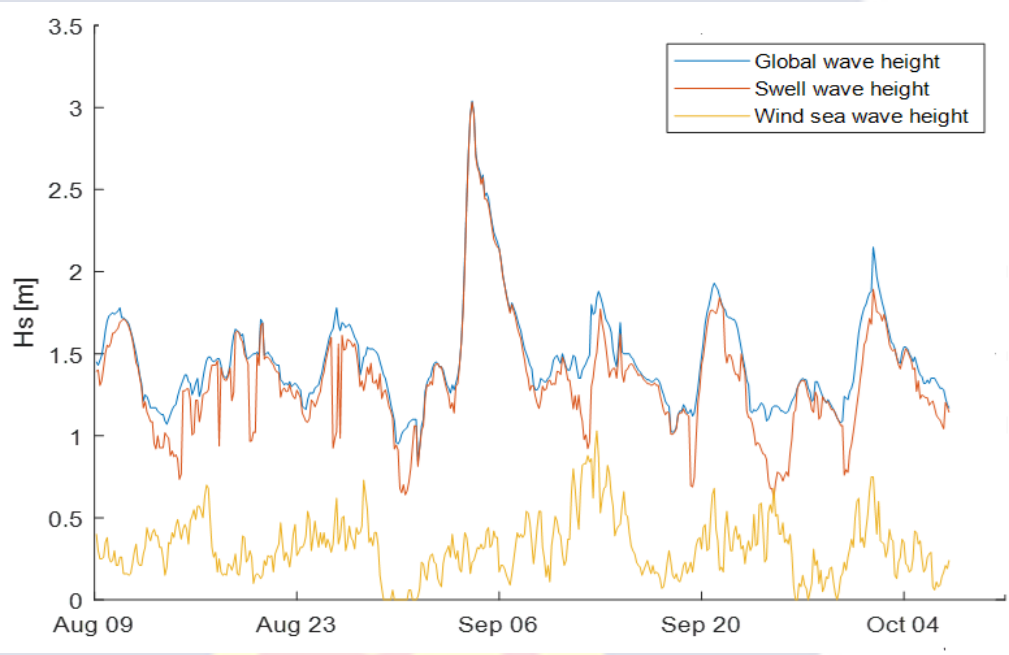

Figure 17: Example of time series of significant wave height of swell (red) and wind sea (orange) off Ghana between August 9, 2016 and October 9, 2016. The Hs of the combined wind sea and swell is also plotted (blue)

Analysis of the time series of the other three regions (Ivory Coast, Togo/Benin, and Nigeria) gave similar results. The results for these regions can be found in the appendix.

Contribution to the Total Energy of Wind Sea and Swell

A pie chart of the contribution to the total energy of sea state of wind sea and swell is shown in Figure 18 for the four regions. It is observed that the waves

of the West Africa region are dominated by swell. The proportion of swell to wind sea in these areas is 97.88% to 2.12% for Ivory Coast, 95.12% to 4.88% for Ghana, 95.18% to 2.82% for Togo/Benin and 97.66% to 2.34% for Nigeria.

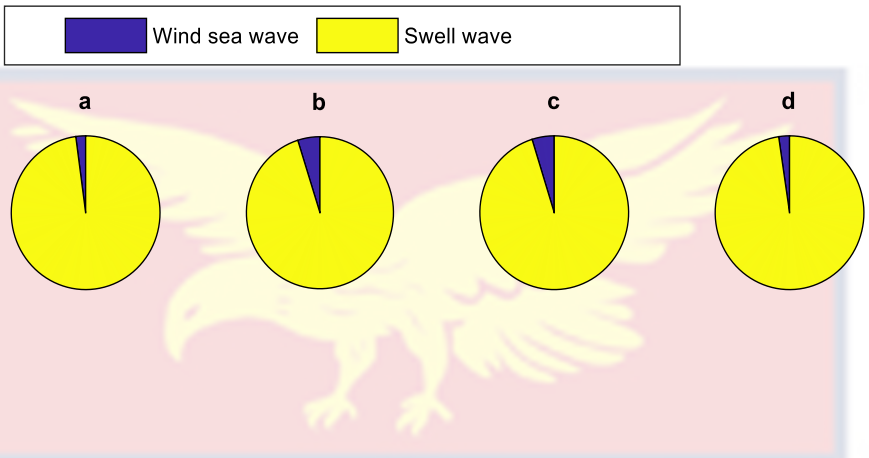

Figure 18: A pie chart depicting the proportion of Hs of wind sea and swell for (a) Ivory Coast, (b) Ghana, (c) Togo/Benin and (d) Nigeria

Distribution of Significant Wave Height of Wind Sea and Swell

A histogram with a density curve was plotted depicting the significant wave height, Hs of wind sea, and swell for the selected regions.

The Hs of wind sea and swell off Ghana were analyzed by plotting a histogram plot with a density curve.

According to Figure 19, the minimum Hs of wind sea and swell were 0.05 m and 0.26 m, respectively and the maximum Hs of wind sea and swell were determined to be 1.57 m and 3.03 m with 0.21 m as the mode of wind sea and 1.10 m as the mode of swell.

Also, 50% of Hs of wind sea were estimated to be less than 0.29 m and that of swell was 1.17m while 10% Hs of wind sea and swell were estimated to be greater than 0.5 9m and 1.66 m, respectively.

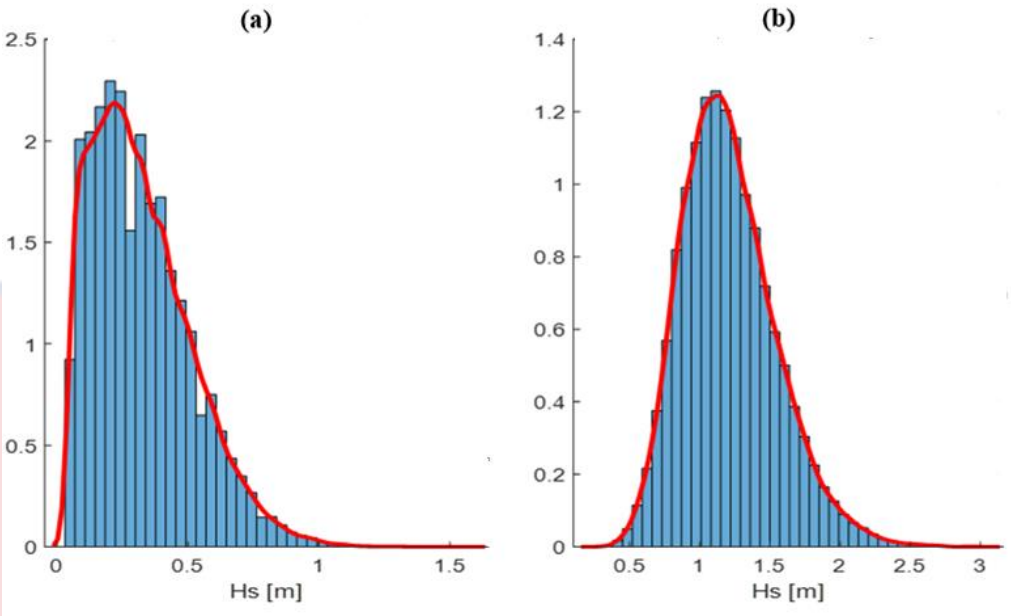

Figure 19: Histogram with density curve of Hs of **(a)** wind sea and **(b)** swell off Ghana

The same analysis was done for the other regions and the results are similar and can be seen in the appendix.

Direction of Wind Sea and Swell

The mean wave direction of the wind sea and swell were also analyzed. According to Figure 20a, 48% of wind sea are coming from west (W) and southwest (SW) and 35% are coming from south (S) and southwest (SW). Whereas figure 20b shows that, 60% of the swell are coming from south (S) and southwest (SW) and 40% are from south (S) and southeast (SE) region.

The swells observed in West Africa are mainly generated in the South Atlantic, between off the coast of Argentina or Cape Horn, and the Cape of Good Hope (Prevosto et al. (2013); Nerzic et al. (2007); Olagnon et al. (2014)). These swells are generated by repetitive storms which, following the general atmospheric circulation move from Cape Horn towards the Cape of Good Hope.

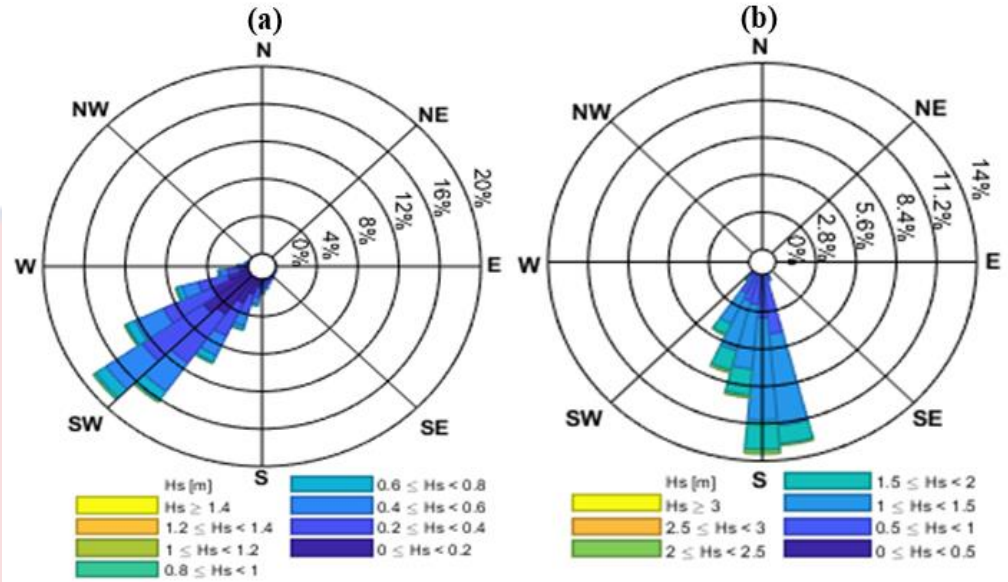

Figure 20: Directional rose for wind sea (a) and swell (b) off Ghana

Analysis for the other three locations gave similar results and can be seen in the appendix.

Seasonal Variability

Seasonal variability in the context of wave climate refers to the regular and predictable variations in ocean wave conditions that take place year-round in a particular location. These variations, which are usually linked to seasonal shifts, can significantly affect a range of maritime and coastal operations. Numerous elements, such as wind patterns, ocean currents, and meteorological conditions, can have an impact on the seasonal fluctuation of wave climate. Seasonal variability of the wave conditions for the entire West Africa region for the 30-year period (January 1993 to December 2022) was analyzed.

Analysis of Global Wave Parameters

Global Significant Wave Height

Analysis of the West Africa region of Hs was examined for the duration to see how the wave conditions vary with respect to seasonal changes. From Figure 20, the months of July and August, the global Hs is very high. Even at the coast of this region, Hs of 1.8 m in average is obtained in the month of August whereas for January and February, only 1.4 m is obtained in the same area.

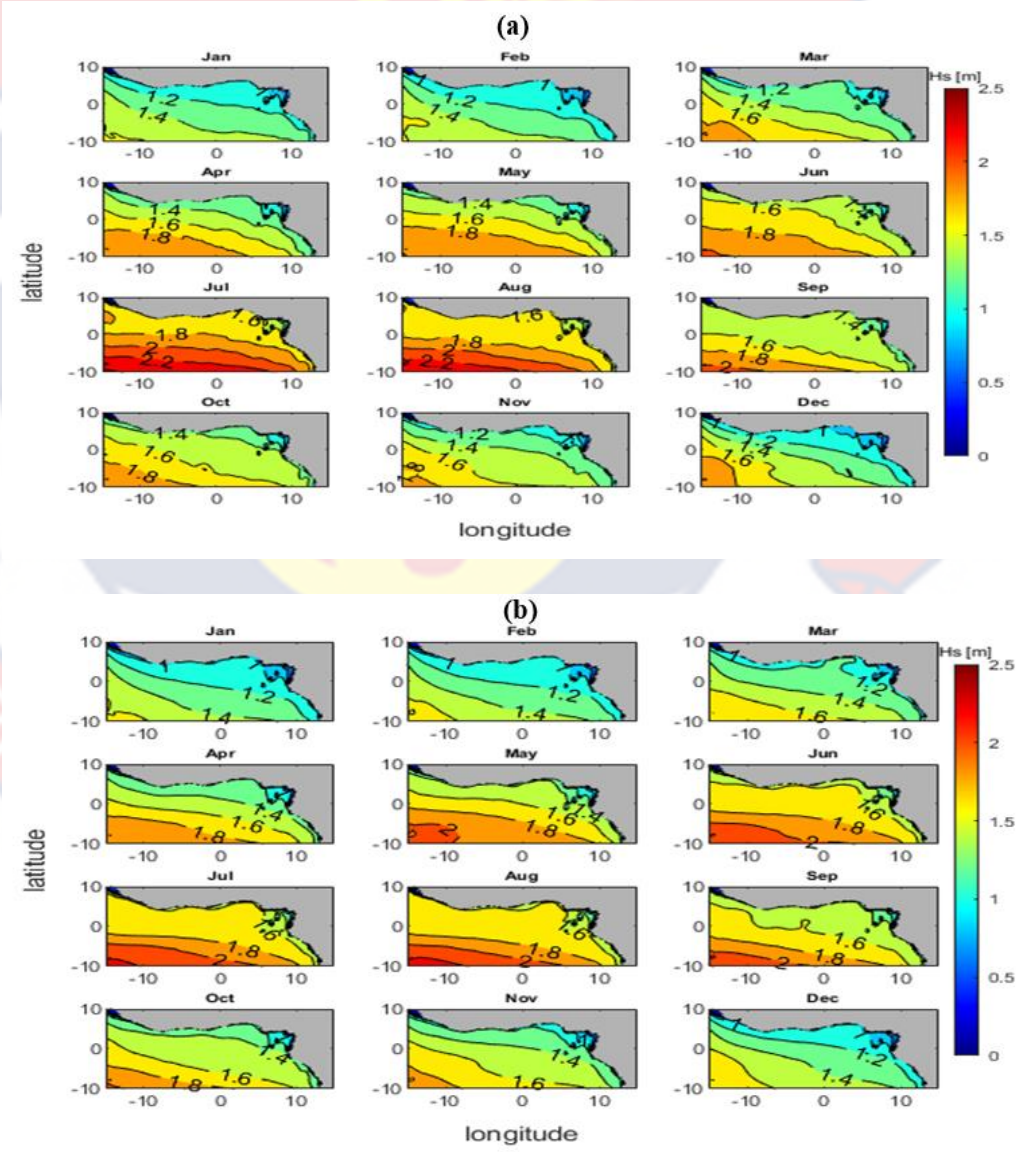

Figure 21: Maps of monthly average of Hs for the duration (a). 1993 to 2020

with a spatial resolution of ~20km and (b). 2021 to 2022 with a spatial resolution of ~8km

A box plot analysis of seasonal variations of global Hs with their mean curve for the four selected regions for the Duration of January 1993 to December 2022 is presented in Figure 22. Monthly box plots of global Hs with their mean curve were plotted to describe the season changes.

For Ghana, the minimum mean global Hs was determined to be 1.06 m which occurred in the month of January, and increased consistently till it reached the maximum mean global Hs, which was determined to be 1.66 m. The maximum global wave values were recorded in the months of June, July, and August and started decreasing consistently after the month of August.

The seasonal variation of Hs for the remaining locations yields a similar result to that of Ghana.

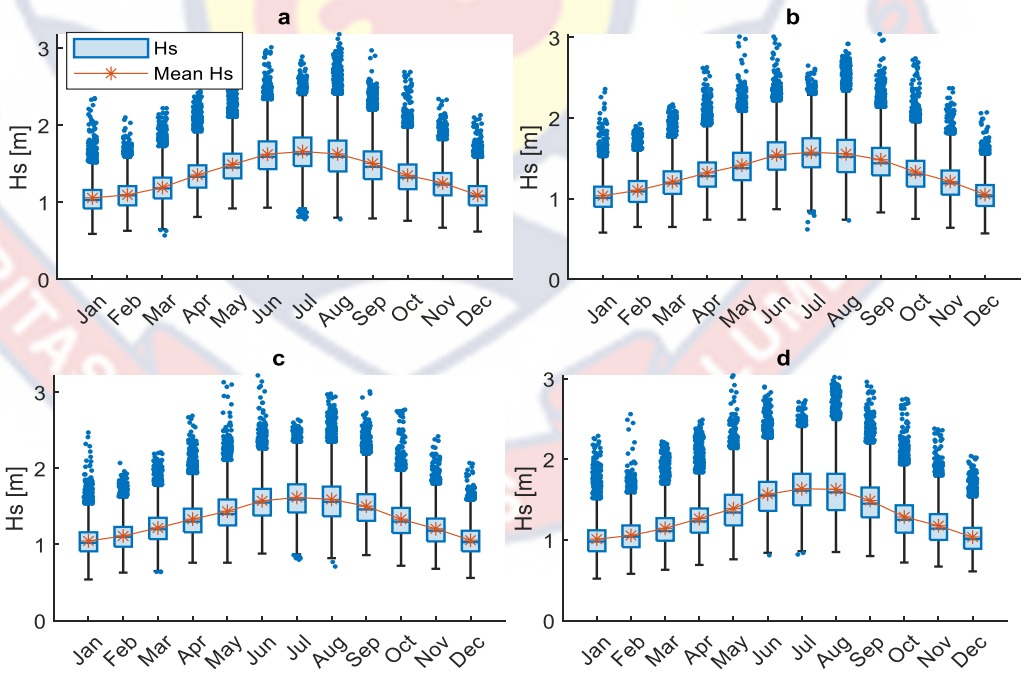

Figure 22: Box plot of seasonal variation of monthly mean global Hs of **(a)** Ivory Coast, **(b)** Ghana, **(c)** Togo/Benin and **(d)** Nigeria

From Figure 23, the directional rose of waves off Ghana according to seasons was presented.

The seasonal directional roses depict that the waves come from the same direction (south and southwest) whatever the season. Analysis of the other locations rendered similar results and can be found in the appendix.

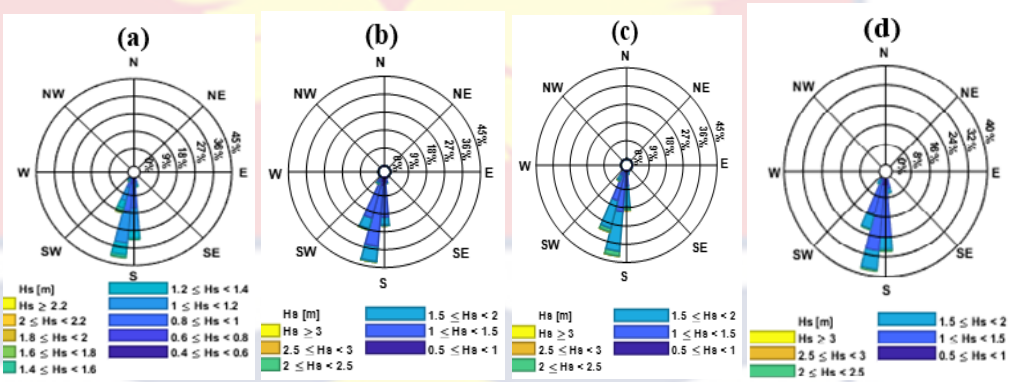

Figure 23: Directional roses of waves according to seasons: (a) December, January, and February, (b) March, April, and May, (c) June, July, and August and (d) September, October, and November

Global Wave Period

For the duration, an analysis of Tp of the entire West African region was conducted to understand how seasonal variations affect wave conditions.

A seasonal map of the global Tp covering the years 1993 –2022 is shown in Figure 24. It shows how seasonal variations affect the global Tp for the West Africa region. It is evident that the global Tp reaches an extremely high level during the months of July and August. Also, in the months of January, February and March, the global Tp low at the coast of the West Africa regions.

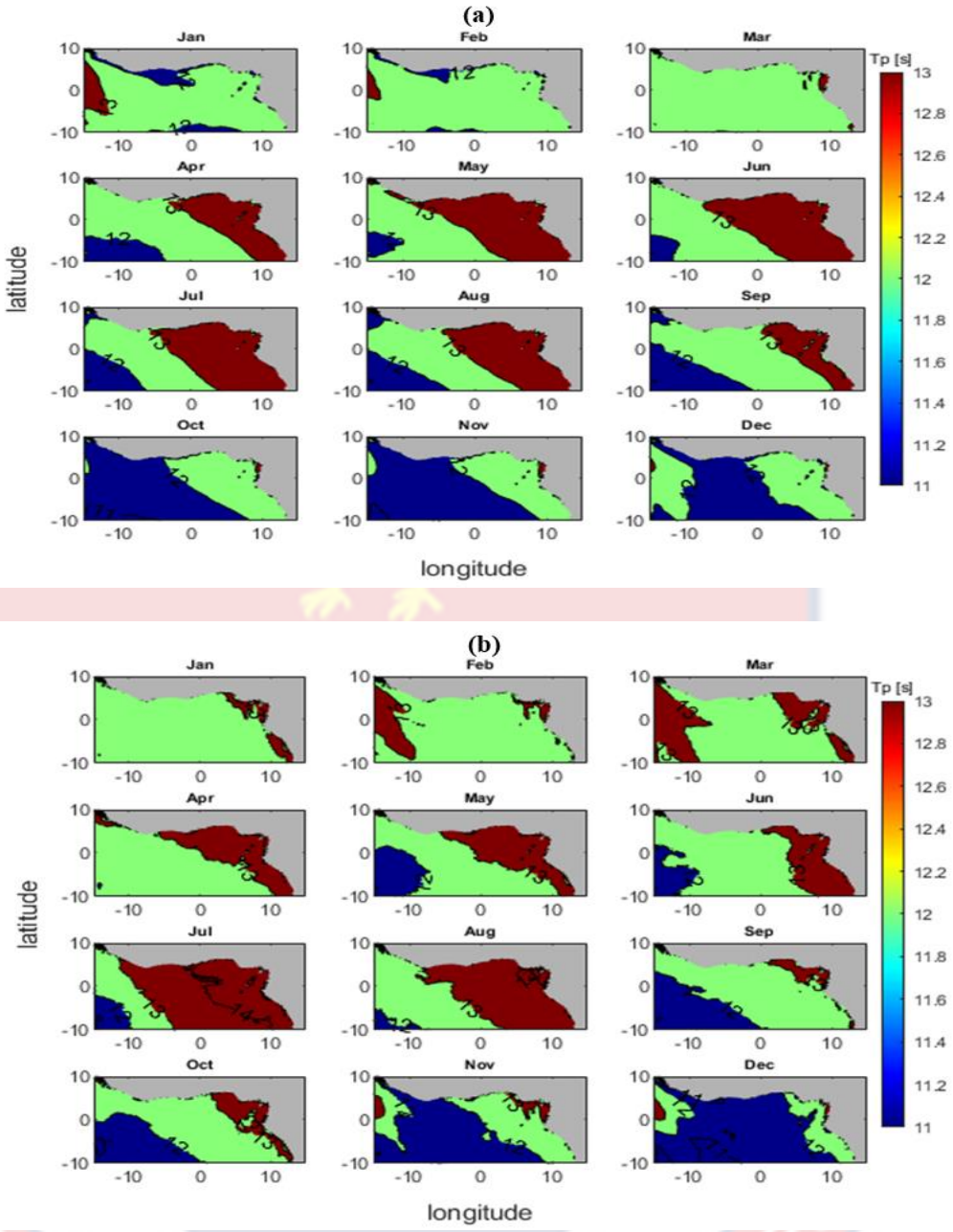

Figure 24: Maps of monthly average of Tp for the duration (a). 1993 to 2020 with a spatial resolution of ~20km and (b). 2021 to 2022 with a spatial resolution of ~8km

To further illustrate the seasonal variations, monthly box plots of the mean global Tp with their mean curve were created to see the distribution. Figure 25 shows how global Tp is distributed over the years.

For Ghana, the lowest mean global Tp value was determined to be 12.08 s which occurred in January, while the highest mean global Tp value was determined to be 13.53 s and occurred in July, as shown in Figure 25b. The other regions gave a similar result.

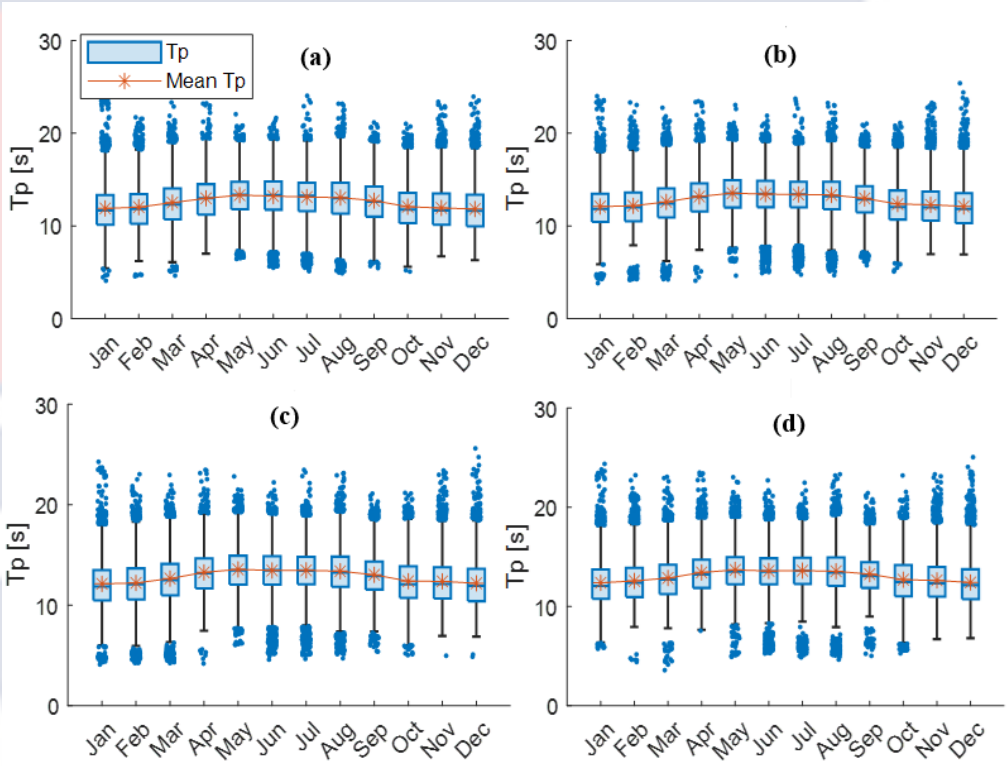

Figure 25: Box plot of seasonal variation of monthly mean global Tp of (a) Ivory Coast, (b) Ghana, (c) Togo/Benin and (d) Nigeria

Seasonal Variability of Significant Wave Height of Wind Sea and Swell

Seasonal variability analysis of the wave partitions (wind sea and swell) was also examined. This analysis was done to see the impact of wind sea and swell on the global wave.

Wind Sea Hs

Maps depicting the seasonal variation of the wind sea Hs for the entire West Africa region were analyzed to see how it contributes to the global wave height.

A map depicting the Hs of wind sea impact on global Hs for this region is shown in Figure 26.

The contribution of wind sea to the global sea state is small compared to swell off West Africa. Highest wind sea Hs occurred in the months of June, July, and August with Hs of 0.4 m even in the coastal regions of West Africa.

In the months of December, January, and February, the wind sea at the coastal regions is very low with Hs of 0.1 m in average.

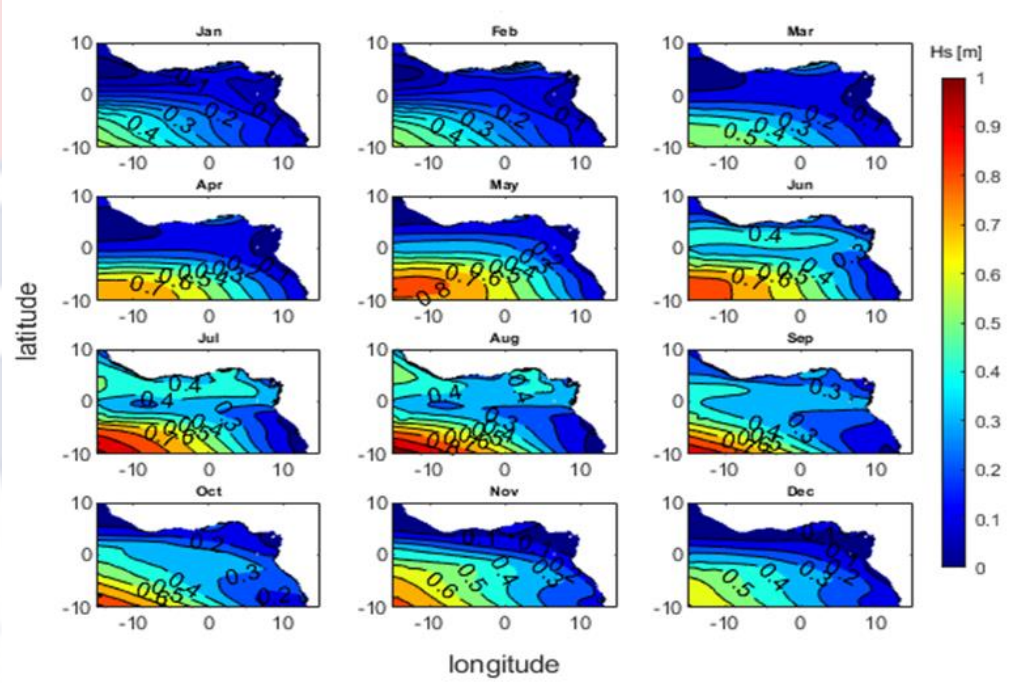

Figure 26: Maps of monthly average of wind sea Hs for the duration 1993 to 2021

To depict the seasonal variations in Ghana, monthly box plots of wind sea, and swell Hs with their mean curve were created.

The wind sea Hs exhibits seasonal modulation, as seen in Figure 27, with two yearly peaks-one in March and a bigger one in July and August. The peaks correspond to the extreme locations of the ITCZ, the passage of the ITCZ over the Bight of Benin coastline being associated with weaker winds

(Almar et. al., 2015). The analysis for the other locations (Figure 27a, Figure 27c and Figure 27d) gave similar results and can be found in the appendix.

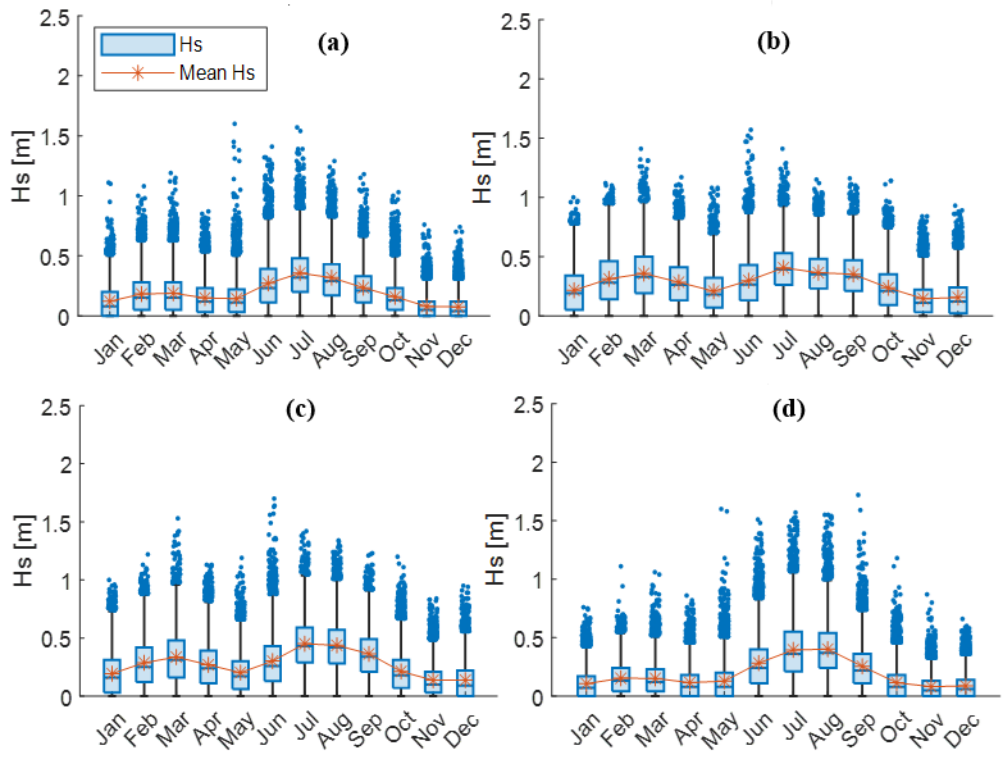

Figure 27: Monthly boxplot of mean Hs of wind sea Hs off (a) Ivory Coast, (b) Ghana, (c) Togo/Benin and (d) Nigeria

Swell Hs

According to Figure 28, the swell in the West African region is at its peak in the months of June, July, and August with average Hs of 1.4 m at the coasts. Indeed, during austral winter (June, July and August) winds are stronger in the South Atlantic, where swells reaching West Africa are generated. This explains the strong swells observed off West Africa during this season. In the months of December, January and February are the months where the lowest swell waves were estimated. The Hs of swell for these months were low as 0.6 m.

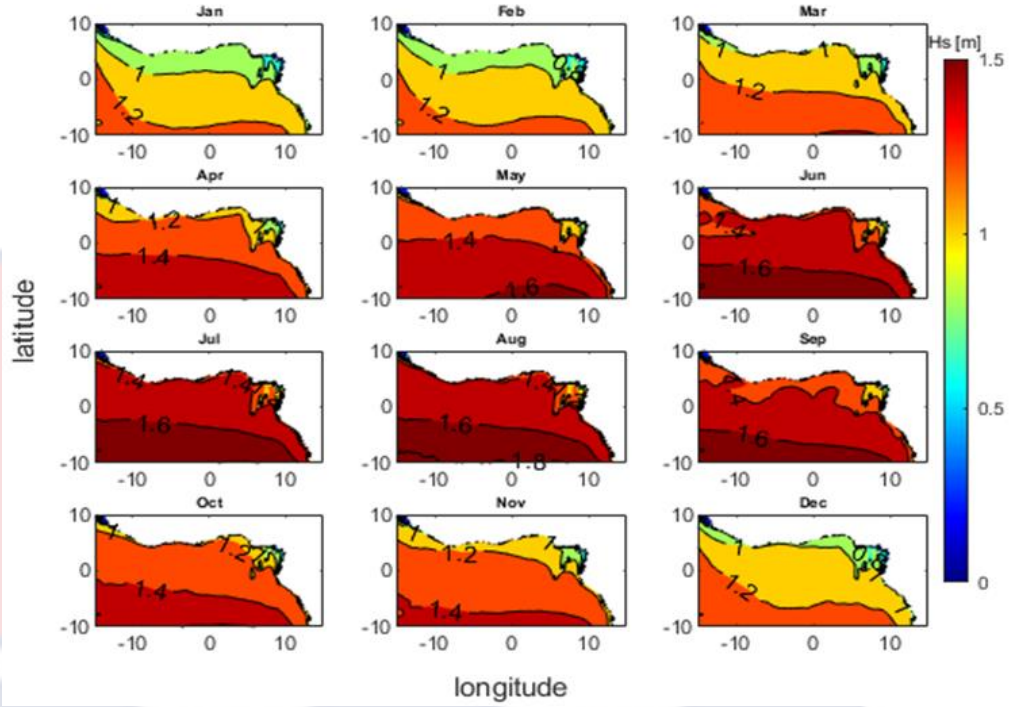

Figure 28: Map of monthly average of swell Hs for the duration 1993 to 2021

Monthly box plots of swell Hs with their mean curve were plotted to describe the seasonal changes in West Africa.

Based on the data presented in Figure 29b (Ghana), the minimum mean Hs of swell of 0.91 m, which happened in January. Subsequently, the mean swell wave height grew steadily until it reached the maximum value of 1.40 m. The highest Hs of swell were seen in June, July, and August; following August, they began to steadily decline. The analysis for the other locations (Figure 29a, Figure 29c, and Figure 29d) gave similar results and can be found in the appendix.

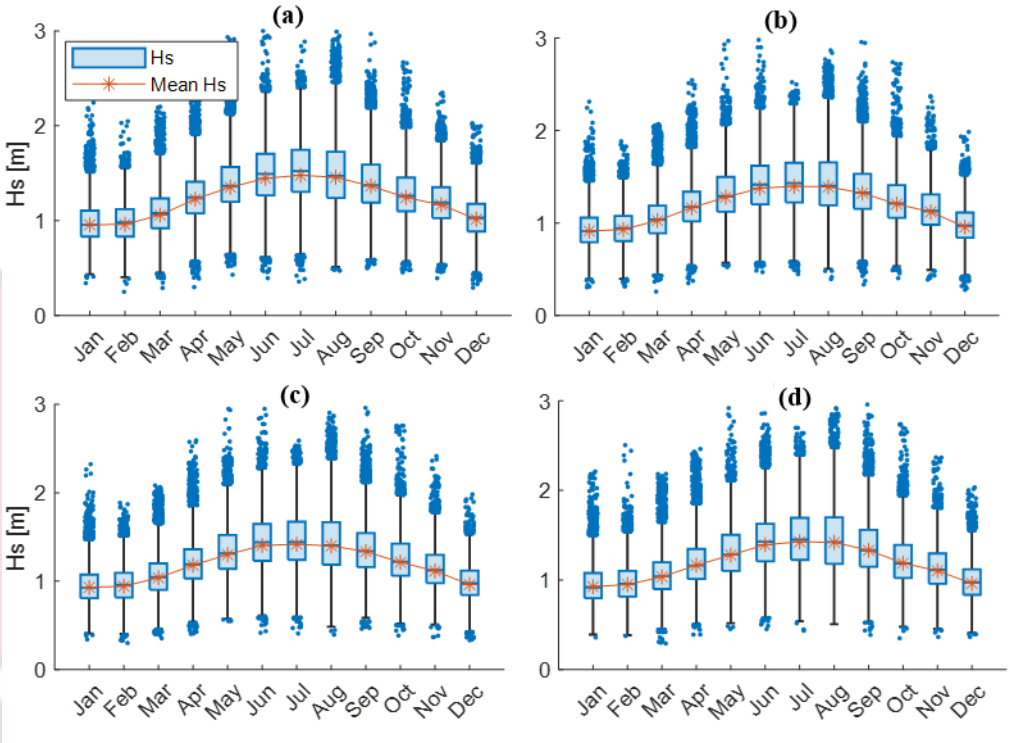

Figure 29: Box plot of seasonal variation of mean swell Hs of (a) Ivory Coast, (b) Ghana, (c) Togo/Benin and (d) Nigeria

Interannual Variability of Wave Condition in West Africa.

Significant Wave Height Anomaly

Anomaly refers to a deviation or departure from the normal or expected wave patterns, specifically in terms of wave height. These anomalies can be either positive or negative.

Positive wave anomalies typically refer to waves that are larger or more energetic than what is typically observed in a particular region during a specific time period. This can be caused by various factors such as storm systems, strong winds, or other meteorological conditions that generate larger waves than usual. Negative wave anomalies, on the other hand, indicate waves that are smaller or less energetic than the typical conditions for a given area and time frame. This

could result from factors like the absence of significant weather systems or wind patterns that usually generate waves.

To describe the interannual variability of wave conditions of West Africa, global Hs anomaly was plotted for the entire West Africa and also the selected regions. According to Figure 30, the average of the whole domain (West Africa) anomaly of Hs from 1993 to 2021. The year 2017 saw the largest anomaly Hs while the year 2010 saw the lowest. Extreme Hs events occurred in 1996, 2011 – 2014, 2016 – 2017. It was also observed that there were more positive anomalies from 2011 onwards than before that year, suggesting an increase in the frequency of extreme events in recent years. Anomaly plots of the four selected regions were analyzed and can be found in the appendix.

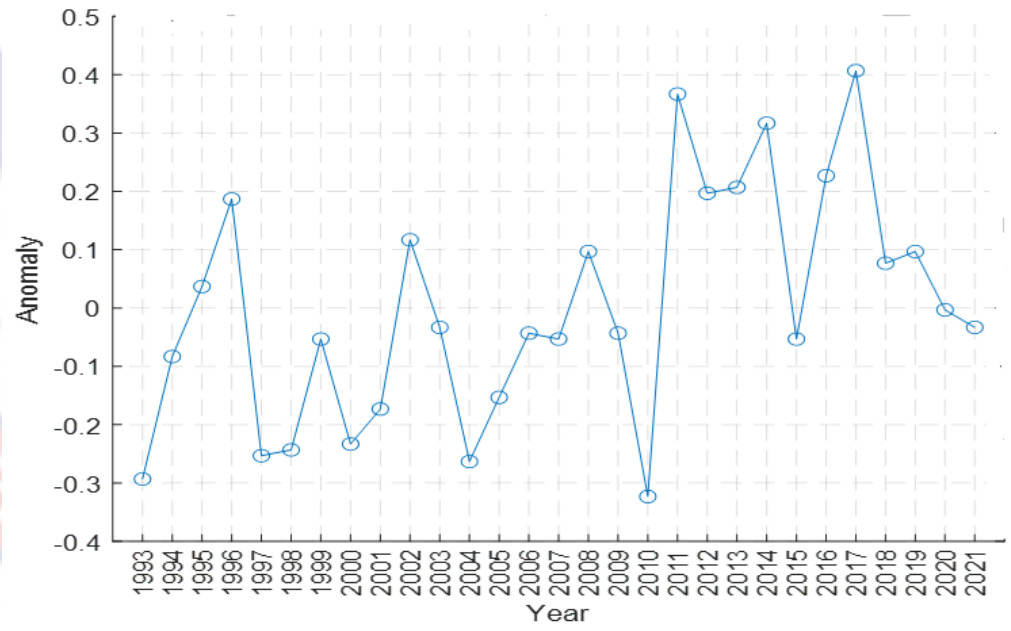

Figure 30: Annual anomaly plot of global Hs for the entire West Africa.

Wave Power

It is crucial to investigate the wave power at a certain site for a number of reasons. The fact that it clarifies the possibilities of wave energy as a

renewable energy source is one of the main justifications. Wave energy has the potential to power distant islands and coastal villages that presently rely on costly, carbon-intensive diesel imports.

The average wave power for the whole West African region from 1993 to 2021 is shown in Figure 31. Wave power is often expressed in terms of wave energy flux, which represents the amount of energy carried by the waves per unit of time and per unit of crest length. The wave energy flux can be calculated using Equation 4. The minimum wave power, which occurred in the year 2005, was 10.21 kW/m, and the maximum wave power, which occurred in the year 2018, was 13.31 kW/m. From 1993 to 2021, it seems that the wave power increases at an average rate of approximately 0.048 kW/m per year.

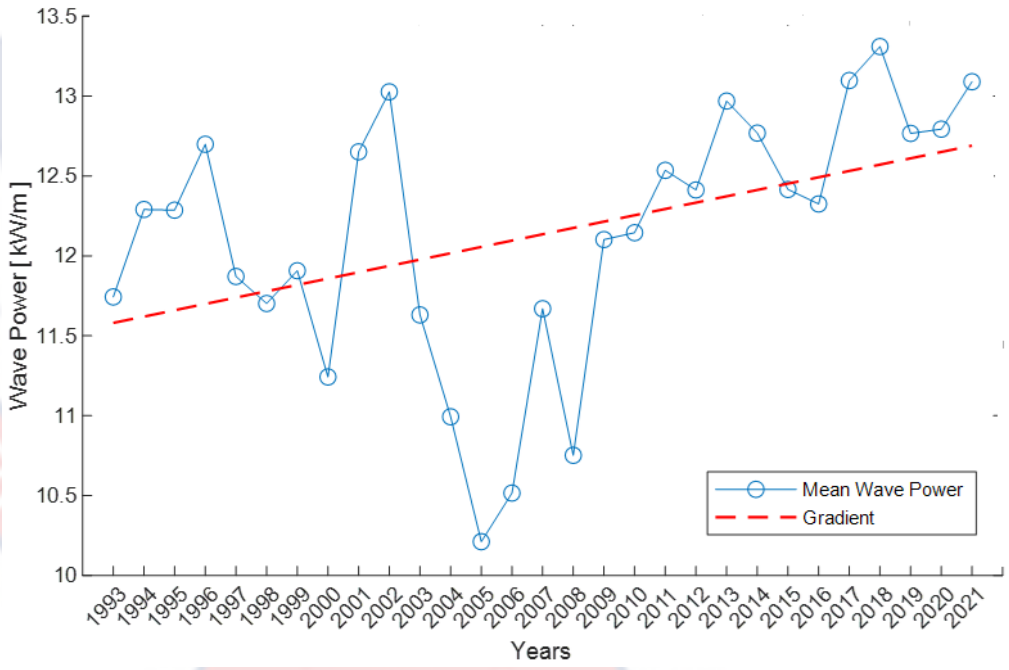

Figure 31: Interannual variability of wave power off West Africa

Extreme Wave Events

In this study, we analyzed the extreme wave events for the four selected regions (Ivory Coast, Ghana, Togo/Benin and Nigeria). For this first analysis, the chosen threshold is equivalent to the 99% quantile of the Hs of each region.

In figure 32 time series of Hs is shown with threshold (red horizontal line) and Hs_e of extreme wave events (green stars) for the regions of Ivory Coast (a), Ghana (b), Togo/Benin (c) and Nigeria (d).

The 99% quantile of Hs (defined threshold value) for Ivory Coast, Ghana, Togo/Benin, and Nigeria were estimated to be 2.28 m, 2.20 m, 2.25 m, and 2.31 m respectively.

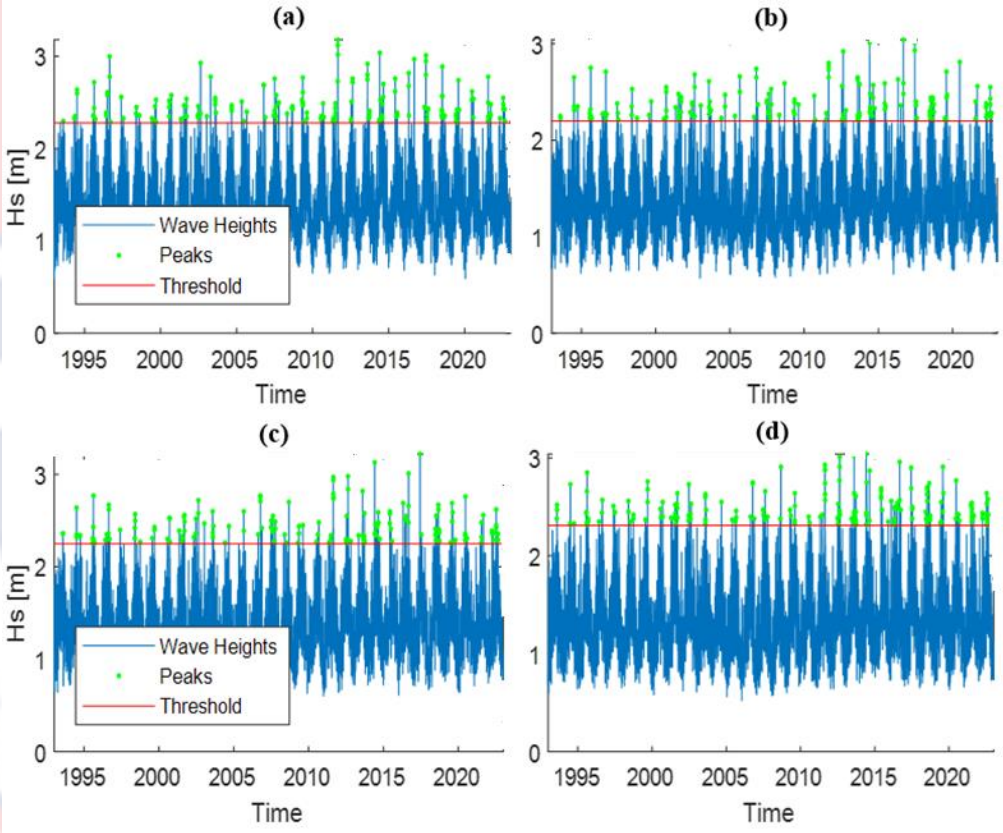

Figure 32: Time series of Hs with threshold (red) and Hs_e of selected extreme events (green stars) off (a) Ivory Coast, (b) Ghana, (c) Togo/Benin and (d) Nigeria

According to Table 3, Nigeria was where many events were recorded, which was determined to be 114 with the highest peak of 3.04 m with a duration of 126 hours, followed by the region of Ivory Coast, with the number of extreme events 113, having 3.18 m as the highest peak recorded with a duration of 87

hours, Togo/Benin being the next with the number of events 105, the highest event being 3.22 m which lasted for 57 hours and with Ghana having the least number of events of 102.

Table 3: Statistical Analysis for the Extreme Wave Event

Statistics	Ivory Coast	Ghana	Togo/Benin	Nigeria
Lowest peak (m)	2.3	2.23	2.26	2.33
Date	Aug 7, 1993	Aug 7, 1993	Sep 13, 1995	Jun 24, 1994
Duration (hrs)	3	12	3	3
Highest peak (m)	3.18	3.04	3.22	3.04
Date	Aug 27, 2011	Sep 4, 2016	Jun 11, 2017	May 31, 2014
Duration (hrs)	87	48	57	126
Number of events	113	102	105	114

Source: Researcher, 2023

Marginal Distributions

The distribution of Hs_e off Ivory Coast (a), Ghana (b), Togo/Benin (c) and Nigeria (d) is depicted in Figure 33. In Ivory Coast, the extreme event's minimum and maximum Hs_e values were estimated to be 2.29 m and 3.18 m, with a modal value of 2.35 m. Approximately less than 50% of the extreme events had an Hs_e of 2.43m, while 10% were estimated to be greater than 2.77 m. Moving to Ghana, the corresponding Hs_e values for the extreme event ranged from 2.21 m to 3.04 m, with a modal value of 2.23 m. Less than 50% of the extreme events in Ghana had an Hs_e of 2.37 m, and 10% were projected to be greater than 2.69 m. For Togo/Benin, the minimum and maximum Hs_e values were estimated at 2.26 m and 3.22 m, with a modal value of 2.26 m. 10% of the extreme events were projected to exceed 2.70 m, while an Hs_e of 2.42 m was anticipated to be less than 50%. In Nigeria, the extreme event was calculated to

have a modal Hs_e of 2.38 m, with the lowest and highest values at 2.33 m and 3.04 m, respectively. 10% of the extreme events in Nigeria were projected to surpass 2.76 m, and an Hs_e of 2.45 m was estimated to exceed 50% of the extreme event.

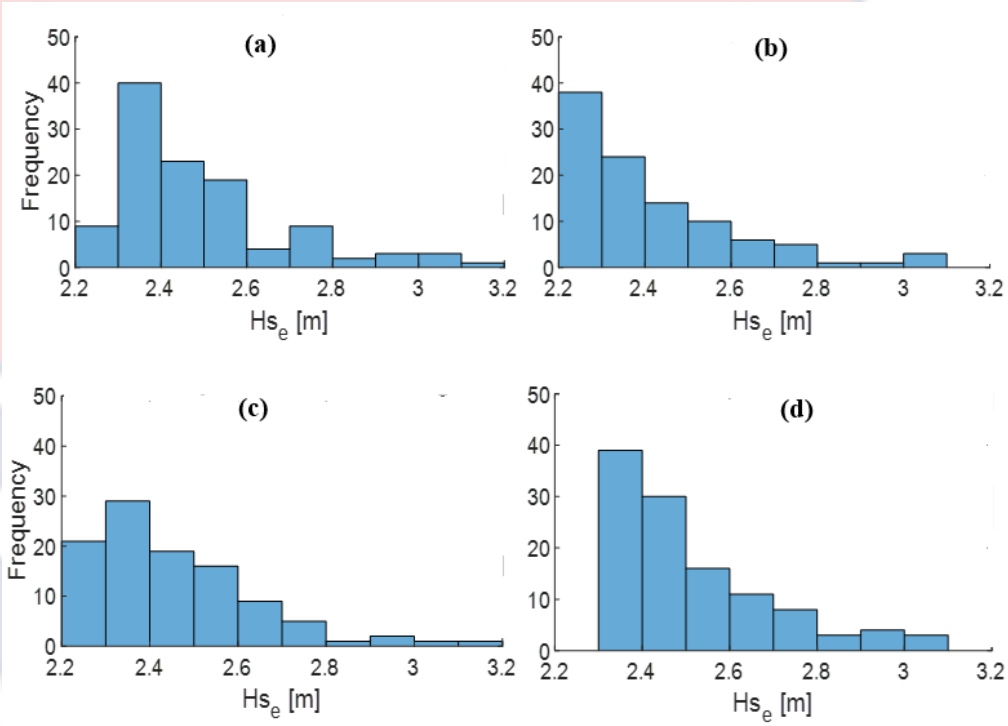

Figure 33: Histogram of the extreme events of Hs_e that occurred off (a) Ivory Coast, (b) Ghana, (c) Togo/Benin and (d) Nigeria

The distribution of Tp_e off (a) Ivory Coast, (b) Ghana, (c) Togo/Benin and (d) Nigeria is shown in Figure 34. The extreme event in Ivory Coast was assessed to have a modal value, Tp_e of 13.29 s and lowest and maximum peak Tp_e values of 11.97 s and 19.17 s, respectively. 10% of the extreme occurrences were predicted to have a time point larger than 17.76 s, with a predicted Tp_e of 16.10 s for less than 50% of the extreme events. Going on to Ghana, there was a modal value of 13.93 s and matching Tp_e values for the extreme event ranging from 12.43 s to 18.82 s. The Tp_e of 16.03 s was estimated to be less than 50%,

and the Tp_e of 17.94 s was estimated to be larger than 10% of the extreme events. With a modal value of 13.38 s, the lowest and maximum Tp_e values for Togo/Benin were assessed to be 12.39 s and 19.13 s. 10% of the extreme events were anticipated to have a time point larger than 17.99 s, with a Tp_e of 16.31 s estimated to be less than 50%. The minimum and maximum Tp values of the severe event in Nigeria were calculated to be 11.82 s and 19.29 s, respectively, with a modal value of 14.83 s. 10% of the extreme occurrences were predicted to have a time point larger than 17.90 s, with the Tp_e of 16.08 s being less than 50%.

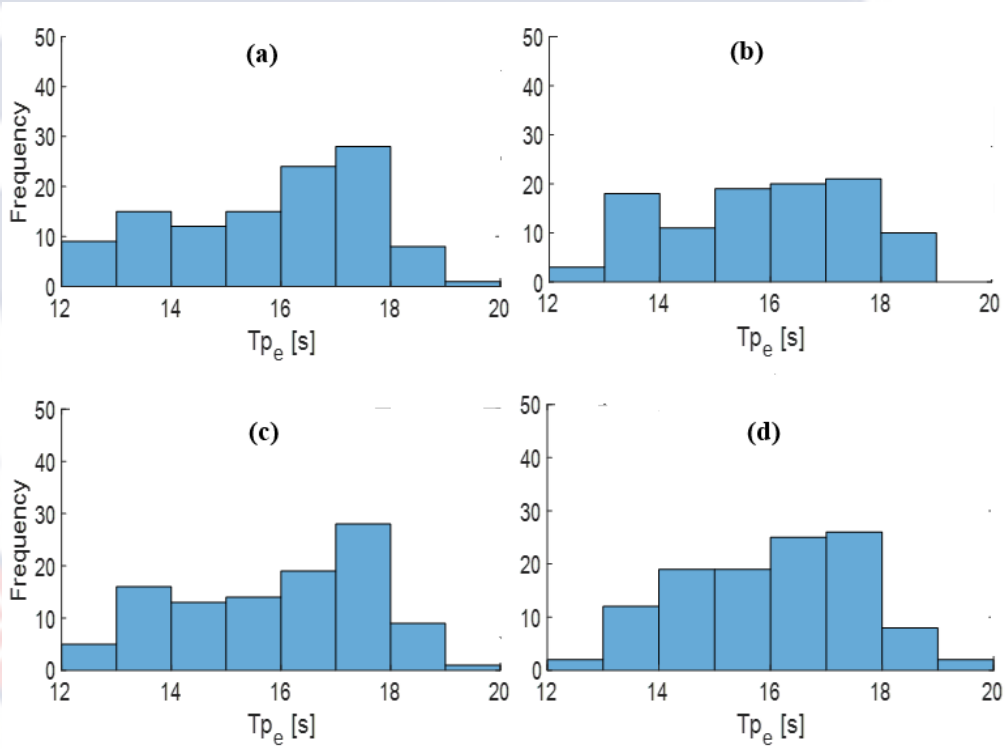

Figure 34: Histogram of the extreme events of Tp_e off (a) Ivory Coast, (b) Ghana, (c) Togo/Benin and (d) Nigeria

Analysis on the marginal distribution of the duration of the extreme wave events was presented in Figure 35. In Ivory Coast, the minimum and maximum duration of the events of the extreme event were estimated to be 3

hours and 99 hours, respectively, with a modal duration of 3 hours. Additionally, 15 hours of the event duration was estimated to be less than 50%, while 10% of the events were projected to have a duration greater than 57 hours. Moving to Ghana, the corresponding duration for the extreme event ranged from 3 hours to 117 hours, with a modal duration of 3 hours. Similarly, 18 hours of the event duration were estimated to be less than 50%, and 10% of the events were estimated to have a duration greater than 60 hours. For Togo/Benin, the minimum and maximum duration of the extreme event's events were estimated at 3 hours and 114 hours, with a modal duration of 3 hours. Additionally, 18 hours of the event duration were projected to be less than 50%, while 10% of the events were estimated to have a duration greater than 69 hours. In Nigeria, the extreme event was calculated to have a minimum and maximum duration of 3 hours and 126 hours, respectively, with a modal duration of 3 hours. Moreover, 12 hours of the event duration were estimated to be less than 50%, and 10% of the events were projected to have a duration greater than 57 hours.

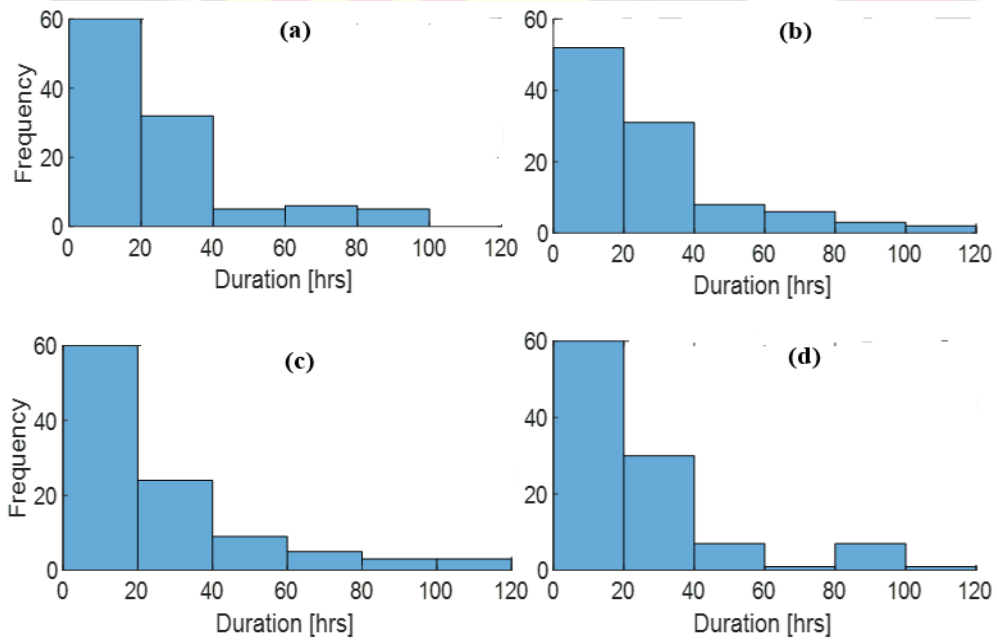

Figure 35: Marginal distribution of the duration of extreme events off (a) Ivory Coast, (b) Ghana, (c) Togo/Benin and (d) Nigeria

Joint Distribution of Hs_e, Tp_e, and Duration

A joint distribution of Hs_e against Tp_e for all the extreme events that occurred with the event duration as the color bar for the regions is depicted in figure 36. It can be observed from all the regions that most events with a Hs_e greater than 2.8 m generally lasted more than 48 hours. In addition, there is a positive correlation between Hs_e and Tp_e: events with high Hs_e generally have longer periods.

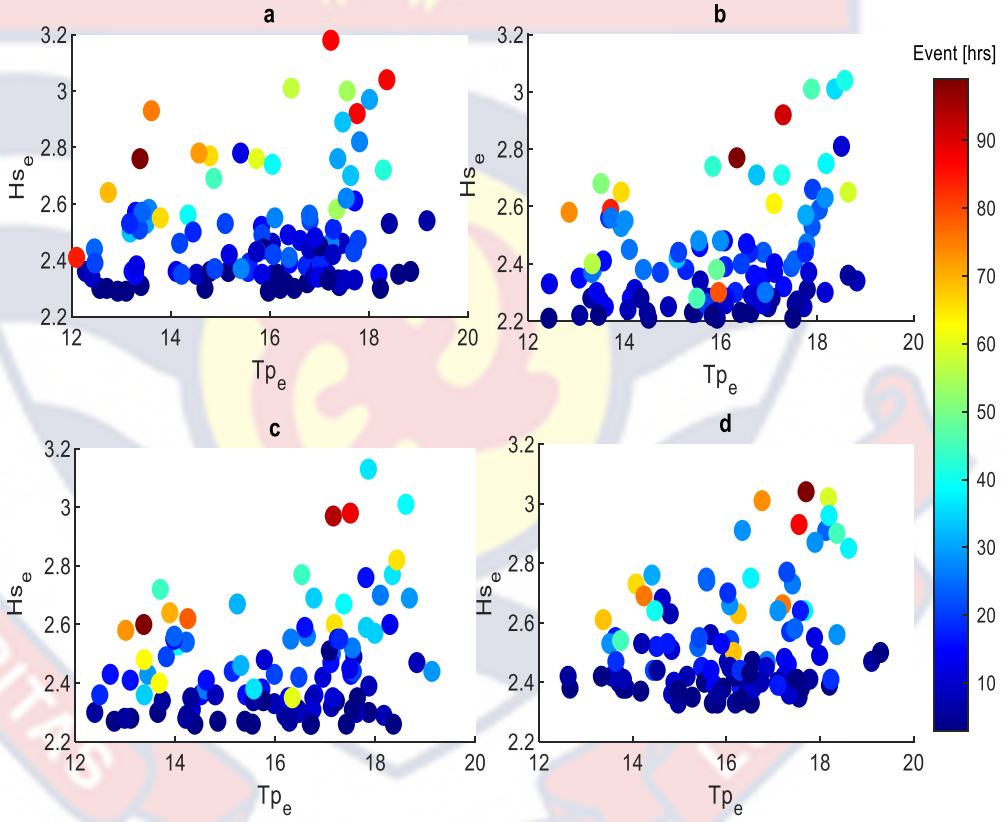

Figure 36: Scatter plot of the extreme events occurrences off (a) Ivory Coast, (b) Ghana, (c) Togo/Benin and (d) Nigeria

POT/GPD results

Threshold selection

The choice of threshold is an important practical problem, which is mainly based on a compromise between bias and variance. The threshold must be high enough for the excess over the threshold to converge to the GPD, meantime the sample size should be large enough to ensure that there are enough data points left for satisfactory determination of the GPD parameters.

To select the threshold for the POT approach, we used the classic parameter stability method, which consists of plotting he GPD fits for some range of thresholds and look for shape and scale parameters stability. To take account of local variations, this method is applied separately to 4 regions (Ivory Coast, Ghana, Benin/Togo, Nigeria). This has led to different thresholds for these 4 regions, even though the thresholds are not very different.

In this study, the approach that was used to select the threshold is to plot the GPD fits for some ranges of thresholds and look for parameter stability. Figure 37 shows a GPD fits for threshold range from quantile 90% to quantile 99.9% for the regions of Ivory Coast, Ghana, Togo/Benin and Nigeria respectively. For Ivory Coast a threshold greater than 2.3 m seems to be too high. A reasonable threshold is 2.2 m. Similarly, reasonable thresholds for Ghana, Togo/Benin and Nigeria are respectively 2.20 m, 2.25 m and 2.28 m.

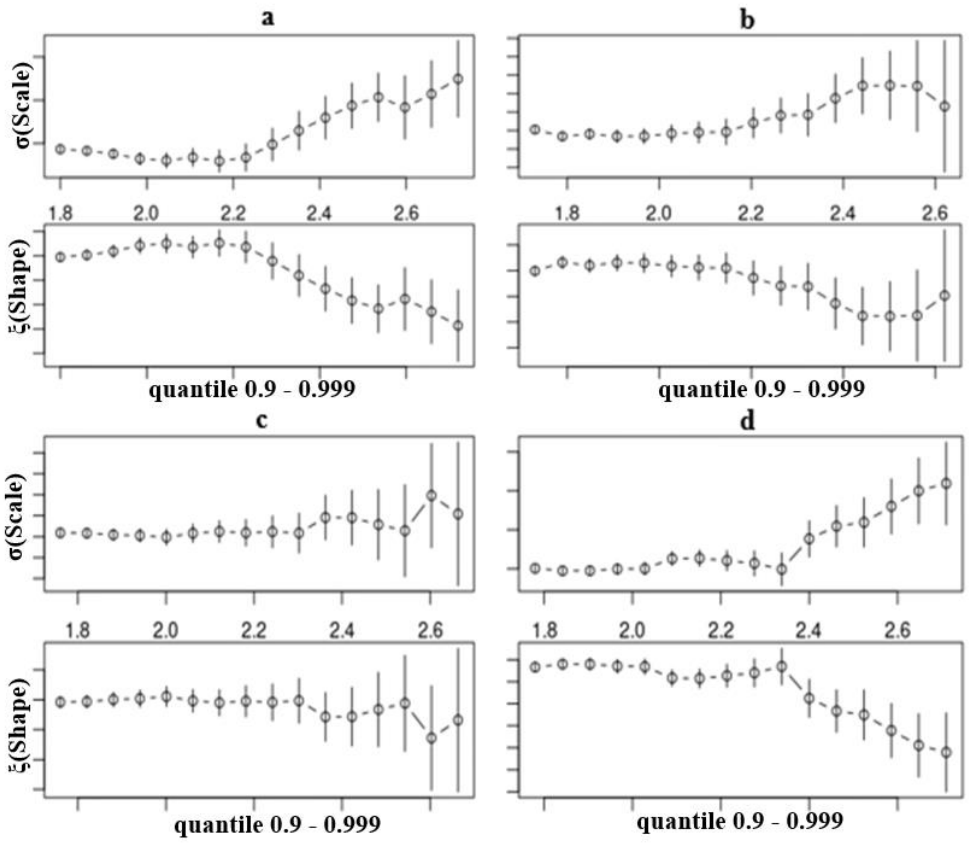

Figure 37: GPD fitting graph for the threshold of quantile 0.9 – 0.999 for the regions off (a) Ivory Coast, (b) Ghana, (c) Togo/Benin and (d) Nigeria

GPD fitting results

In this research, maximum likelihood (ML) was the method employed to fit GPD. ML estimators are preferable over other methods for parameter estimation because they possess desirable properties such as consistency, asymptotic normality, and asymptotic efficiency. Additionally, they have strong theoretical foundations and offer a unified approach to parameter estimation, making them ideal for comparing different models. ML estimation is also flexible and can be used for a wide range of models under a variety of assumptions.

From Figure 38, the diagnostic of GPD fit for the four regions was shown. Quantile plot for empirical data and quantile plot for model simulated data along with a density estimate plot and return-level plot for the POT data. Since much of the data lines up on the diagonal of the goodness of fit plots we can conclude that the GPD fit the data well.

The return level plot plots the return period against the return level and also includes 95% confidence interval and in which all the data points fall within the confidence band. The 100-year return values obtained from POT approach is 3.2 m for Ivory Coast, 3.1 m for Togo/Benin and 3.0 m for Ghana and Nigeria. A summary of the shape and scale parameters as well as the 50-year and 100-year return periods are presented in the Table 4.

a

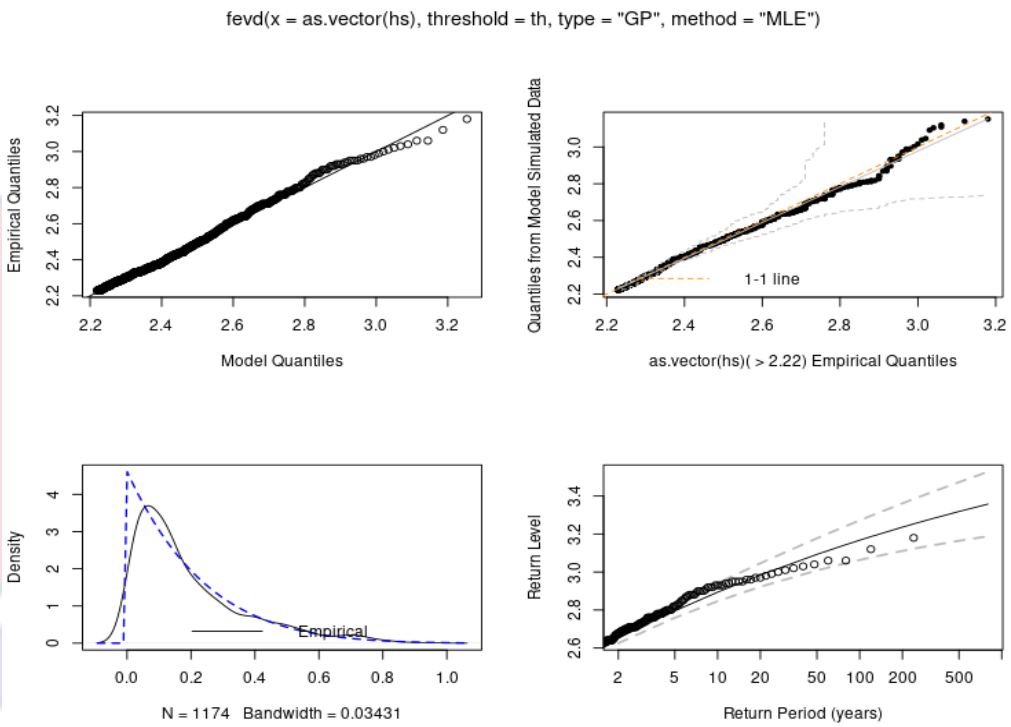

b

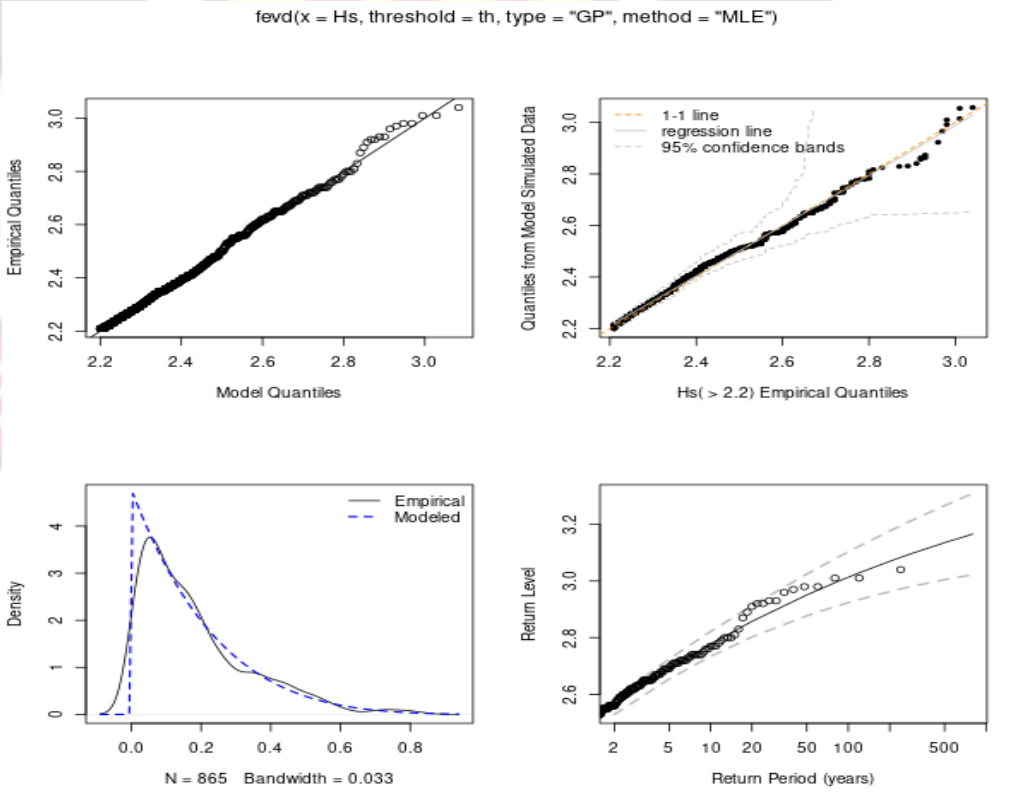

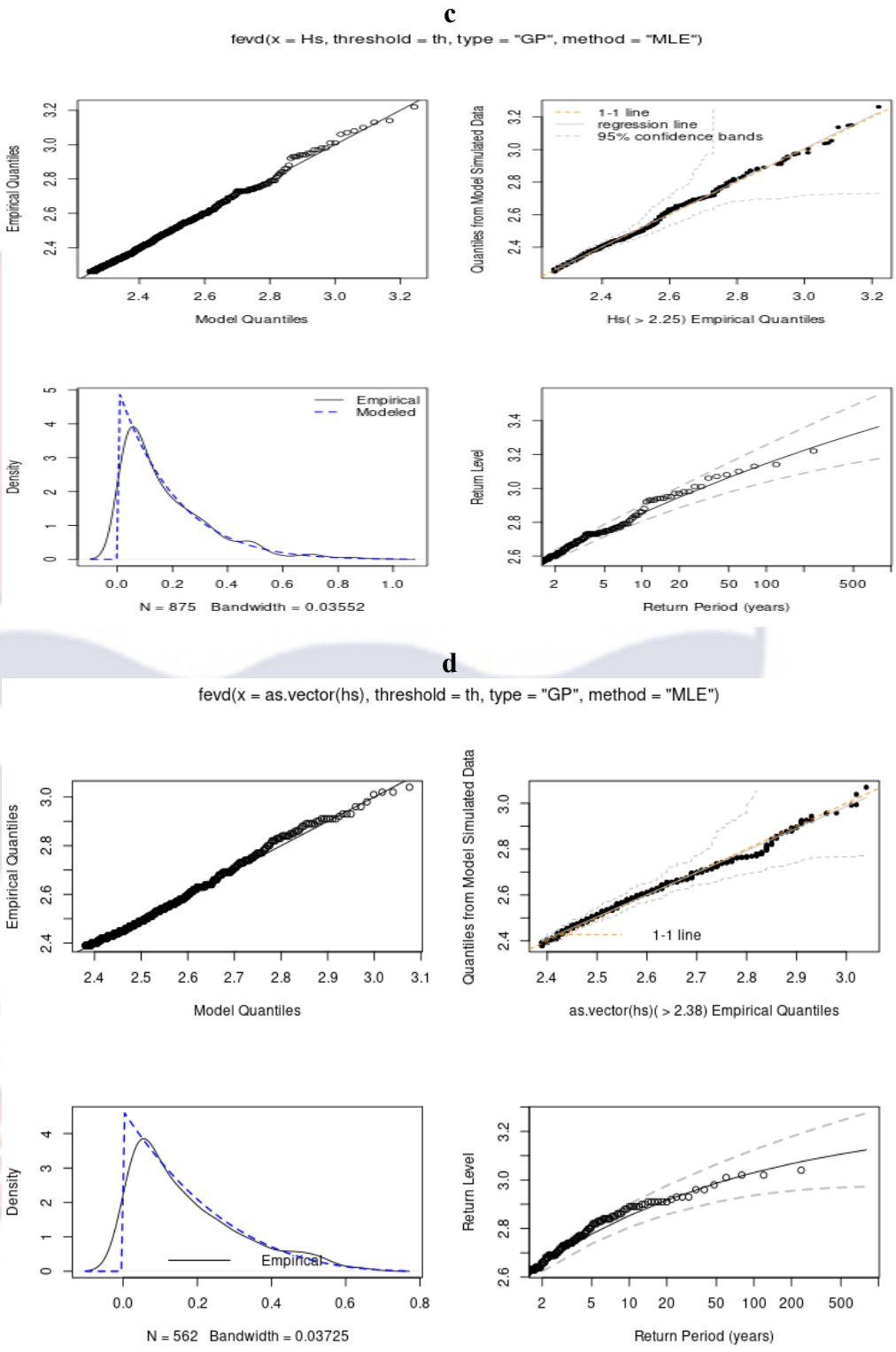

Figure 38: GPD fitting graph with the empirical quantile against modeled quantile and estimated return periods off (a) Ivory Coast, (b) Ghana (c) Togo/Benin and (d) Nigeria

Table 4: GPD fit scale and shape parameters with the return period for the four regions

Threshold (m)	σ(Scale)	ξ(Shape)	Hs of the Return period (m)	
			50 years	100 years
Ivory Coast				
2.22	0.2167	- 0.1197	3.070	3.173
Ghana				
2.20	0.2093	- 0.1523	2.928	3.013
Togo/Benin				
2.25	0.1962	- 0.0907	3.035	3.146
Nigeria				
2.38	0.2144	- 0.2416	2.982	3.054

Source: Researcher, 2023

A summary of the shape and scale parameters as well as the 50-year and 100-year return periods of GPD fits.

Chapter Summary

From 1993 to 2021, West Africa's Atlantic Ocean wave parameters exhibited distinct patterns. The general analysis of the region revealed a global significant wave height ranging from a minimum of approximately 0.57 m to a maximum of around 3.20 m. The global wave period ranged from a minimum of approximately 3.8 s to a maximum of about 25.0 s, with predominant wave directions within the South and Southwest regions. Further partitioning of waves showed that wind sea significant wave height varied from a minimum of approximately 0.05 m to a maximum of around 1.50 m, mainly concentrated in the South and Southeast, as well as Southwest and West regions. Swell significant wave height exhibited a range from approximately 0.25 m to 3.00 m,

with directions predominantly in the south-southeast, as well as the south-southwest regions.

In general, the waves in the West Africa region are dominated by swell which is about 95% of the global waves of this area and the remaining 5% are wind sea waves.

Seasonal analysis of West Africa's Atlantic Ocean waves demonstrated fluctuations in significant wave height and wave period. General analysis indicated that the global mean significant wave height reached a minimum of about 1.0 m in December and January, while it peaked at around 1.6 m in June, July, and August. The global mean wave period exhibited a minimum of about 12.0 s during December and January and a maximum of about 13.5 s in June, July, and August.

The swell waves of West Africa are generated from sources far from the West African ocean environment in South Atlantic between Cape Horn and Cape of Good Hope.

In examining the extreme wave conditions, the analysis was conducted over three decades, from January 1992 to December 2022, using the CMENS dataset. By choosing four points—Ivory Coast, Ghana, Togo/Benin, and Nigeria—it created a 100-year return level map for the West African region. The POT method was used in all cases, and fitting all excesses above a high threshold with a Generalized Pareto Distribution.

The number of events that occurred in these regions were 113, 102, 105 and 114 for Ivory Coast, Ghana, Togo/Benin and Nigeria respectively. The highest Hs recorded for these events with their respective durations were 3.18 m for 87 hours, 3.04 m for 48 hours, 3.22 m for 57 hours and 3.04 m for 126

hours for the regions of for Ivory Coast, Ghana, Togo/Benin and Nigeria. From the analysis, it was found that, the events with high Hs had the highest duration.

From the GPD, the 100-year return period of Hs was found to be 3.1 m, 3.0 m, 3.1 m and 3.0 m for the regions of Ivory Coast, Ghana, Togo/Benin and Nigeria respectively. This analysis is based on CMENS data in which the extremes are underestimated. It is obvious that the "true" values corresponding to the 100-year return period of the Hs are slightly higher than the values obtained in this study.

CHAPTER FIVE

SUMMARY, CONCLUSIONS AND RECOMMENDATIONS

Overview

The study analyzed wave conditions in West Africa's Atlantic Ocean from 1993 to 2021, revealing patterns in significant wave height, wave period, and direction. It found that significant wave heights ranged between 0.57 m and 3.20 m, with wave periods from 3.8 s to 25.0 s, predominantly from the south and southwest. Swell waves were the dominant force, constituting 95% of the wave energy, and primarily originated in the South Atlantic. Seasonal fluctuations showed higher wave activity between June and August, while extreme wave events were also analyzed using the CMENS dataset. The study highlighted the importance of understanding wave variability and the implications of extreme wave events on coastal management, recommending the use of CMENS data for designing offshore and coastal structures.

The study further conducted a comparative assessment between the ERA5 and CMENS datasets to determine which was more effective for West Africa's wave conditions. CMENS proved to be the more reliable dataset, especially for coastal infrastructure design and flood warning systems. Extreme wave conditions were analyzed for four West African regions (Ivory Coast, Ghana, Togo/Benin, and Nigeria), providing insights into significant wave height and event duration. The study's findings contribute to coastal planning and risk management, with recommendations for resilient infrastructure, early warning systems, and continued research for adaptive coastal management in response to wave climate dynamics and climate change.

Summary

From 1993 to 2021, wave parameters in West Africa's Atlantic Ocean exhibited distinct patterns. Significant wave heights ranged from 0.57 m to 3.20 m, with wave periods between 3.8 s and 25.0 s, and predominant wave directions from the South and Southwest. Wind sea wave heights varied between 0.05 m and 1.50 m, while swell wave heights ranged from 0.25 m to 3.00 m, primarily from the south-southeast and south-southwest. Swell waves dominated the region, accounting for 95% of the global waves, with the remaining 5% being wind sea waves. Seasonally, significant wave heights reached a minimum of 1.0 m in December and January, peaking at 1.6 m in June to August, while wave periods ranged from 12.0 s to 13.5 s. These swell waves originated far from West Africa, between Cape Horn and the Cape of Good Hope in the South Atlantic.

Extreme wave conditions were also analyzed using the CMENS dataset from MFWAM, spanning 30 years (1992–2022), and focused on four locations: Ivory Coast, Ghana, Togo/Benin, and Nigeria. A 100-year return level map was created for these regions using the Peaks Over Threshold (POT) method, fitting wave height excesses above a threshold with a Generalized Pareto Distribution (GPD). The number of extreme events recorded were 113, 102, 105, and 114 for each region, with the highest significant wave heights (Hs) being 3.18 m, 3.04 m, 3.22 m, and 3.04 m, with durations of 87, 48, 57, and 126 hours, respectively. The study found a correlation between higher wave heights and longer event durations. Based on GPD analysis, the estimated 100-year return wave heights were 3.1 m for Ivory Coast and Togo/Benin, and 3.0

m for Ghana and Nigeria, though these values are likely underestimated due to limitations in the CMENS dataset.

Conclusions

In conclusion, this study successfully achieved its primary goals. First and foremost, a thorough comparison between CMENS and ERA5 datasets was conducted, specifically focusing on their effectiveness in describing wave conditions off the West African coast. This comparative analysis provided valuable insights into the strengths and limitations of each dataset, aiding in the identification of the more accurate model for this specific geographical context. Second, the study met its objective of estimating the wave climate off West Africa, contributing to a comprehensive understanding of the region's dynamic oceanic conditions. Lastly, the analysis of extreme wave events, crucial for assessing the potential impacts on coastal areas, was successfully undertaken. By accomplishing these goals, the study not only advances our knowledge in oceanography but also provides essential information for coastal management and resilience planning in West Africa.

As the in-situ data for the other sea state parameters were not available, the comparison between the two reanalysis was made using only the significant wave height. The data used was from the Akpo buoy off Nigeria and data from the HY-2B and HY-2C satellites as reference data.

The use of HY-2B and HY-2C is crucial as the wave models generating the reanalysis do not assimilate Hs data from these altimeters. This deliberate exclusion ensures the independence of HY-2B and HY-2C data, providing a

unique opportunity for a robust comparison and enhancing the reliability of the study's findings regarding wave conditions off West Africa.

This study clearly shows that for studies requiring the use of wave reanalysis data, it is preferable to use CMENS data, which better describe the sea state conditions in West Africa, compared with ERA5 data, which have been used up to now for studies relating to coastal infrastructure development, coastal erosion or the design of offshore structures. For example, to estimate the 100-year return period for wave heights, which is useful for the design of offshore structures and coastal protection, it would be wise to use CMENS data and therefore the values produced in this study.

If one wish to set up a coastal flood warning system, the results of the wave climate established in this study and the results obtained from the analysis of extreme events, together with the analysis of the tide, will help to define the specific warning thresholds.

The comprehensive analysis of West Africa's Atlantic Ocean wave parameters spanning the period from 1993 to 2022 has yielded insightful findings that contribute significantly to our understanding of the region's wave climate. The distinct patterns observed in significant wave height, wave period, and wave directions reflect the complex interplay of oceanic factors influencing the West African coastal environment.

Significant wave height off West Africa varies between 0.57 m and 3.18 m with a mean value of around 1.22 m. The wave period ranged from a minimum of approximately 3.8 s to a maximum of about 25.0 s.

The general analysis of the region's wave climate revealed a dominance of swell waves, accounting for approximately 95% of the global wave energy. Wind sea

waves, constituting the remaining 5%, exhibited intriguing patterns, with low wave heights in specific months and peaks in others. The waves of West Africa are generated from sources far from the West African ocean environment in the South Atlantic between Cape Horn and Cape of Good Hope.

Seasonal analysis showcased fluctuations in significant wave height and wave period, emphasizing the dynamic nature of the wave climate with high Hs and Tp between July and August. Notably, the austral winter and summer seasons play distinct roles in shaping wave dynamics, driven by extratropical storms, westerly winds, and atmospheric systems. The intricate interaction of these elements contributes to unique seasonal patterns, requiring careful consideration in coastal planning and management strategies.

The dynamic character of wave patterns in West Africa, as highlighted by the intricate interaction of various oceanic elements, has far-reaching implications for coastal management and marine activities. The findings underscore the need for adaptive strategies that account for the seasonal variability and dominant swell wave conditions. Coastal infrastructure, resource utilization, and disaster preparedness must be informed by a nuanced understanding of the complex wave climate dynamics observed in the region.

The interannual variability off the West African coast was also analyzed with a minimum wave power of 10.21 kW/m and a maximum wave power of 13.31 kW/m. Also, there was an average increment of wave power of 0.048 kW/m annually.

The extreme wave conditions along the West African coastline using the CMENS dataset, focusing on the Ivory Coast, Ghana, Togo/Benin, and Nigeria regions. Utilizing the Peaks Over Threshold (POT) method and fitting excesses

above a high threshold with a Generalized Pareto Distribution (GPD). The findings provide valuable insights into extreme wave events and their characteristics, particularly concerning significant wave height (Hs) and their return periods.

The examination of extreme wave events (considering a threshold equal to quantile 99%) revealed significant variations in both the number of events and their corresponding characteristics across the selected regions. Ivory Coast, Ghana, Togo/Benin, and Nigeria experienced 113, 102, 105, and 114 events, respectively. The highest Hs recorded for these events with their respective durations were 3.18m for 87 hours, 3.04 m for 48 hours, 3.22 m for 57 hours and 3.04 m for 126 hours for the regions of Ivory Coast, Ghana, Togo/Benin and Nigeria respectively. The highest recorded significant wave heights for these events, along with their durations, demonstrated notable differences, emphasizing the regional specificity of extreme wave occurrences.

A noteworthy observation from the analysis was the positive correlation between significant wave height (Hs) and event duration. Events with higher Hs values tended to have longer durations, suggesting a potential link between the magnitude of extreme waves and their persistence over time. This finding is crucial for understanding the temporal dynamics of extreme wave conditions and their implications for coastal resilience.

The 100-year return period analysis, conducted through the Generalized Pareto Distribution (GPD), provided key insights into the extreme wave conditions expected over a longer timeframe. The calculated 100-year return levels for significant wave height (Hs) were found to be 3.1 m, 3.0 m, 3.1 m, and 3.0 m for the regions of Ivory Coast, Ghana, Togo/Benin, and Nigeria, respectively.

These values serve as essential benchmarks for assessing the recurrence interval of extreme wave events and informing risk assessment and mitigation strategies. Given that the analysis relies on CMENS data, it is essential to note that the extremes in this dataset tend to be underestimated. Specifically, the study acknowledges that the "true" values corresponding to the 100-year return period of significant wave height (Hs) are likely slightly higher than the values derived from CMENS. This acknowledgment underscores the importance of interpreting the study's findings within the context of this underestimation, emphasizing the need for caution in extrapolating results, especially when considering extreme wave events and their potential impact on coastal conditions.

The outcomes of this study carry significant implications for coastal planning and management along the West African coastline. Understanding the characteristics and recurrence intervals of extreme wave events is crucial for designing resilient coastal structures, implementing effective risk management measures, and safeguarding coastal communities and infrastructure.

Recommendations

Based on the comprehensive analysis of West Africa's Atlantic Ocean wave parameters and the examination of extreme wave conditions, several recommendations emerge to enhance coastal management, infrastructure design, and risk mitigation strategies in the region:

Infrastructure Resilience Planning: Given the distinct seasonal variations and extreme wave conditions observed, there is a need to incorporate these findings into coastal infrastructure planning. Designing resilient structures

that can withstand the peak wave heights and durations, especially during the months of June, July, and August, is crucial to minimizing the risk of damage.

Coastal Zoning and Land Use Planning: Understanding the dominance of swell waves and their distant sources can inform coastal zoning and land use planning. Identifying areas more prone to extreme wave impacts and restricting certain activities in those regions can enhance overall safety and minimize potential damage.

Public Awareness and Early Warning Systems: Establishing effective early warning systems and increasing public awareness about the seasonal variations in wave conditions can aid in timely evacuation and preparedness for extreme events. Local communities should be informed about the periods when waves are expected to reach their peak, allowing for proactive measures. To do this, these extreme wave data need to be supplemented with tide and to a lesser extent, storm-surge data.

Climate Change Adaptation Strategies: Considering the potential impact of climate change on wave patterns is essential for long-term planning. Integrating adaptive strategies into coastal management plans will help mitigate the evolving risks associated with changing wave climates in West Africa.

Continued Monitoring and Research: The study highlights the importance of continuous monitoring of wave conditions in the West Africa region. Future research efforts should focus on refining models, incorporating additional datasets, and expanding the geographical scope to ensure the most accurate and up-to-date information for coastal decision-makers. Intensifying efforts in in-situ wave measurements to supplement remote sensing and reanalysis data. Additionally, a specialized regional wave model for the West

African coast is crucial for more accurate predictions and better management of coastal hazards. These measures collectively contribute to a more comprehensive understanding of wave dynamics in the region, supporting informed decision-making in coastal planning and management.

International Collaboration: Recognizing that swell waves are generated in the South Atlantic, collaboration with international organizations and neighboring countries is crucial. Sharing data and insights on wave patterns and extreme conditions can contribute to a collective understanding and joint efforts in managing the impacts of these waves.

Implementing these recommendations will contribute to a more resilient and adaptive approach to coastal management in West Africa, safeguarding both communities and infrastructure against the challenges posed by the dynamic wave climate observed in the region.

REFERENCES

Abdul, M., Kumar, R., Hounkpe, N., & Haque, A. (2020). Coastal vulnerability assessment in West Africa: a review. *Journal of Coastal Conservation*, 24(1), 1-18.

Almar Kestenare, E., Reyns, J., Jouanno, J., Anthony, E.J., Laibi, R., Hemer, M., Du Penhoat, Y. and Ranasinghe, R. (2015) Response of the Bight of Benin (Gulf of Guinea, West Africa) Coastline to Anthropogenic and Natural Forcing, Part 1: Wave Climate Variability and Impacts on the Longshore Sediment, R., Transport. *Continental Shelf Research*, 110, 48-59. https://doi.org/10.1016/j.csr.2015.09.020

Almar, R., Stieglitz, T., Addo, K.A. *et al.* Coastal Zone Changes in West Africa: Challenges and Opportunities for Satellite Earth Observations. *Surv Geophys* 44, 249–275 (2023). https://doi.org/10. 1007/s10712-022-09721-4

Amponsah, J., Asare, E., & Addae, J. (2021). Coastal flooding in Ghana: Causes, impacts, and mitigation strategies. *Journal of Ocean and Coastal Management*, 214, 105758.

Angnuureng, D. B., Brempong, K. E., Jayson-Quashigah, P. N., Dada, O. A., Akuoko, S. G. I., Frimpomaa, J., Mattah, P. A., & Almar, R. (2022). Satellite, drone and video camera multi-platform monitoring of coastal erosion at an engineered pocket beach: A showcase for coastal management at Elmina Bay, Ghana (West Africa). *Regional Studies in Marine Science*, 53, 102437. https://doi.org/10.1016/j.rsma.2022.102437

Appeaning Addo, K., Larbi, L., Amisigo, B., & Ofori-Danson, P. K. (2011). Impacts of Coastal Inundation Due to Climate Change in a CLUSTER of Urban Coastal Communities in Ghana, West Africa. *Remote Sensing*, *3*(9), 2029–2050. MDPI AG. http://dx.doi.org/10.3390/rs3092029

Ardhuin, F., Babanin, A. V., & Rogers, W. E. (2010). Wave Climate and Variability in the Atlantic Ocean as Observed by Waverider Buoys from 1994 to 2007. *Journal of Physical Oceanography*, 40(6), 1250–1266. https://doi.org/10.1175/2010JPO4324.1

Ardhuin F., Stopa J. E., Chapron B., Collard F., Husson R., Jensen R. E., Johannessen J., Mouche A., Passaro M., Quartly G. D., Swail V. & Young I. (2019). Observing Sea States. *Front. Mar. Sci*. 6:124. https://doi.org/10.3389/fmars.2019.00124

Caires, S., & Sterl, A. (2005). 100-year return value estimates for ocean wind speed and significant wave height from the ERA-40 data. *Journal of Climate*, *18*(7), 1032-1048.

Caires, S., Donlon, J., Sterl, A., et al. (2005). Global wave climate from TOPEX/Poseidon and ERS-1/2. *Journal of Geophysical Research: Oceans,* 110(C12), C12003.

Camus, P., Mendez, F. J., Medina, R., & Cofiño, A. S. (2011). Analysis of clustering and selection algorithms for the study of multivariate wave climate. *Coastal Engineering*, *58*(6), 453-462.

Collins, M. B., Grifoll, M., Quaresma, L., & Bolaños, R. (2015). The validation of WAVERYS reanalysis wave data in the north-east Atlantic. *Ocean Science*, 11(5), 685–695. https://doi.org/10.5194/os-11-685-2015

Damen, M. O., El Gamal, H., & Caire, G. (2003). On maximum-likelihood detection and the search for the closest lattice point. *IEEE Transactions on information theory*, *49*(10), 2389-2402.

De Carlo, M., Ardhuin, F., & Le Pichon, A. (2020). Atmospheric infrasound generation by ocean waves in finite depth: unified theory and application to radiation patterns. *Geophysical Journal International*, *221*(1), 569-585.

Dodet, G., Bertin, X., & Taborda, R. (2010). Wave climate variability in the North-East Atlantic Ocean over the last six decades. *Ocean modelling*, *31*(3-4), 120-131.

Dong, S., Tao, S., Lei, S., & Guedes Soares, C. (2013). Parameter estimation of the maximum entropy distribution of significant wave height. *Journal of Coastal Research*, 29(3), 597-604. Coconut Creek (Florida), ISSN 0749-0208

European Centre for Medium-Range Weather Forecasts (ECMWF). (2019). ERA5: Fifth generation of ECMWF atmospheric reanalyses of the global climate. Copernicus Climate Change Service Climate Data Store (CDS). https://doi.org/10.24381/cds.adbb2d47

Foli, B.A.K., Appeaning Addo, K., Ansong, J.K. *et al.* Evaluation of ECMWF and NCEP Reanalysis Wind Fields for Long-Term Historical Analysis and Ocean Wave Modelling in West Africa. *Remote Sens Earth Syst Sci* **5**, 26–45 (2022). https://doi.org/10.1007/s41976-021-00052-3

Folley, M. (2017). The Wave Energy Resource. In: Pecher, A., Kofoed, J. (eds) Handbook of Ocean Wave Energy. *Ocean Engineering &*

Oceanography, vol 7. Springer, Cham. https://doi.org/10.1007/978-3-319-39889-1_3

Folorunsho, R., Salami, M., Ayinde, A. and Gyuk, N. (2023) The Salient Issues of Coastal Hazards and Disasters in Nigeria. *Journal of Environmental Protection*, **14**, 361-372. http://doi.org/10.4236/jep. 2023.145021

Grimshaw, S. D. (1993). Computing maximum likelihood estimates for the generalized Pareto distribution. *Technometrics*, *35*(2), 185-191.

Guillaume D., Angélique M., Fabrice A., Xavier B. & Déborah I. (2019). The Contribution of Wind-Generated Waves to Coastal Sea-Level Changes. *Surveys in Geophysics*, 2019, 40 (6), pp.1563-1601. ff10.1007/s10712-019-09557-5ff.

Hafez, K., Abouelfadl, W. & Leheta, H. (2012). Comparative Dynamic Response Analysis of a Fixed Offshore Platform Using Deterministic and Spectral Wave Approaches. *Proceedings of the International Conference on Offshore Mechanics and Arctic Engineering - OMAE*. 2. 10.1115/OMAE2012-83845.

Hersbach, H., Bell, B., Berrisford, P., Biavati, G., Horányi, A., Muñoz Sabater, J., Nicolas, J., Peubey, C., Radu, R., Rozum, I., Schepers, D., Simmons, A., Soci, C., Dee, D., & Thépaut, J.-N. (2020). The ERA5 global reanalysis. *Quarterly Journal of the Royal Meteorological Society*, 146(730), 1999–2049. https://doi.org/10.1002/qj.3803

Hersbach, H., & Dee, D. P. (2016). The ERA5 global reanalysis: Preprocessing and first analysis results. *Quarterly Journal of the Royal Meteorological Society*, 142(693), 3479-3514.

Hounguè, G.H., Kounouhéwa, B.B., Almar, R., Sohou, Z., Lefebvre, J-P., Houépkonhéha, M., & Tokpohozin, B. (2018). Waves forcing climate on Bénin coast, and the link with climatic index, Gulf of Guinea (West Africa). *In*: Almar, R.; Almeida, L.P.; Trung Viet, N., and Sall, M. (eds.), Tropical Coastal and Estuarine Dynamics. *Journal of Coastal Research, Special Issue No.* 81, pp. 130–137. Coconut Creek (Florida), ISSN 0749-0208.

Hounkpe, N. M., Gervais, S., & Lepennec, A. (2019). Coastal vulnerability assessment in West Africa: an overview. *Journal of Coastal Conservation*, 23(3), 363-380.

Ishmael Y. D., Alex B. O. & Osman Adams (2016). Analysis of Shoreline Change along Cape Coast-Sekondi Coast, Ghana. *Geography Journal*. 1868936, 9. https://doi.org/10.1155/2016/1868936

Ismail A. J. & Nining S. N. (2020). Extreme wave height analysis in Natuna sea using Peak-Over Threshold method. IOP Conf. Series: *Earth and Environmental Science* 618 (2020) 012024. https://doi.org/10.1088/1755-1315/618/1/012024

Jiang, X., Xie, B., Bao, Y., & Song, Z. (2023). Global 3-hourly wind-wave and swell data for wave climate and wave energy resource research from 1950 to 2100. *Scientific data*, *10*(1), 225. https://doi.org/10.1038/s41597-023-02151-w

Law-Chune S., Aouf L., Dalphinet A. et al. (2021). WAVERY: a CMENS global wave reanalysis during the altimetry period. *Ocean Dynamics* 71, 357-378. http://doi.org/10.1007/s10236-020-01433-w

Liu, T., Yu, J., Yu, Y., Zhang, X., Zhou, B., & Yin, L. (2023). Characterization of Wave Power Resources off the Coast of Guangdong. *Processes*, *11*(7), 2221. MDPI AG. http://dx.doi.org/10.3390/pr11072221

Munoz Sabater J., (2019). ERA5-Land hourly data from 1950 to present. Copernicus Climate Change Service (C3S) Climate Data Store (CDS). http://doi.org/10.24381/cds.e2161bac

Olagnon, M., Kpogo-Nuwoklo, K. A., & Guédé, Z. (2014). Statistical processing of West Africa wave directional spectra time-series into a climatology of swell events. *Journal of Marine Systems*, *130*, 101-108.

Okeke, P. N., Okeke, F. N., & Ajaegwu, N. E. (2020). Assessing the effects of coastal erosion on shoreline retreat in Lagos State, Nigeria. *Journal of Coastal Research*, 95(sp1), 311-315.

Pang, T., Wang, X., Nawaz, R. A., Keefe, G., & Adekanmbi, T. (2023). Coastal erosion and climate change: A review on coastal-change process and modeling. *Ambio*, *52*(12), 2034-2052. https://doi.org/10.1007/s13280-023-01901-9

Rusu, L., Raileanu, A., & Onea, F. (2018). A Comparative Analysis of the Wind and Wave Climate in the Black Sea Along the Shipping Routes. *Water*, *10*(7), 924. MDPI AG. http://dx.doi.org/10.3390/w10070924

Sample reference for comparing reanalysis data: González-Riancho, P., Olabarrieta, M., Castro, M., & Castanedo, S. (2019). Comparing wave hindcast data sets for the Bay of Biscay: An intercomparison of wind,

wave and spectral statistics. *Ocean Modelling*, 136, 65–81. https://doi.org/10.1016/j.ocemod.2019.01.008

Sterl, A., & Caires, S. (2005). Climatology, variability and extrema of ocean waves: The Web-based KNMI/ERA-40 wave atlas. *International Journal of Climatology: A Journal of the Royal Meteorological Society*, *25*(7), 963-977.

Stopa, J. E. (2007). A comparison of global wave reanalyses. *Ocean Modelling*, 19(1), 1-23.

Tatem, A. J., Goetz, S. J., & Hay, S. I. (2008). Fifty Years of Earth Observation Satellites: Views from above have lead to countless advances on the ground in both scientific knowledge and daily life. *American scientist*, *96*(5), 390–398. https://doi.org/10.1511/2008.74.390

Teena, N., Sanil Kumar, V., Kotteppad, S., & Sajeev, R. (2012). Statistical analysis on extreme wave height. *Natural Hazards*. https://doi.org/10.1007/s11069-912-0229-y

Uppala, S. M., Kållberg, P. W., Simmons, A. J., Andrae, U., Bechtold, V. D. C., Fiorino, M. & Woollen, J. (2005). The ERA-40 re-analysis. *Quarterly Journal of the Royal Meteorological Society: A journal of the atmospheric sciences, applied meteorology and physical oceanography*, *131*(612), 2961-3012.

Wimbush, M., Cox, C.S., & Clarke, A.J. (2021, May). Ocean waves. *AccessScience*. Retrieved September 27, 2023, from https://doi.org/10.1036/1097-8542.463900.

APPENDIX

Appendix A

Results on the Analysis of the other Three Regions

Time Series Analysis for Wind Sea and Swell for the Three Regions.

As stated in chapter four, the time series analysis of the Ivory Coast, Togo/Benin and Nigeria are examined.

Ivory Coast.

Time series comparing global Hs to that of wind sea and swell of when the highest global Hs was observed. From Figure 39, the highest global Hs for the period of 1993 to 2022 occurred on 27th August 2011 which was 3.18 m. The maximum Hs of swell within the duration of 1993 to 2022 occurred on 27th August 2011 which was also 3.15 m. For this period at (27th August 2011 to 30th September 2011), the maximum Hs of wind sea was recorded to be 1.02 m.

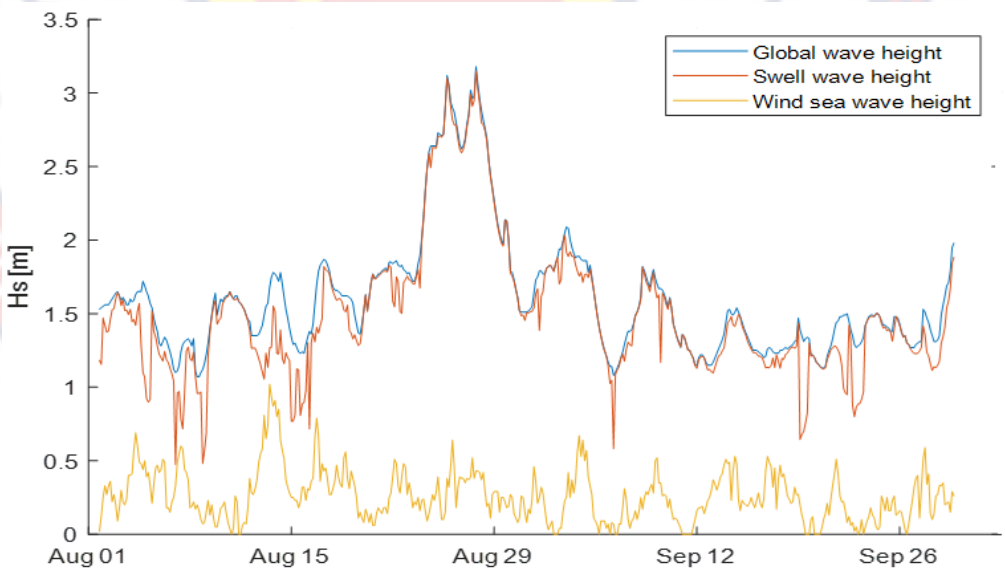

Figure 39: Time series of when the highest wave height, Hs, was recorded off Ivory Coast.

Togo/Benin.

Time series showing when the highest global Hs was recorded, along with comparisons to wind sea, and swell values. According to Figure 40, the highest global Hs for the period of 1993 to 2022 occurred on 11th June 2017 which was 3.22 m. The maximum Hs of swell within the duration of 1993 to 2022 occurred on 11th June 2017 which was also 3.22 m. For the same duration, the maximum wind sea Hs was recorded to be 1.11 m.

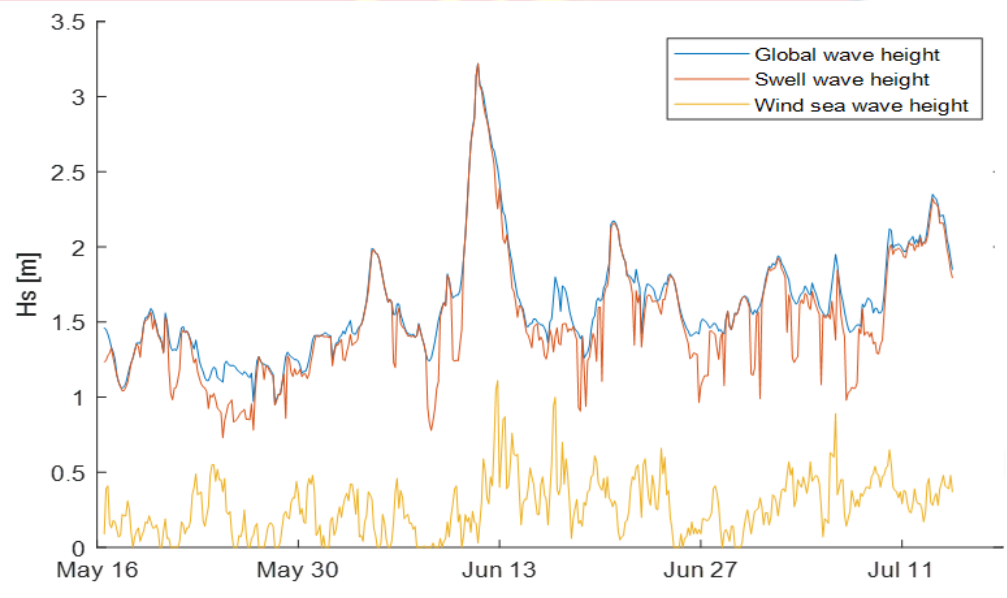

Figure 40: Time series of when the highest wave height was recorded off Togo/Benin.

Nigeria.

Time series showing when the highest global Hs was recorded, along with comparisons to wind sea, and swell values. Figure 41 shows that on May 31, 2014, at 3.04 m, the highest global Hs for the years 1993 to 2022 occurred. The highest swell Hs recorded in the period from 1993 to 2022 was 3.03 m on May

31, 2014. The maximum wind sea wave during the period of May 5, 2014, to July 3, 2014, was measured to be 1.31 m.

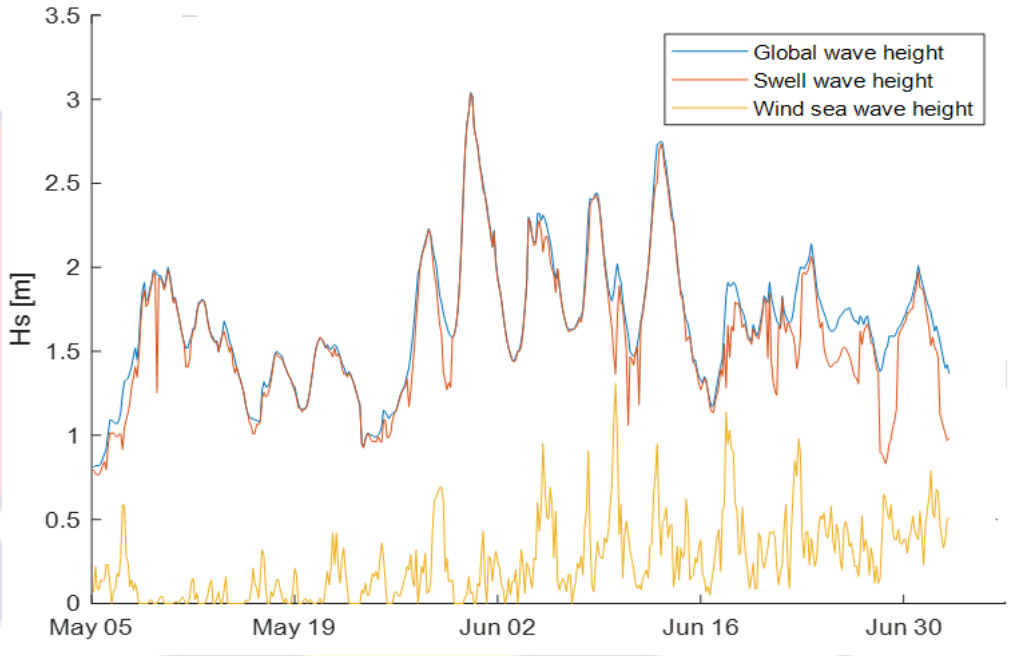

Figure 41: Time series of when the highest wave height was recorded off Nigeria

Interannual Variability of Global Wave Parameters

Map analysis of interannual variability of global Hs and Tp of West Africa for all August were analyzed to see distribution over the 30-year period.

Global Significant Wave Height

Figure 42 and Figure 43 are maps that show the global Hs condition for all the August for the 30-year period. This analysis was done due to the fact that Hs for August in the seasonal map (Figure 20) depicted the highest wave condition in the month of August. Of all the August of the years, the Hs of the waves at the coast are within the range of 1.6 m to 1.8 m. The months of July

and August experience the highest significant wave heights (Hs) in the West Africa region. This phenomenon can be attributed to the waves generated by strong winds originating from the South Atlantic, particularly near Argentina. These winds tend to produce swells during the winter season, and it's during July and August that the West African region is most affected by these wave conditions.

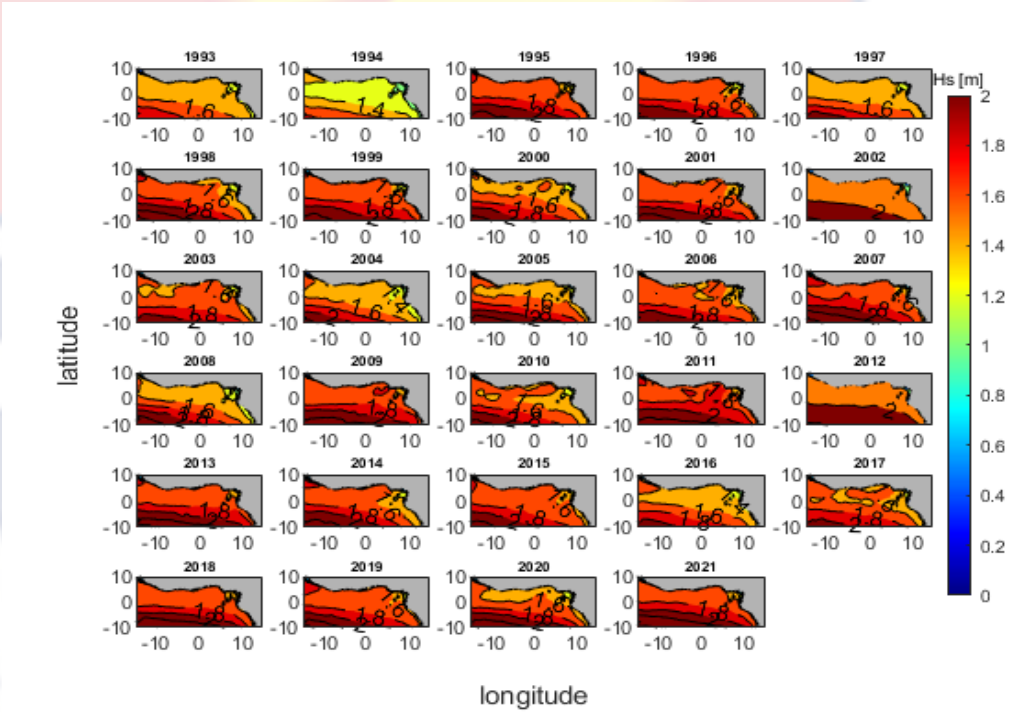

Figure 42: Map of global Hs for August for the duration 1993 to 2021

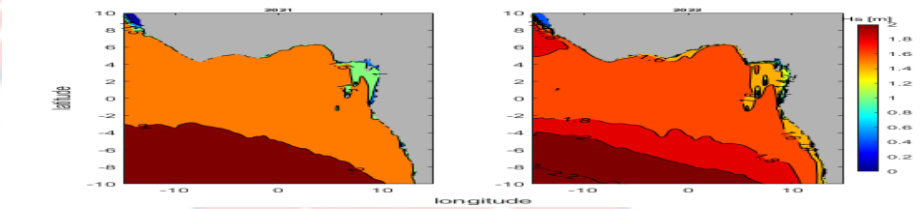

Figure 43: Map of global Hs for August for the duration of 2021 and 2022.

Global Wave Period

Figure 44 and Figure 45 are maps depicting the global Tp for all the August for the 30-year period. This was done to see the correlation of all the August for each year. The Tp is at its peak for this season with the range of 13 s to 15 s even at the coast of the West African region. Even though August proved to have the highest global Tp, there was a need to examine the annual changes.

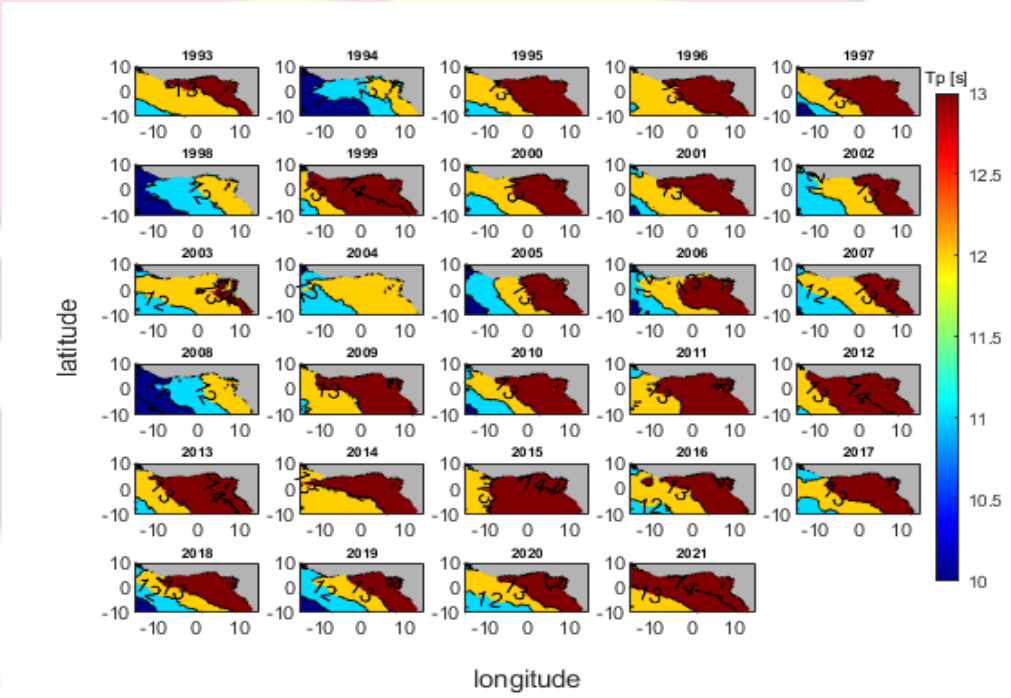

Figure 44: Map of global Tp for August for the duration 1993 to 2021.

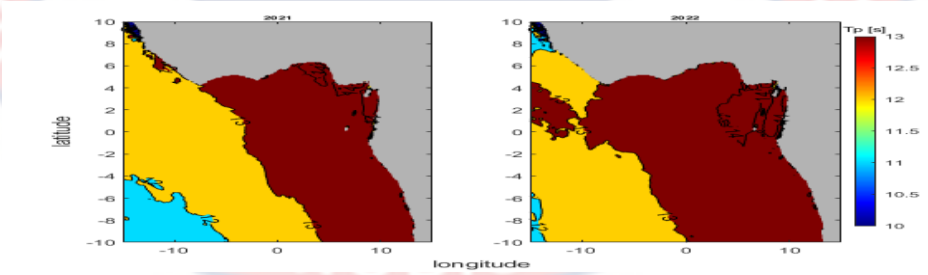

Figure 45: Map of global Tp for August for the duration of 2021 and 2022.

Distribution of Hs of Wind Sea and Swell Waves for the three other locations

As stated in Chapter Four, the histogram distribution of the wave partition (wind sea and swell) was analyzed.

Ivory Coast

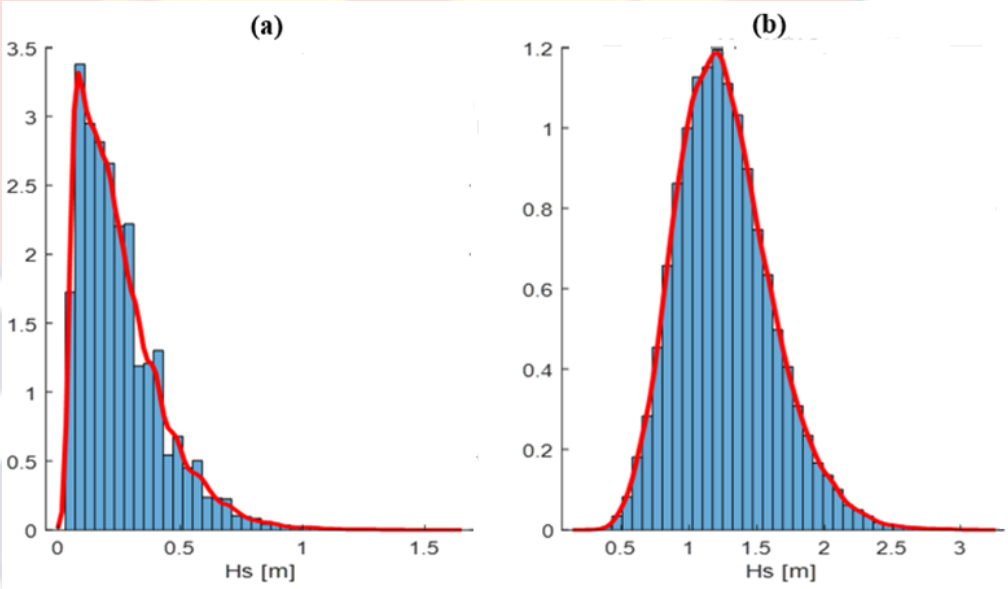

Figure 46: Histogram with density curve of Hs of **(a)** wind sea and **(b)** swell off Ivory Coast.

Table 5: Statistical Analysis for Wind Sea and Swell off Ivory Coast.

Statistical Analysis	Wind sea	Swell
Minimum wave height value (m)	0.05	0.25
Maximum wave height value (m)	1.60	3.15
Modal wave height value (m)	0.07	1.20
50% quantile value (m)	0.21	1.23
90% quantile value (m)	0.48	1.72

Source: Researcher, 2023

Togo/Benin.

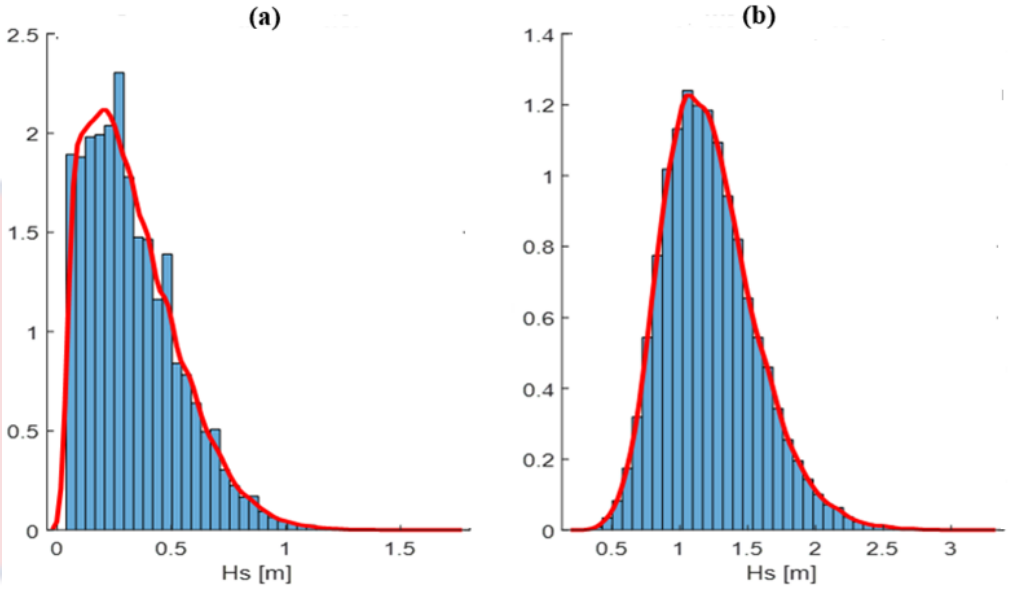

Figure 47: Histogram with density curve of Hs of **(a)** wind sea and **(b)** swell off Togo/Benin.

Table 6: Statistical Analysis for Wind Sea and Swell off Togo/Benin

Statistical Analysis	Wind sea	Swell
Minimum wave height value (m)	0.05	0.30
Maximum wave height value (m)	1.70	3.22
Modal wave height value (m)	0.21	1.02
50% quantile value (m)	0.29	1.18
90% quantile value (m)	0.61	1.67

Source: Researcher, 2023

Nigeria.

The Hs of wind sea and swell of Nigeria were analyzed by plotting a histogram plot with a density curve.

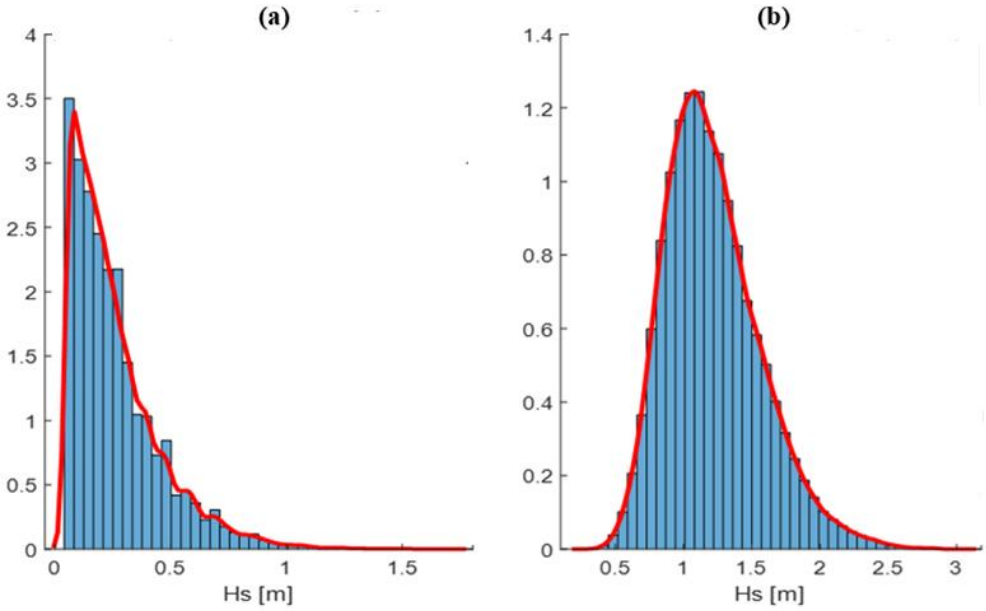

Figure 48: Histogram with density curve of Hs of **(a)** wind sea and **(b)** swell off Nigeria.

Table 7: Summary of the Statistical Analysis for Figure 48.

Statistical Analysis	Wind sea	Swell
Minimum wave height value (m)	0.05	0.29
Maximum wave height value (m)	1.72	3.03
Modal wave height value (m)	0.05	1.10
50% quantile value (m)	0.21	1.17
90% quantile value (m)	0.53	1.69

Source: Researcher, 2023

The direction of wind sea and swell for the three other regions as stated in Chapter Four.

The analysis of the direction of the Hs of wind sea and swell for Ivory Coast, Togo/Benin and Nigeria was also estimated.

Ivory Coast

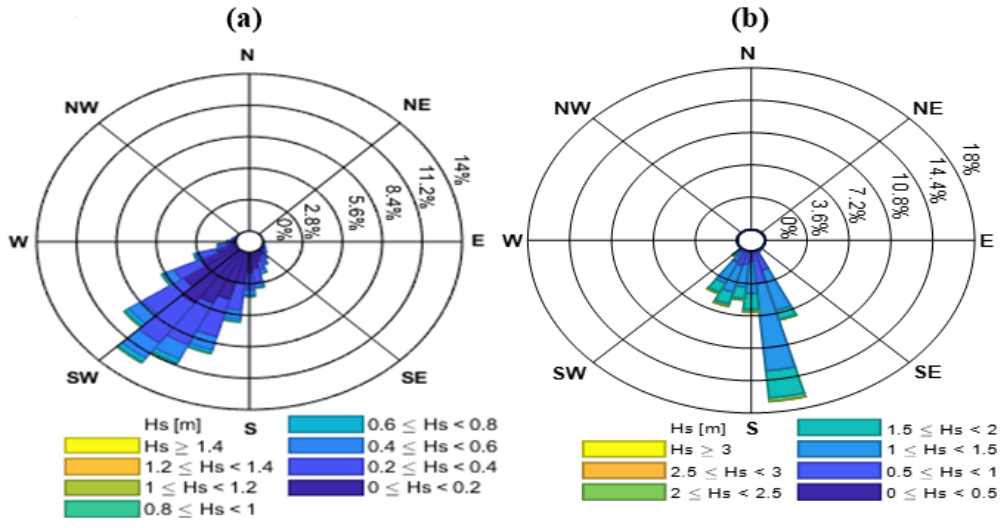

Figure 49: Directional rose for Hs of **(a)** wind sea and **(b)** swell.

Table 8: Summary of the Wave Direction off Ivory Coast.

Analysis	Wind sea	Swell
Mean wave direction	Within W-SW and SW-S region	Within S-SW and S-SE region

Source: Researcher, 2023

Togo/Benin

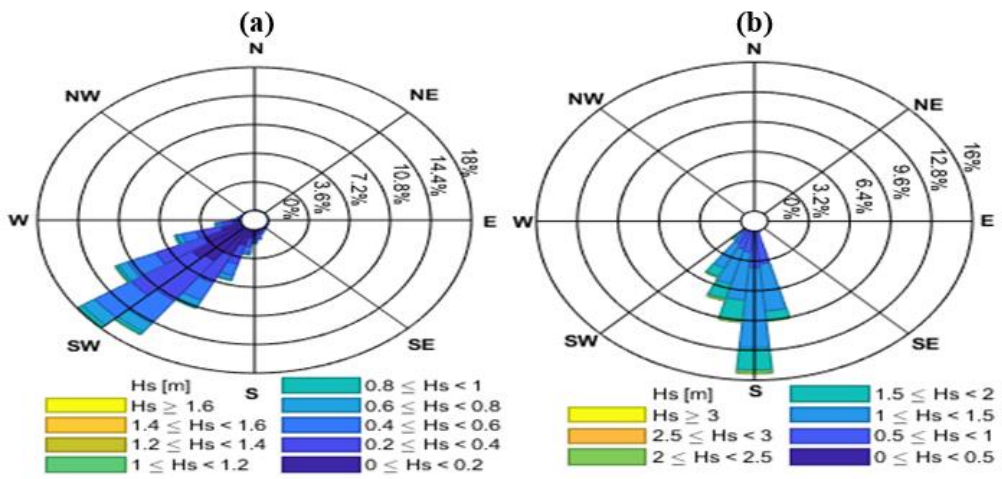

Figure 50: Directional rose for mean Hs for **(a)** wind sea and **(b)** swell for Togo/Benin

Table 9: Summary of the Wave Direction off Togo/Benin.

Analysis	Wind sea	Swell
Mean wave direction	Within W-SW and SW-S region	Within SW-S and S-SE region

Source: Researcher, 2023

Nigeria

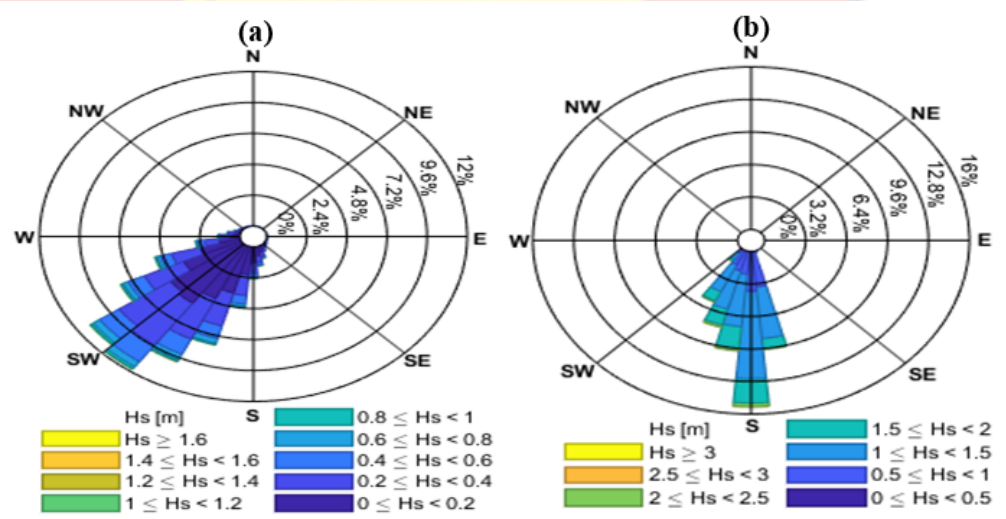

Figure 51: Directional rose for mean Hs for **(a)** wind sea and **(b)** swell

Table 10: Summary of the Wave Direction off Nigeria

Analysis	Wind sea	Swell
Mean wave direction	Within W-SW and SW-S region	Within SW-S and S-SE region

Source: Researcher, 2023

Seasonal Analysis of Global Significant Wave Height and Wave Period for Ivory Coast, Togo/Benin and Nigeria

Box plot analysis of seasonal variations of global Hs and its mean were analyzed for the other three regions for the Duration of January 1993 to December 2022.

Global Significant Wave Height

Figure 52 is the analysis of global Hs for Ivory Coast, Togo/Benin and Nigeria.

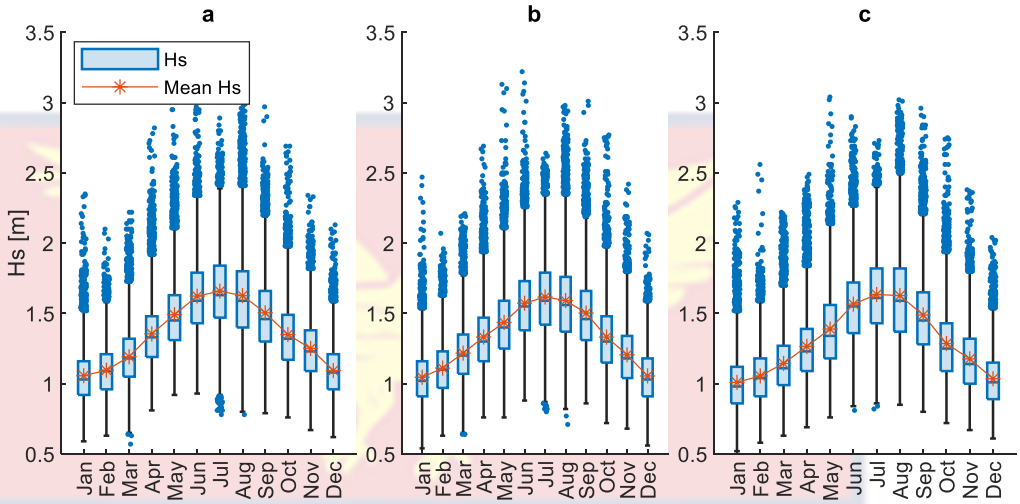

Figure 52: Box plot of seasonal variation of global Hs of **(a)** Ivory Coast, **(b)** Togo/Benin and **(c)** Nigeria

Table 11: Summary of Seasonal Variation of Global Hs off (a) Ivory Coast, (b) Togo/Benin and (c) Nigeria

Statistical Analysis	Ivory Coast	Togo/Benin	Nigeria
Minimum value (m)	1.06	1.05	1.01
Maximum value (m)	1.66	1.62	1.63
50% quantile (m)	1.35	1.33	1.28
90% quantile (m)	1.64	1.60	1.63

Source: Researcher, 2023

Figure 53, Figure 54 and Figure 55 are directional rose plots indicating where the global waves of the seasons originated from for the locations of Ivory Coast, Togo/Benin and Nigeria respectively.

Seasonal global Hs analysis for Ivory Coast.

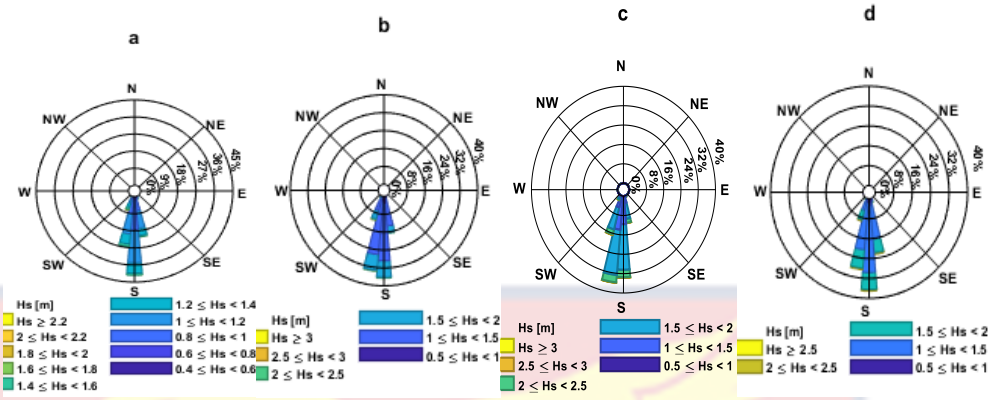

Figure 53: Seasonal global wave direction of Ivory Coast in **(a).** December, January, and February, **(b).** March, April, and May, **(c).** June, July, and August **(d).** September, October and November.

Table 12: Analysis of the Wave Direction of the Seasons of (a). | Dec | Jan | Feb|, (b). | Mar | Apr | May |, (c). | Jun | Jul | Aug | and (d). | Sep | Oct | Nov | of Ivory Coast.

Season	|Dec|Jan|Feb|	|Mar|Apr|May|	|Jun|Jul|Aug|	|Sep|Oct|Nov|
Wave Direction	SW-S (36%)	SW-S (42%)	SW-S (60%)	SW-S (40%)
	S (40%)	S (40%)	S (32%)	S (38%)
	S-SE (24%)	S-SE (18%)	S-SE (8%)	S-SE (22%)

Source: Researcher, 2023

Seasonal global Hs analysis for Togo/Benin.

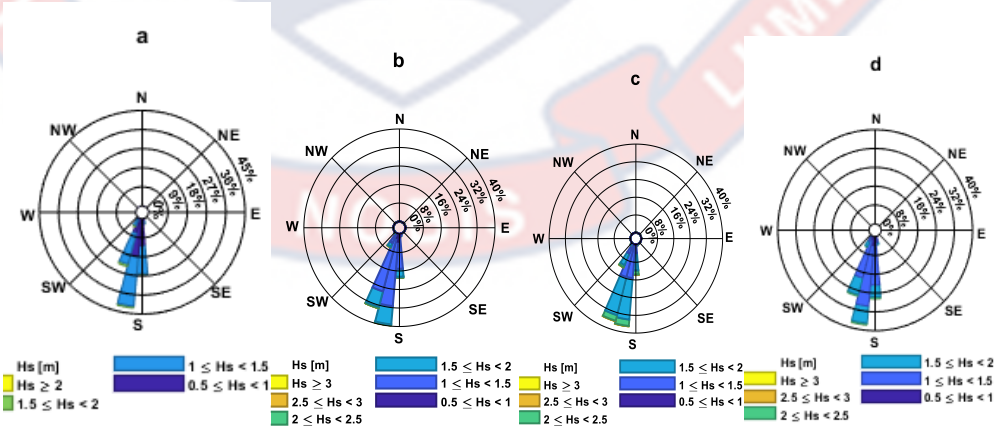

Figure 54: Seasonal global wave direction of Togo/Benin in **(a).** December,

January, and February, **(b).** March, April, and May, **(c).** June, July, and August **(d).** September, October and November.

Table 13: Analysis of the Wave Direction of the Seasons of (a). | Dec | Jan | Feb |, (b). | Mar | Apr | May |, (c). | Jun | Jul | Aug | and (d). | Sep | Oct | Nov | of Togo/Benin.

Season	|Dec|Jan|Feb|	|Mar|Apr|May|	|Jun|Jul|Aug|	|Sep|Oct|Nov|
Wave Direction	SW-S (81%) S (16%) S-SE (3%)	SW-S (80%) S (20%)	SW-S (86%) S (14%)	SW-S (70%) S (26%) S-SE (4%)

Source: Researcher, 2023

Seasonal global Hs analysis for Nigeria.

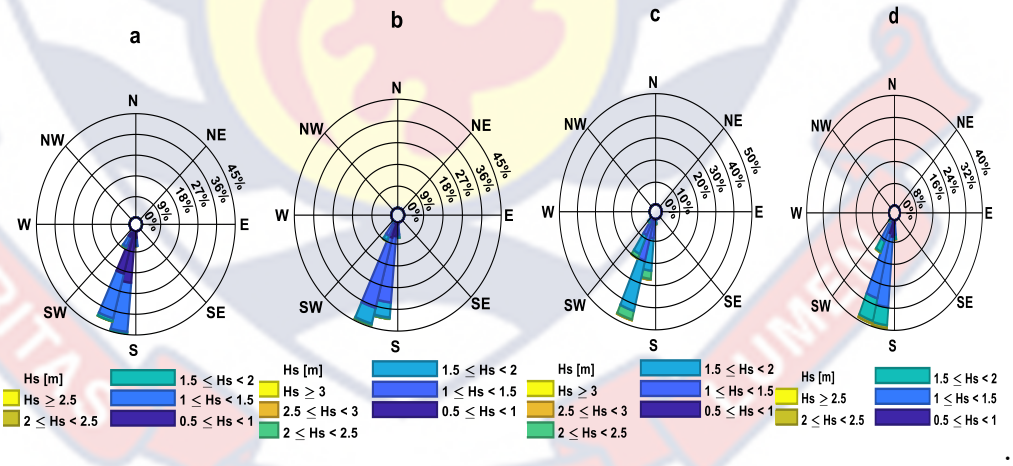

Figure 55: Seasonal global wave direction of Nigeria in **(a).** December, January, and February, **(b).** March, April, and May, **(c).** June, July, and August **(d).** September, October and November.

Table 14: Analysis of the Wave Direction of the Seasons of (a). | Dec | Jan | Feb |, (b). | Mar | Apr | May |, (c). | Jun | Jul | Aug | and (d). | Sep | Oct | Nov | of Nigeria

Season	|Dec|Jan|Feb|	|Mar|Apr|May|	|Jun|Jul|Aug|	|Sep|Oct|Nov|
Wave Direction	SW-S (96%) S (4%)	SW-S (96%) S (4%)	SW-S (100%)	SW-S (100%)

Source: Researcher, 2023

Global wave period

Figure 56 is the analysis of global Tp for Ivory Coast, Togo/Benin and Nigeria.

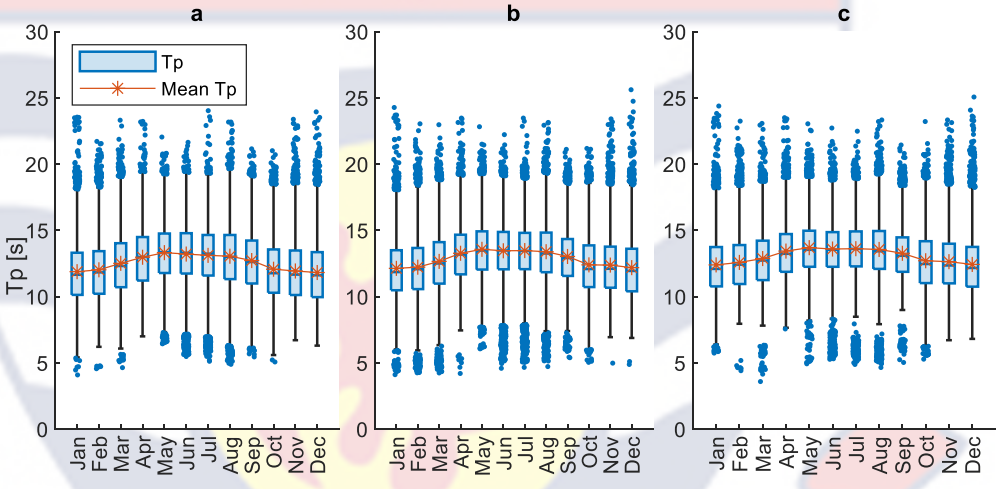

Figure 56: Box plot of seasonal variation of global Tp of **(a)** Ivory Coast, **(b)** Togo/Benin and **(c)** Nigeria

Table 15: Statistical Analysis of Global Tp for Ivory Coast, Togo/Benin and Nigeria.

Statistical Analysis	**Ivory Coast**	**Togo/Benin**	**Nigeria**
Minimum value (s)	11.82	12.13	12.39
Maximum value (s)	13.32	13.57	13.69
50% quantile (s)	12.62	12.84	13.07
90% quantile (s)	13.24	13.50	13.64

Source: Researcher, 2023

Seasonal Analysis of Significant Wave Height of Swell and Wind Sea for Ivory Coast, Togo/Benin and Nigeria

Box plot analysis of seasonal variations of Hs of swell and wind sea to the global wave were analyzed for the other three regions for the Duration of January 1993 to December 2022.

Swell Significant Wave Height

Figure 57 is the analysis of swell waves of the regions of Ivory Coast, Togo/Benin and Nigeria.

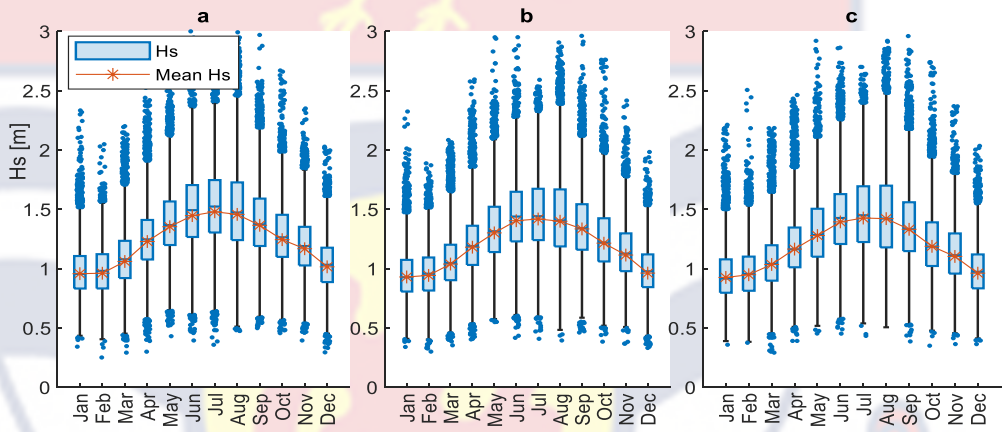

Figure 57: Box plot of seasonal variation of swell Hs of **(a)** Ivory Coast, **(b)** Togo/Benin and **(c)** Nigeria

Table 16: Statistical Analysis of Seasonal Variations of Swell Hs off Ivory Coast, Togo/Benin and Nigeria

Statistical Analysis	Ivory Coast	Togo/Benin	Nigeria
Minimum wave height value (m)	0.96	0.93	0.93
Maximum wave height value (m)	1.48	1.42	1.43
50% quantile value (m)	1.24	1.20	1.18
90% quantile value (m)	1.46	1.41	1.42

Source: Researcher, 2023

Wind Sea Significant Wave Height

Figure 58 is the analysis of wind sea waves of the regions of Ivory Coast, Togo/Benin and Nigeria.

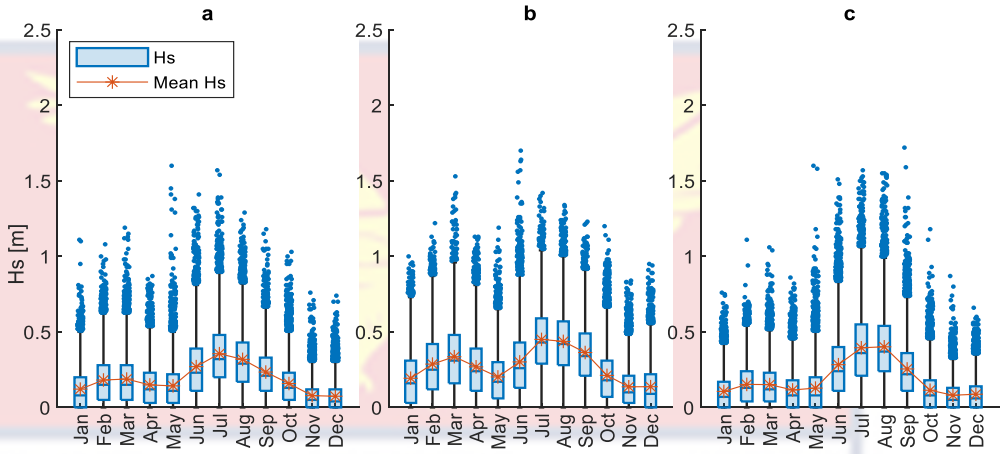

Figure 58: Box plot of seasonal variation of wind sea Hs of **(a)** Ivory Coast, **(b)** Togo/Benin and **(c)** Nigeria

Table 17: Statistical Analysis of Seasonal Variations of Wind Sea Hs off Ivory Coast, Togo/Benin and Nigeria

Statistical Analysis	Ivory Coast	Togo/Benin	Nigeria
Minimum wave height value (m)	0.07	0.14	0.08
Maximum wave height value (m)	0.36	0.45	0.40
50% quantile value (m)	0.17	0.28	0.14
90% quantile value (m)	0.33	0.44	0.40

Source: Researcher, 2023

Interannual Variability of Wave Condition in the Four Regions.

Figure 59 is the interannual variability anomaly plot of wave conditions of global significant wave height, Hs was for the selected regions.

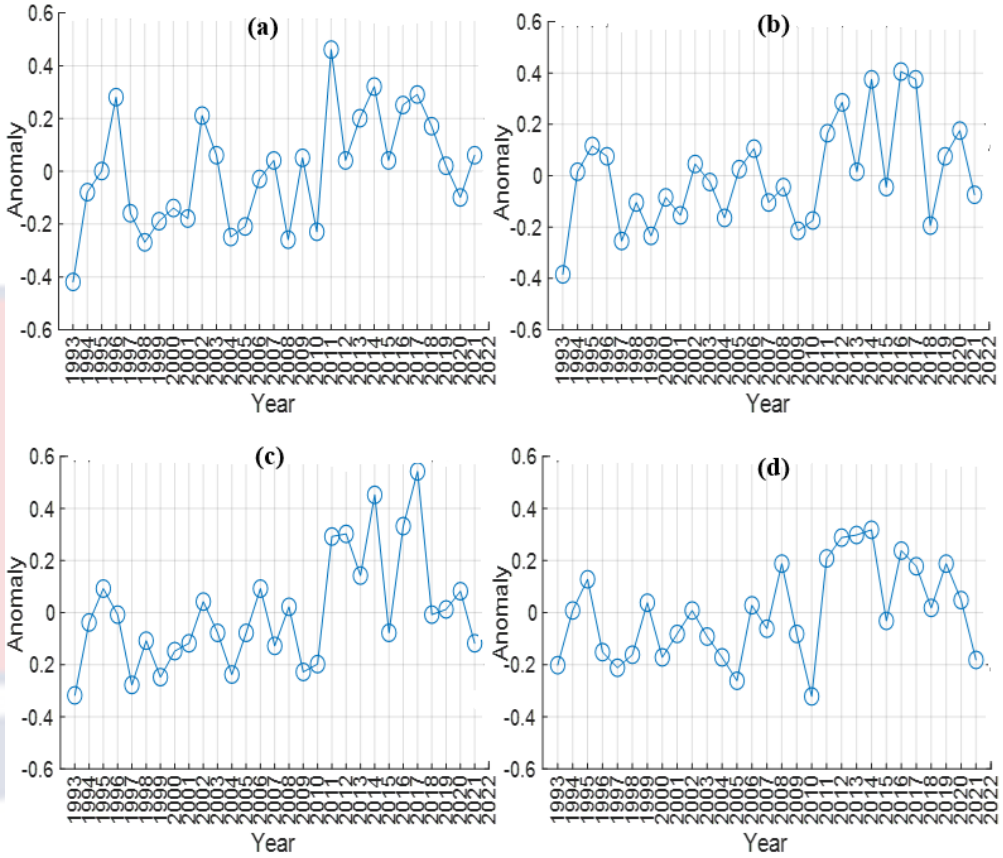

Figure 59: Annual anomaly plot of global Hs of **(a)** Ivory Coast, **(b)** Ghana, **(c)** Togo/Benin and **(d)** Nigeria

Table 18: A Summary of the Annual Anomaly of Global Hs off Ivory Coast, Ghana, Togo/Benin and Nigeria.

Statistical Analysis	Ivory Coast	Ghana	Togo/Benin	Nigeria
Minimum anomaly	-0.46	-0.38	-0.32	-0.32
Maximum anomaly	0.46	0.41	0.54	0.32
50% quantile anomaly	0.02	-0.03	-0.04	0.01
90% quantile anomaly	0.29	0.34	0.32	0.27

Source: Researcher, 2023

Wave power

Figure 60 exhibit the interannual variability of wave power over the period of 1993 to 2022 for Ivory Coast (a), Ghana (b), Togo/Benin (c) and Nigeria (d).

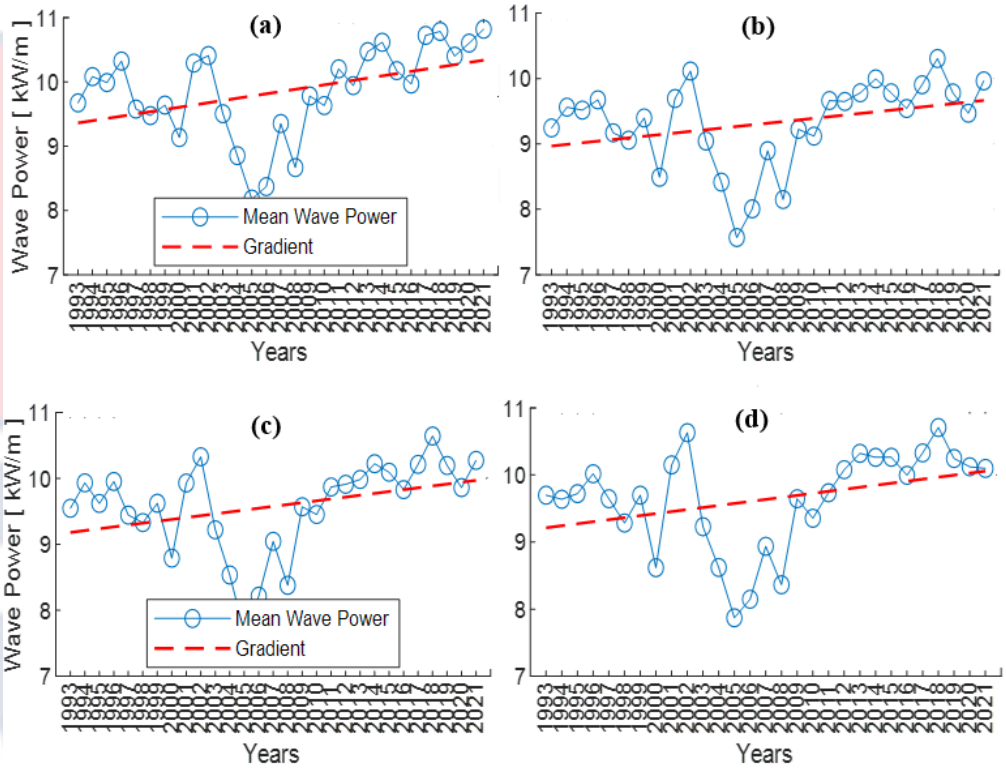

Figure 60: Interannual variability of wave power of (a) Ivory Coast, (b) Ghana, (c) Togo/Benin and (d) Nigeria

Ivory Coast: The minimum wave power was estimated to be 8.18 kW/m which occurred in 2005 and that of the maximum wave power was estimated to be 10.82 kW/m which occurred in 2021.

Ghana: The minimum wave power was estimated to be 7.57 kW/m which occurred in 2005 and that of the maximum wave power was estimated to be 10.31 kW/m which occurred in 2018.

Togo/Benin: The minimum wave power was estimated to be 7.68 kW/m which occurred in 2005 and of the maximum wave power was estimated to be 10.64 kW/m which occurred in 2018.

Nigeria: The minimum wave power was estimated to be 7.87 kW/m which occurred in 2005 and that of the maximum wave power was estimated to be 10.71 kW/m which occurred in 2018.

The annual average wave power was estimated to be 0.04 kW/m, 0.025 kW/m, 0.026 kW/m and 0.013 kW/m for the regions of Ivory Coast, Ghana, Togo/Benin and Nigeria respectively.